2016-03-23

A Role for the Lipid Droplet Protein HIG2 in Promoting Lipid Deposition in Liver and Adipose Tissue: A Dissertation

Marina T. DiStefano
University of Massachusetts Medical School

A ROLE FOR THE LIPID DROPLET PROTEIN HIG2 IN PROMOTING LIPID DEPOSITION IN LIVER AND ADIPOSE TISSUE

A Dissertation Presented

By

MARINA T. DISTEFANO

Submitted to the Faculty of the
University of Massachusetts Graduate School of Biomedical Sciences, Worcester
in partial fulfillment of the requirements for the degree of

DOCTOR OF PHILOSOPHY

MARCH 23, 2016

INTERDISCIPLINARY GRADUATE PROGRAM

A ROLE FOR THE LIPID DROPLET PROTEIN HIG2 IN PROMOTING LIPID DEPOSITION IN LIVER AND ADIPOSE TISSUE

A Dissertation Presented
By

MARINA T. DISTEFANO

The signatures of the Dissertation Defense Committee signify completion and approval as to style and content of the Dissertation

_____
Michael P. Czech, Ph.D., Thesis Advisor

_____
Andrew S. Greenberg, M.D., Member of Committee

_____
David A. Guertin, Ph.D., Member of Committee

_____
Amy Walker, Ph.D., Member of Committee

_____
Pranoti Mandrekar, Ph.D., Member of Committee

The signature of the Chair of the Committee signifies that the written dissertation meets the requirements of the Dissertation Committee

_____
Roger J. Davis, Ph.D., Chair of Committee

The signature of the Dean of the Graduate School of Biomedical Sciences signifies that the student has met all graduation requirements of the school.

_____
Anthony Carruthers, Ph.D.,
Dean of the Graduate School of Biomedical Sciences

Interdisciplinary Graduate Program

March 23, 2016

Dedication

I would like to dedicate this work to the late Paula M. Pitha-Rowe, Ph.D., my undergraduate Principal Investigator and mentor. I thank her for always approaching research with a contagious vivacity and curiosity. I thank her for all of the countless hours of instruction and mentorship. I thank her for all of the conversations and the delicious meals she has cooked for me. This work is dedicated to her because she convinced me to apply to a school she loved and often visited, the University of Massachusetts Medical School. Without her, I would not be where I am today.

Acknowledgements

I am very lucky to be surrounded by a strong support system of family and friends. I would like to thank my thesis mentor, Mike Czech for introducing me to the world of adipose tissue biology, for giving me experimental independence, for teaching me how to make and give a stellar presentation, and for demonstrating how to write an attention-grabbing abstract. These last six years have flown by and I have learned innumerable lessons during my time in the lab. I would like to thank my thesis committee for their encouragement and innovative suggestions. I know that mentoring a graduate student requires a significant time commitment and I am grateful for all of the time and advice they have provided.

I would also like to thank all of the past and present members of the Czech lab for helpful discussions and critical experimental advice. Thank you to Rachel Roth Flach for acting as a lab mentor, editor, and valuable friend. Thank you to Joe Virbasius for all of the editing, thoughtful discussions, necessary experimental criticism, and friendship. Thank you to Ozlem Senol-Cosar and Laura V. Danai for extra experimental hands, advice, and making each day in the lab enjoyable.

Finally, I would like to thank my family and friends. Thank you to Bill Monis, Ly-Sha Ee, and Sungwook Choi for friendship from that first day of GSBS orientation to now. Thank you to my parents for love, support, and

encouragement. Thank you to my sisters for keeping tabs on me and visiting me. As always, thank you to my husband for his unwavering love, support, and for humoring me and listening to thousands of scientific dinner conversations.

Abstract

Chronic exposure of humans or rodents to high calorie diets leads to hypertriglyceridemia and ectopic lipid deposition throughout the body, resulting in metabolic disease. Cellular lipids are stored in organelles termed lipid droplets (LDs) that are regulated by tissue-specific LD proteins. These proteins are critical for lipid homeostasis, as humans with LD protein mutations manifest metabolic dysfunction. Identification of novel components of the LD machinery could shed light on human disease mechanisms and suggest potential therapeutics for Type 2 Diabetes.

Microarray analyses pinpointed the largely unstudied Hypoxia-Inducible Gene 2 (Hig2) as a gene that was highly expressed in obese human adipocytes. Imaging studies demonstrated that Hig2 localized to LDs in mouse hepatocytes and the human SGBS adipocyte cell line. Thus, this work examined the role of Hig2 as a LD protein in liver and adipose tissue.

Hig2 deficiency reduced triglyceride deposition in hepatocytes; conversely, ectopic Hig2 expression promoted lipid deposition. Furthermore, liver-specific Hig2-deficient mice displayed improved glucose tolerance and reduced liver triglyceride content. Hig2 deficiency increased lipolysis and β-oxidation, accounting for the reduced triglyceride accumulation.

Similarly, adipocyte-specific Hig2-deficient mice displayed improved glucose tolerance, reduced adipose tissue weight and brown adipose tissue that

was largely cleared of lipids. These improvements were abrogated when the animals were placed in thermoneutral housing and brown adipocyte-specific Hig2-deficient mice also displayed improved glucose tolerance, suggesting that active brown fat largely mediates the metabolic phenotype of Hig2 deletion. Thus, this work demonstrates that Hig2 localizes to LDs in liver and adipose tissue and promotes glucose intolerance.

Table of Contents

List of Tables

List of Figures

CHAPTER I

CHAPTER II

CHAPTER III

List of Symbols, Abbreviations or Nomenclature

TG - triglyceride

FA - fatty acid

LD - lipid droplet

WAT- white adipose tissue (epididymal [eWAT], inguinal [iWAT])

BAT- brown adipose tissue

SVF- stromal vascular fraction

T2D - Type 2 Diabetes

HSL - hormone sensitive lipase

ATGL - adipose triglyceride lipase

DNL - *de novo* lipogenesis

NAFLD - non-alcoholic fatty liver disease

UCP1 - uncoupling protein-1

CIDE - cell death-inducing DNA fragmentation factor 45-like effector

Hig2 - hypoxia-inducible gene 2

G0S2 - G0/G1 switch protein 2

Ubc - ubiquitin C

HFD - high fat diet

ND - normal diet

SGBS - Simpson-Golabi-Behmel syndrome

GTT - glucose tolerance test

CHAPTER I: INTRODUCTION

Part1: Lipid Deposition in health and disease

Lipids act as a critical energy reservoir. Their formation, storage and breakdown are tightly controlled by signaling pathways that will be detailed below. Two organs that function as master regulators of lipid synthesis and storage are the liver and adipose tissue. In healthy animals, both liver and adipose tissue synthesize lipids to be stored largely in white adipose tissue. Thus, the first part of chapter 1 will focus on the roles of liver and adipose tissue in lipid deposition.

Liver

Structure

The liver is organized into lobes; hepatocytes, marked by the lineage marker albumin, make up 80% of the cell population (1). Most hepatocytes in mature liver are multinucleated and thus, tetraploid, and function in nutrient processing (2). The remainder of the liver cell population consists of resident immune cells, endothelial cells, and a variety of stem cells. Kupffer cells (KCs), the resident macrophages of the liver, are the most numerous tissue-resident macrophage in the body, and have distinct subpopulations (3). These cells often present the first line of defense for blood-borne infections and KC-depleted mice display 100% lethality when exposed to certain infections (4,5). Hepatic stellate cells (HSCs) store lipids and vitamin A in a healthy liver, but become highly proliferative and fibrinogenic in a chronically inflamed liver (3). The liver has a

remarkable capacity for regeneration and the role of pluripotent stem cells and multipotent oval cells in this process is still debated, as hepatocytes appear to divide and regenerate the majority of liver after partial hepatectomy (6).

Function

The liver is a master regulator of immune surveillance, detoxification, serum protein synthesis, and whole body metabolism. The hepatic immune system differs from that of other organs because it must maintain a level of immunosuppression due to its exposure to LPS, a bacterially-derived polysaccharide, but it must be capable of being fully activated when exposed to blood-borne infections (3). The liver removes and breaks down circulating toxic compounds such as ammonia, bilirubin, and ethanol (7). The liver also functions in secretion of plasma proteins such as albumin and clotting factors (8). As discussed in detail below, the liver acts as a master regulator of whole body metabolism (Figure 1.1). During times of caloric excess, the liver synthesizes and exports or stores lipids and during fasting or starvation, it synthesizes and exports glucose. The liver also plays a key role in the synthesis and recycling of glycogen and bile acids (9,10).

Figure 1.1 Lipid metabolism in liver

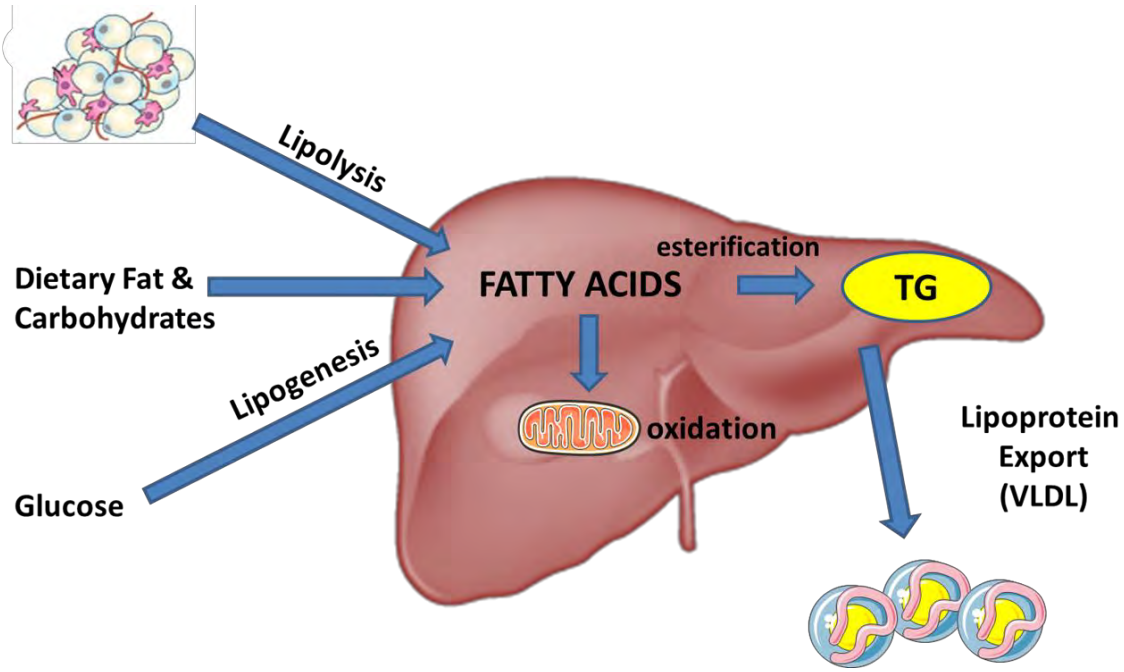

FIGURE 1.1 Lipid metabolism in liver. The liver is a master regulator of lipid metabolism. Fatty acids that are esterified into triglycerides (TG) in the liver can come from multiple sources, such as adipose tissue lipolysis, the diet, or synthesis directly from glucose via *de novo* lipogenesis. Triglycerides can be packaged and exported in very low-density (VLDL) lipoprotein particles or can be broken down to fatty acids and oxidized by the mitochondria. TG; triglyceride, VLDL; very low-density lipoprotein.

De Novo Lipogenesis

De novo (DNL) lipogenesis is the postprandial synthesis of lipids from protein or carbohydrate metabolites. Both liver and adipose tissue synthesize lipids via the *de novo* lipogenic pathway and the contribution of each tissue is often species-specific (11). Experiments suggest that in humans and rodents, DNL predominantly occurs in liver, while in ruminants, the adipose tissue synthesizes most of the lipids (11). DNL builds FAs from acetyl units, which usually come from glucose or acetate, and acetyl-CoA. Glucose enters the cell via the glucose transporter Glut2 (12). Glucose is converted to pyruvate by glycolysis and pyruvate is converted to citrate within the TCA cycle. ATP citrate lyase (ACLY) converts citrate and CoA to acetyl-CoA. Acetyl-CoA carboxylase (ACC) is the rate-limiting enzyme for FA synthesis and converts acetyl-CoA to malonyl-CoA. Fatty acid synthase (FAS) synthesizes the FA palmitate from malonyl-CoA and acetyl-CoA. Other FAs are synthesized by elongation and/or desaturation of palmitate. Two FA molecules are esterified to a molecule of glycerol phosphate by the enzyme Glycerol-P Acyl-Transferase (GPAT) to form triglyceride (TG) (11). DNL is highly coupled to nutrient availability and the transcription factors that regulate the expression of most lipogenic enzymes are upstream stimulatory factors (USFs), Sterol regulatory-element binding protein 1 (SREBP1), Carbohydrate regulatory-element binding protein (ChREBP), and Liver x receptor LXR (13). Transcription of lipogenic enzymes, such as FAS, is

increased by insulin and decreased by fasting, coupling them with nutrient availability (11,14). TGs synthesized *de novo* can either be stored in hepatic lipid droplets (LDs) or exported into circulation as very low density lipoprotein (vLDL) particles.

Lipid uptake and secretion

The liver functions both in the secretion of lipid-containing lipoprotein particles and the uptake of lipoprotein remnants. The synthesis and secretion of vLDL occur in hepatocytes and are well-characterized. TGs and cholesterol are synthesized in the smooth ER and transferred to lipoprotein particles containing apolipoprotein B-100 (ApoB-100) by microsomal triglyceride transfer protein (Mttp). Lipid and ApoB-100-containing vesicles diffuse to the Golgi where they are glycosylated and bud off. The vesicles fuse with the hepatocyte sinusoidal membrane and are released into circulation (11).

Conversely, dietary FAs from chylomicrons, which are circulating cholesterol, phospholipid, and TG-containing lipoprotein particles from the intestine, are taken up by muscle and adipose tissue, leaving chylomicron remnants (CR) (15). Hepatocytes take up CR via the hepatic low density lipoprotein receptor (LDLR) or LDLR-related protein 1 (LRP1) (16-19). Delipidated vLDL remnants are similarly recycled (15).

Hepatic Glucose Production

During prolonged fasting, the liver must synthesize and export glucose to maintain blood glucose concentrations. Initially, glucose is formed from glycogenolysis, the breakdown of stored hepatic glycogen (20). Upon depletion of glycogen stores, glucose is synthesized from glycerol, lactate, or amino acids (AAs) by gluconeogenesis. These substrates, which are often derived from muscle or adipose tissue, enter the cytoplasm via transporters, and are converted to pyruvate. Pyruvate is converted to oxaloacetate by pyruvate carboxylase (PC), then converted to phosphoenolpyruvate (PEP) by phosphoenolpyruvate carboxykinase (PEPCK). In a series of steps, PEP is converted to fructose 6-phosphate, then glucose 6-phosphate and finally to glucose by glucose-6-phosphatase (Glu-6-Pase), which can then be released into the bloodstream (21).

Gluconeogenic enzyme activity is increased by both glucagon and glucocorticoids and decreased by insulin, coupling gluconeogenesis with fed-fasting state (21-23). The transcription factors that promote gluconeogenic enzyme expression are Forkhead box O1 (FOXO1), peroxisome proliferator-activated receptor gamma coactivator 1 alpha (PGC1α), cAMP-responsive element binding protein (CREB)/ CREB-regulated transcription coactivator 2 (Crtc2), CCAAT enhancer-binding proteins (C/EBPs), and hepatocyte nuclear factors (HNFs). During fasting, these factors translocate to the nucleus and activate gluconeogenic genes (24-27). Although it has been established that

hormones control hepatic glucose production, the precise mechanisms whereby this happens are unclear. One hypothesis, which couples adipose tissue lipolysis to hepatic glucose production suggests that insulin suppresses adipose tissue lipolysis, which reduces the availability of the substrate acetyl-CoA for hepatic gluconeogenesis, thereby reducing gluconeogenic enzyme levels (particularly PC) and hepatic gluconeogenesis (28).

Glycogen Synthesis

Glycogen consists of large branched polymers of glucose stored in cytoplasmic granules in hepatocytes and it functions as a ready glucose supply in liver. During fasting, glycogen is the first source of glucose released by the liver to maintain euglycemia (10). Glycogen stores can also be found in skeletal muscle. Glycogen is converted first to glucose 1-phospate then glucose 6-phosphate by phosphoglucomutase and finally to glucose by Glu-6-Pase, which can then be released into the bloodstream (10). Glycogen synthesis and breakdown are hormonally regulated, coupling glucose availability to fed-fasting state (20).

Adipose Tissue

The adipose tissue is a critical energy reservoir and an endocrine organ. What was once considered an inert fat storage organ has evolved into a key regulator of whole body metabolism. Adipose tissue is actively involved in lipid and glucose uptake, *de novo* lipid synthesis, lipolysis, and the secretion of

adipose-specific cytokines, termed adipokines. The necessity of adipose tissue is confirmed by the metabolic disease and related comorbidities of patients that lack functional adipose tissue. The role of adipose tissue in health and disease will be discussed in detail below.

Structure

The adipose tissue is a heterogeneous organ comprised of fat cells, also known as adipocytes, which can number up to two-thirds of the cell population, and a range of other cells including stem cells, fibroblasts, endothelial cells, blood cells, and neuronal cells (29,30). These cells, when digested and fractionated from the adipocytes, are collectively called the stromal vascular fraction or the SVF (31). Experiments have established that multipotent cells capable of forming fat pads *in vitro* and *in vivo* reside in the SVF (32-34). Although the exact developmental origin of these adipose tissue stem cells is still unclear, numerous hypotheses exist. One hypothesis suggests that these stem cells arise from a vascular niche as a subset of perivascular mural cells (33), while another suggests that endothelial cells and/or hematopoietic cells can change cell fate to give rise to adipocyte stem cells (35-38). Adipose tissue resides in many different depots in mammals and these depots are formed and remodeled throughout the life of the organism. Three classifications of adipose tissue, which have differing structures and functions will be described below.

White Adipose Tissue

White adipose tissue (WAT) is the primary site of energy storage in animals. White adipocytes store energy in the form of neutral lipids in a large, unilocular organelle termed a lipid droplet (LD), which will be described in detail later in the chapter (39). The prominent WAT depots in humans are the visceral, consisting of the omental, mesenteric, and retroperitoneal depots and the subcutaneous, consisting of the abdominal and gluteofemoral depots (40). The prominent WAT depots in mice are the visceral, consisting of the perigonadal, the retroperitoneal, the perirenal, and the mesenteric depots and the subcutaneous, consisting of the inguinal, interscapular, subscapular, axillary and cervical depots (39,41). Experimental evidence suggests that the subcutaneous and visceral depots are phenotypically distinct by a number of measures. The subcutaneous depot is associated with insulin sensitivity, is resistant to lipolysis, and expands primarily via hypertrophy during obesity (42-44). In mice, transplanting subcutaneous adipose tissue but not visceral adipose tissue into a visceral depot improves metabolic health, thus, this depot is considered a beneficial adipose depot (45). The visceral fat depot, perhaps due to its proximity to other organs and the liver portal vein, is prone to inflammation during metabolic disease, is highly lipolytic and, expands by both hypertrophy and hyperplasia during obesity (42-44,46).

Brown Adipose Tissue

Brown adipose tissue (BAT) is characterized by multilocular adipocytes, a high vascular density, and large numbers of mitochondria, which contribute to its brown color (39). A primary function of BAT is to generate heat by nonshivering thermogenesis, which occurs by uncoupling of oxidative metabolism (47). BAT forms during embryonic development in mammals and has its own specific gene expression program, which will be discussed below (48). While adult mice have BAT depots, until recently it was thought that BAT was only present in neonatal humans to generate necessary heat, but it was determined through analysis of fluorodeoxyglucose positron emission tomography (FDG-PET) scans that humans retain some portion of BAT through adulthood (49-51). The primary BAT depots in humans are located in the supraclavicular and subscapular regions, while mice have interscapular, subscapular, cervical, periaortic, and perirenal BAT depots (40,47,52). Retrospective analysis of FDG-PET scans demonstrate that BAT is associated with insulin sensitivity in humans and inversely associated with BMI, age, and fasting glucose levels (53,54).

Beige/Brite Adipose Tissue

Although WAT and BAT comprise the majority of adipose tissue in humans and rodents, beige (55) or brite (brown in white) (56) adipose tissue is being thoroughly investigated due to its inducible therapeutic potential. Interestingly, certain depots of adipose tissue have demonstrated plasticity depending on ambient temperature (57). For instance, cold temperatures

increase catecholamine levels thereby activating BAT to maintain body temperature. Conversely, it is less active at warm temperatures (39). Additionally, in colder temperatures, catecholamines activate certain populations of cells in WAT, particularly those in the subcutaneous depots. These beige/brite cells acquire more mitochondria and multilocular LDs, much like brown adipocytes (58). As these adipocytes possess characteristics of both white and brown adipocytes, they are termed beige/brite adipocytes. Although the source of these cells (conversion from mature white cells (59) vs *de novo* differentiation of precursors (42)) is controversial, the act of certain WAT cells expressing beige adipocytes markers is often called “browning” and, along with catecholamine-stimulation in cold temperatures, many stimuli have been claimed to “brown” WAT (60). The browning of WAT is an active area of investigation because beige adipocytes increase energy expenditure and improve metabolic health in rodents (48). Additionally, studies have shown that humans contain cells with a beige gene signature and that these cells are correlated with reduced BMI and insulin sensitivity (53,54,61). As such, beige adipocytes may prove useful for weight loss therapy in humans.

Function

Adipose tissue as an endocrine organ

The adipose tissue secretes a number of factors termed adipokines that modulate whole body metabolism (62). Two of these potent signaling factors are

adiponectin and leptin. Adiponectin is considered a beneficial adipokine that promotes insulin sensitivity (63). Its overexpression in mice promotes healthy adipose tissue expansion (64). Adiponectin levels negatively correlate with BMI and insulin resistance (63). Leptin is largely produced by WAT and is a hormone that is required for satiety; it inhibits food intake, along with altering energy expenditure, angiogenesis and sexual maturity (62). Leptin levels are increased with BMI in humans and obesity is often associated with leptin resistance (65,66).

Lipid Handling

WAT is a critical energy storage organ; thus, many of the signaling pathways of the adipocyte control storage and breakdown of lipids (Figure 1.2). Like liver, WAT converts protein or carbohydrate metabolites into stored lipids through the process of DNL (67). Additionally, adipocytes can directly uptake circulating lipids from chylomicrons for storage as TGs (68).

Figure 1.2 Lipid metabolism in adipose tissue

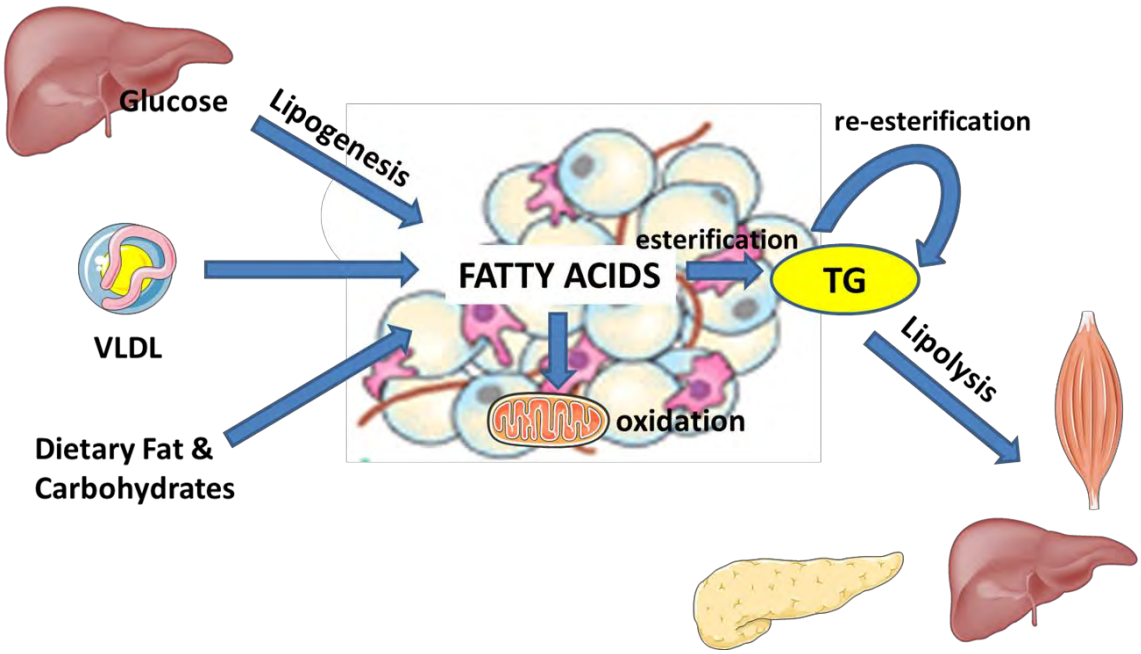

FIGURE 1.2 Lipid metabolism in adipose tissue. Adipose tissue processes and stores fatty acids as triglyceride (TG) in lipid droplets. These fatty acids can come from a variety of sources, including the diet, very low-density lipoprotein (VLDL) particles released by the liver, or direct synthesis from glucose via *de novo* lipogenesis. Triglycerides can be broken down via lipolysis and released into circulation to be taken up by other tissues, such as muscle liver or pancreas. Additionally, fatty acids liberated by lipolysis can be re-esterified into triglyceride or oxidized by the mitochondria. TG; triglyceride, VLDL; very low-density lipoprotein.

De novo lipogenesis

DNL in the adipocyte is defined by a well-characterized metabolic pathway with identical enzymes to hepatic DNL (67). Although the pathways and enzymes of adipose tissue and liver DNL are identical, experimental evidence suggests adipose tissue and liver DNL may be differentially regulated and serve distinct functions. For instance, obesity increases hepatic DNL and decreases adipose tissue DNL in mice and humans (69-73). In humans, increased hepatic DNL is associated with insulin resistance, hepatic steatosis and increased adipocyte size, while increased adipose tissue DNL is negatively correlated with these measures (74-77). In adipocytes, glucose, a major substrate for DNL, is transported into the cell by the adipocyte-specific transporter, Glut4 (78). As in liver, SREBP1 and ChREBP are the two transcription factors that control expression of most genes required for DNL. They are activated by both glucose and insulin, coupling them to overall metabolic homeostasis (79). Although FA uptake and esterification of circulating dietary lipids account for most of stored TGs, DNL may be required for the synthesis of key signaling lipids (80-82). For instance, DNL in adipocytes may be involved in synthesizing endogenous ligands for PPARγ (82,83), a master regulator of adipogenesis, and DNL in hepatocytes may be involved in synthesizing endogenous ligands for PPARα (80,81,84). While eicosanoids and poly unsaturated FAs activate PPARγ *in vitro (85-87)*, the

hypothesized endogenously synthesized ligands have yet to be specifically identified *in vivo* (84).

Lipolysis

Conversely, lipolysis is the breakdown of triglycerides (TGs) into FAs and glycerol. Lipolysis usually occurs during fasting; it liberates FAs to fuel muscle and liver. Briefly, β_3-adrenergic receptor stimulation, usually by catecholamines, activates GTP stimulatory (Gs) proteins, which in turn activate adenylyl cyclase (AC), increasing the concentration of cyclic AMP (cAMP). This activates Protein Kinase A (PKA), which phosphorylates lipases and other proteins, including lipid droplet proteins, some of which will be detailed below (88). A previous prevailing hypothesis suggested that one lipase, hormone sensitive lipase (HSL) was responsible for majority of TG hydrolysis; this hypothesis was challenged when HSL null animals did not display lipolytic defects or major alterations in obesity, but accumulated DGs in adipose tissue, muscle and testis (89-91). Animal studies identified an additional lipase termed adipose triglyceride lipase/desnutrin (ATGL) and suggest that it is the major TG lipase in adipocytes (92-94). These studies were later confirmed when human ATGL mutations were discovered and characterized (95-98); these will be discussed in detail later in the chapter. Thus, in adipocytes there are three identified lipases that coordinate the breakdown of a molecule of TG into three molecules of FA and one molecule of glycerol. Adipose triglyceride lipase (ATGL) catalyzes the primary reaction and hydrolyzes

TG to diacylglycerol (DG) (92-94). Hormone sensitive lipase (HSL) preferentially hydrolyzes DG to monoacylglycerol (MG). Finally, monoglyceride lipase (MGL) hydrolyzes MGs (99). FAs are then transported to other tissues, such as liver and muscle for fuel or re-esterified into TG at the LD. Synthesis of glycerol 3-phosphate from glucose or pyruvate via glyceroneogenesis controls the rate of FA re-esterification (100). Lipase binding partners will be discussed later in the chapter.

Thermogenesis

Although brown adipocytes also perform DNL and lipolysis to store lipids, their primary function is to generate heat through nonshivering thermogenesis. Thus, brown adipocytes have a specific gene expression signature in order to perform this task. PR Domain Containing 16 (Prdm16), C/ebpβ, Pgc1α, Early B-Cell Factor 2 (Ebf2), and peroxisome proliferator activated receptor alpha (PPARα) are transcription factors that are required for brown adipocyte identity and the thermogenic gene program (48). Prdm16 activates the transcription of genes important for BAT function, including uncoupling protein-1 (UCP1), the protein responsible for thermogenesis through uncoupling of oxidative phosphorylation (101). UCP1 is located in the mitochondrial membrane and uncouples the electron transport chain by facilitating a proton leak, which generates energy in the form of heat (102). UCP1 protein steadily increases with the differentiation of brown adipocytes (103) and without it, mice become cold-

sensitive when housed at room temperature (20-23°C) (104) and obese when housed at thermoneutrality (30°C) (105), a temperature that eliminates thermal stress. Although certain adult human BAT depots are more similar in appearance and gene expression signature to rodent beige cells (106), cold exposure in humans still promotes glucose and FA uptake in BAT (107); this uptake is correlated with leanness (108). Furthermore, cold exposure in humans leads to increases in insulin sensitivity and energy expenditure (61,109). Taken together, this evidence suggests that humans indeed have functional BAT and that activating this BAT can improve metabolic health.

Beige/brite adipose tissue function and gene expression overlaps with both WAT and BAT. Beige/brite cells also express the transcription factors Prdm16, C/ebpβ, and Pgc1α (101). UCP1 is also expressed, but not nearly to the extent of BAT (60). The markers that are uniquely beige/brite include Cd137, Tbx1, Tmem26, Cited1, and Shox2 (48). The current contributions of beige/brite cells to metabolism, particularly in humans, are unclear, but current knowledge suggests that they have therapeutic potential.

The insulin/glucagon axis

Insulin is an anabolic hormone that is secreted by the β-cells of the pancreatic islet in response to postprandial blood glucose and amino acid (AA) increases (110-112). Among its primary effects is to stimulate glucose clearance from circulation. Numerous tissues contain insulin receptors, including adipose

tissue, muscle, and liver. In liver, insulin binds to insulin receptors, which recruit and phosphorylate substrate adaptors, such as the insulin receptor substrates 1 and 2 (IRS1/2) (113,114). IRS 1/2 bind Phosphoinositide 3-kinase (PI3K), which generates the lipid second messenger phosphatidylinositol-3,4,5-triphosphate (PIP_3), thereby activating 3-phosphoinositide-dependent protein kinase 1 (PDK1) and, in turn, activating isoforms of Protein Kinase B (PKB/AKT) (115,116). This node of the insulin signaling pathway is critical for metabolic responses to insulin. The PI3K/Ras-mitogen-activated protein kinase (MAPK) signaling node controls insulin-responsive differentiation and growth and will not be discussed in detail here (117). AKT is a kinase with critical downstream functions, such as preventing hepatic gluconeogenesis through FOXO1 inhibition, activating glycogen synthesis through Glycogen synthase kinase 3 (GSK3), promoting glucose uptake via Akt substrate of 160 kDa (AS160), and enhancing protein synthesis via Mammalian target of rapamycin (mTOR) (118). Additionally, Insulin induces FA and TG synthesis by activating the key lipogenic transcription factors SREBP1, USF1 and LXR (117).

Conversely, glucagon is a catabolic hormone secreted by the α-cells of the pancreatic islet in response to fasting, low blood glucose levels, and increases in circulating FAs and AAs (119). Glucagon binds to the Glucagon receptor (GCGR), a g-protein coupled receptor (120), which activates the stimulatory g protein alpha ($G_{s\alpha}$) subunit. $G_{s\alpha}$ activates AC, increasing the

generation of the second messenger cAMP and activating PKA (121). PKA stimulates both hepatic glycogenolysis and gluconeogenesis. PKA also blocks DNL by direct inhibition of ACC phosphorylation and by reduction of pyruvate levels (20). Thus, insulin and glucagon exert opposing functions to maintain euglycemia.

Lipid deposition in disease

Two organs that function as master regulators of lipid synthesis and storage are the liver and adipose tissue. In healthy animals, both liver and adipose tissue synthesize lipids to be stored in largely in white adipose tissue. In times of caloric excess, these processes become dysregulated; one hypothesis suggests that adipose tissue reaches its storage capacity and lipids are ectopically deposited in other organs such as liver, muscle, and pancreas, which may result in metabolic disease. Thus, the second part of chapter 1 will focus on the roles of liver and adipose tissue in lipid deposition in disease.

Liver Dysfunction

The liver is a master regulator of whole body glucose metabolism. It maintains blood glucose levels by alternating between catabolic and anabolic signaling pathways. Chronic exposure of humans or rodents to high calorie diets leads to obesity, which is often associated with steatosis, insulin resistance, and derangements in hepatic metabolic signaling.

Obesity/Insulin Resistance

Chronic caloric excess leads to obesity, which promotes derangements in liver metabolism, although the mechanisms for this are multifactorial, complex, and far from clear. Obesity is characterized by hyperglycemia, hyperinsulinemia, and dyslipidemia (122). Glucose, insulin, and FAs are critical for the regulation of liver metabolism. Thus, prolonged exposure of hepatocytes to these three signaling molecules has deleterious consequences.

Glucose activates hepatic DNL. As such, chronic exposure to high levels of circulating glucose strongly upregulates key lipogenic transcription factors SREBP1, ChREBP, and induces the expression of the adipogenic transcription factor, Peroxisome proliferator-activated receptor gamma (PPARγ), further promoting hepatic lipid deposition (123). Hyperglycemia, by upregulating DNL, also indirectly promotes liver vLDL release, increasing plasma TG levels (124). High glucose levels also increase hepatic TG content by decreasing mitochondrial β-oxidation (125).

Hyperinsulinemia is detrimental because when the liver is exposed to high insulin levels, insulin signaling components are downregulated, promoting hepatic insulin resistance (126). Additionally, hepatic insulin resistance promotes dysregulated hepatic gluconeogenesis as insulin no longer suppresses gluconeogenic genes, leading to uncontrolled glucose production by the liver, furthering hyperglycemia (126,127). The cause of this dysregulated hepatic

gluconeogenesis is unclear, but one hypothesis suggests that uncontrolled adipose tissue lipolysis raises hepatic acetyl-coA levels and promotes PC activation to facilitate hepatic glucose production (28). Circulating FAs, often stemming from uncontrolled adipose tissue lipolysis, can promote hepatic lipid deposition and general hepatocyte dysfunction (128). An excess of long-chain FAs can lead to formation of peroxidated lipids and reactive oxygen species (ROS) by peroxisomes in the hepatocyte (129). Fatty liver and its associated metabolic derangements often lead to T2D, although, in rare cases the two can be dissociated (130).

The spectrum of NAFLD

Hepatocytes rarely store lipids except during fasting or obesity (11). Non-alcoholic fatty liver disease (NAFLD) refers to a liver disease spectrum which begins with benign and reversible TG accumulation, often due to excess caloric intake (131). Prolonged exposure of hepatocytes to lipotoxic FAs leads to hepatocyte ballooning and death, activating KC and promoting inflammatory cascades, progressing to non-alcoholic steatohepatitis (NASH). Chronic inflammation activates HSCs, promoting fibrosis and transitioning the disease to cirrhosis. Prolonged cirrhosis can progress to hepatocellular carcinoma (132).

Adipose tissue dysfunction

Obesity

Healthy adipose tissue expansion is critical for metabolic health. One hypothesis suggests that during chronic overfeeding, adipose expands until its capacity is reached; expanded adipose tissue is characterized by increased fibrosis, and inflammation (133,134). Inflamed adipocytes secrete chemoattractant proteins, such as monocyte chemoattractant protein 1 (MCP1), which recruit macrophages to clean up dying adipocytes (122). Chronically inflamed expanded adipose tissue is also characterized by dysregulated lipid signaling. For instance, obesity results in uncontrolled adipocyte lipolysis, which causes increases in circulating FAs and ectopic TG deposition in other tissues, such as liver and muscle (135,136). Increases in serum FAs induce insulin resistance in human subjects (137). Chronic inflammation has also been correlated with insulin resistance (133,138-140). Under conditions of chronic obesity, insulin fails to stimulate glucose uptake into tissues, leading to hyperinsulinemia and high glucose in the blood, which are associated with type 2 diabetes (T2D) (122).

Lipodystrophy

Metabolic disease can occur when an excess of adipose tissue is present. Interestingly, similar metabolic derangements develop with too little adipose tissue. Lipodystrophy is a rare, often monogenic disorder, characterized by partial or generalized adipose tissue deficiency (141). Humans and mice that lack adipose tissue develop fatty liver, hyperlipidemia, and severe insulin resistance

(142). These cases emphasize the importance of proper FA storage for the maintenance of metabolic health. Furthermore, lipodystrophic humans and mice are often lacking beneficial adipokines secreted by the adipose tissue, such as adiponectin and leptin, leading to insulin resistance and hyperphagia (141).

Other Metabolic Tissues: Muscle and Pancreas

In addition to liver and adipose tissue, other tissues are critical for the maintenance of metabolic homeostasis. Skeletal muscle largely consumes postprandial glucose, provides a protein reservoir during starvation, and develops insulin resistance. The pancreas is a critical exocrine and endocrine organ that is dysregulated during obesity. The structure and function of skeletal muscle and pancreas are detailed below.

Structure and Function

Skeletal Muscle

Skeletal muscle is an organ that is critical for both locomotion and metabolism. Muscle consists of multi-nucleated, post mitotic myofibers that are synthesized from fused myocytes. Additionally, muscles contain satellite cells, which are stem cells (143). Skeletal muscle largely functions to generate force and provide structural stability. As these actions are energetically expensive, skeletal muscle consumes a substantial nutrients and is responsible for 75% of the body's glucose clearance; skeletal muscle also stores glycogen and utilizes

FAs liberated from AT (144). Like liver and adipose tissue, skeletal muscle contains insulin receptors that promote insulin-stimulated glucose uptake via the glucose transporter Glut4 (145). Additionally, as muscle fibers contain 50-75% of the body's total protein, they provide a protein reservoir during starvation (146). Muscles fibers can be divided into three classes based on their metabolism; class I is oxidative, class IIA is intermediate, and class IIx is glycolytic (146).

Pancreas

The pancreas is divided into two distinctly functioning parts: the exocrine pancreas and the endocrine pancreas. The exocrine pancreas is a part of the GI system and contains the duct cells, acinar cells, and associated connective tissue. It largely synthesizes and secretes digestive enzymes into the intestine (147). The endocrine pancreas consists of the islets of Langerhans (islets), which contain glucagon-secreting α cells (15%), insulin-secreting β cells (80%), and somatostatin-secreting δ cells (5%) (147,148). The islets comprise 1-2% of the adult pancreas in most mammals and hormones synthesized and secreted by islet cells modify whole body homeostasis (147). The roles of insulin and glucagon are detailed above. Somatostatin inhibits both glucagon and insulin release (149).

Dysfunction

Skeletal Muscle

Typically, healthy skeletal muscle contains minimal TG (.5%) stored in cellular LDs, although endurance athletes demonstrate much larger lipid stores, known as the athlete's paradox (150). However, during obesity, an excess of circulating FAs become deposited in skeletal muscle and lead to a substantial increase in TG content (3.5%) (151). Obesity promotes skeletal muscle insulin resistance and hyperlipidemia has been suggested to exacerbate this (152), although the mechanism for this is far from clear. Insulin resistance alters insulin-stimulated glucose uptake in muscle, and as muscle is such a critical organ for glucose disposal, muscle insulin resistance is considered to be a substantial contributor to T2D (153). Lipodystrophy, as it is a disease of reduced TG storage capacity, leads to similar pathologies and comorbidities in muscle as obesity (141).

Pancreas

As peripheral tissues develop obesity-related insulin resistance and the circulation becomes hyperglycemic, the pancreas increases insulin secretion, leading to hyperinsulinemia. In the short-term, elevated insulin production can lead to β-cell hypertrophy (154). Both hyperglycemia and chronic augmentation of insulin production are correlated with increased ER stress and β-cell death, which may then cause overt diabetes (155). Additionally, increases in circulating FAs can lead to ectopic lipid deposition in pancreas, further promoting pancreatic dysfunction (156).

Part 2: Lipid Droplets as Dynamic Organelles

Organs such as liver and adipose tissue are master regulators of lipid metabolism. Hepatocytes and adipocytes, as do all cells, store cytotoxic FAs as neutral lipids in organelles termed LDs. Although once considered inert lipid storage vesicles, research from the past 20 years suggests that LDs are dynamic organelles that possess a unique proteome and numerous related signaling pathways. LDs are also highly integrated into cellular metabolism and its associated signaling pathways. Furthermore, LD proteins are critical for lipid homeostasis, as humans or mice with LD protein mutations manifest severe metabolic dysfunction. The LD structure, function, and its proteome will be discussed in detail below.

Structure, Formation and Prevalence

The LD is an organelle that functions in the storage of neutral lipids. It consists of a neutral lipid core, which typically contains a mixture of TGs and cholesterol esters (CE), surrounded by a phospholipid (PL) monolayer. Numerous identified proteins, some of which are cell-type specific, are associated with or embedded in this monolayer and are called LD proteins (157). Their functions will be described in detail below. LDs are very heterogeneous organelles, differing in their size, protein coat, and also their lipid composition (158).

The exact mechanism by which LDs are formed is not known, but it is hypothesized that they form from a lipid lens in the ER bilayer (159). Numerous hypothetical LD biogenesis models have emerged from more recent experimental evidence. One hypothesis proposes a model based on the principle of oil dewetting (160). This model suggests that a lipid lens forms in the ER bilayer by the favorable reduction of the contact angle of the lipids with the bilayer surface. The LD then buds off due to thermodynamically favorable reduction of surface tension. Another hypothesis proposes a synchronized, step-wise model (161) that suggests that FA synthesis in the ER promotes TG enrichment, PL synthesis, and “globule formation”. As the “globule” transitions to a nascent LD, the ER membrane bends and proteins are recruited to promote curvature until a nascent LD is formed. Whether or not LDs permanently retain their ER connection is still unclear. Additional experiments are needed to further elucidate the true mechanism of LD biogenesis.

Numerous proteins appear to coordinate LD formation at the ER by activating FAs, synthesizing neutral lipids, or synthesizing PLs for rapidly expanding nascent droplets (161). Two additional ER-resident proteins that may play a more structural role in LD formation are Seipin and Fat storage-inducing transmembrane protein (FIT/FITM) (161). Seipin localizes to ER-LD junctions (162). Although the precise role of Seipin in this process is far from clear, Seipin-deficient cells display aberrant LD size and number (162,163), while 3T3-L1

adipocytes deficient for FIT2 display reduced LD size and number (164). Interestingly, deletion mutants of all of the currently identified proteins alluded to above suggest redundancy in the system, as no single protein is required for LD biogenesis (161).

All cells store neutral lipids in LDs, but adipose tissue is specifically adapted to store large quantities of TGs. LDs in white adipocytes can reach up to 100μM in diameter, relegating other cellular components to the periphery of the cell, and each adipocyte in WAT is typically unilocular (165). Moreover, LDs in non-adipocyte cells are multilocular, much smaller (1-10μM), and more distant from the cell surface, although they can increase in size in steatotic tissues, such as liver and muscle (166).

Function

A primary function of LDs is to store cytotoxic FAs in the form of inert TGs. While LDs in the adipocyte provide long-term TG storage, other cells, such as hepatocytes and myocytes, form LDs much more transiently to facilitate their metabolism (166). Regardless, LDs are highly responsive to lipogenic and lipolytic signaling (167), which will be discussed in detail below. LDs also appear to play a critical role in immune cell function, synthesizing inflammatory signaling lipids and facilitating antigen cross-presentation (168). Furthermore, LDs are present in cancer cells and are associated with poor prognosis in human breast, prostate, and colon cancers (169). In addition to their metabolic functions, LDs

possess critical alternative functions. For instance, they sequester excess proteins (170), such as maternal histones in Drosophila embryos (171). They are also required for the replication cycle of certain viruses, such as the Hepatitis C Virus (172). Thus, research continually proves that LDs are not inert, fat storing organelles, but dynamic, multi-functional signaling bodies.

The LD Proteome

The PAT family

The PAT family, named for its three founding members Perilipin, Adipophilin, and Tail-interacting protein of 47 kDa (Tip47), is one of the most abundant families of LD proteins. The PAT family currently contains five members numbered chronologically based on their discovery and most share a common N-terminal PAT domain of yet unknown function (173). Perilipins are present in vertebrates and insects their expression promotes lipid deposition (174). Each member possesses unique functions and tissue-specific distribution, which will be detailed below.

Perilipin 1

Perilipin 1 was first characterized as a highly phosphorylated protein in the adipocyte fat cake (lipid fraction of the adipocyte) (175). It is expressed in mature white and brown adipocytes (175-177) and to a lesser extent in steroidogenic cells (178). Alternative splicing of the Perilipin 1 transcript produces three isoforms, termed Perilipin A-C. Perilipin A is the most abundant isoform in

adipocytes and murine Perilipin A contains 517 AAs. Perilipin B is less abundant and contains 422 AA in mice, 405 of which are shared with Perilipin A (175,176). The shortest isoform, Perilipin C is solely expressed in steroidogenic cells (178,179). As Perilipin A is highly abundant and the most-characterized of the Perilipin isoforms, it will be the isoform referred to as Perilipin 1 and discussed in the remainder of this work. Its expression steadily increases with adipogenic differentiation and it promotes lipid deposition by inhibiting lipolysis (180-182). This function will be detailed below.

Perilipin 2/Adipose differentiation-related protein (ADRP)/Adipophilin (ADFP)

Perilipin 2 demonstrates the most ubiquitous expression pattern of the PAT family members. As it is unstable in the cytoplasm, it is constitutively localized to LDs (183,184). Perilipin 2 was first characterized as an mRNA with 100-fold induction upon adipogenic differentiation (185). It coats nascent LDs and is subsequently replaced by Perilipin 1 as these LDs mature (183,186). In addition to adipocytes, Perilipin 2 localizes to LDs in most other cell types (187). In the absence of Perilipin 1 or during lipolytic stimulation, Perilipin 2 coats mature LDs, but inhibits lipolysis less effectively (177,188).

Perilipin 3/Tip47

Perilipin 3 was initially identified in a yeast two hybrid screen as a mannose 6-phosphate receptor binding protein (189). Similar to Perilipin 2, it is ubiquitously expressed and localizes to LDs in most tissues. Unlike Perilipin 2,

Perilipin 3 has cytoplasmic stability (190,191). Its partial crystal structure suggests this stems from a C-terminal bundle of 4 amphipathic helices that are structurally similar to Apopliprotein E (ApoE). These helices can remain closed and soluble in solution or open and embed in PLs (192). As the two most similar PAT members, Perilipin 2 and Perilipin 3 share 43% sequence similarity (173).

Perilipin 4/S3-12

Perilipin 4, like other PAT members, was identified as a protein highly induced during adipocyte differentiation (193). It largely coats nascent LDs in white adipocytes, but is also expressed to a lesser extent in muscle and heart (186,194). At 160 kDa, Perilipin 4 is the largest of the PAT proteins and the only member that lacks the N-terminal PAT domain (191). Perilipin 4 and Perilipin 1 are least similar to other PAT family proteins (173).

Perilipin 5/PAT family member expressed in oxidative tissues (OxPAT)/Myocardial LD Protein (MLDP)/LD Storage Protein 5 (LSDP5)

Perilipin 5 is most highly expressed in oxidative tissues, such as heart and skeletal muscle, while lower levels are expressed in liver, WAT and BAT, testis, and adrenal gland (195-197). Like Perilipin 3, Perilipin 5 is stable both on LDs and in the cytoplasm (195).

The CIDE family

The cell death-inducing DNA fragmentation factor 45-like effector (CIDE) family of LD proteins shares sequence homology with the DNA fragmentation

factor 45, a factor cleaved by caspase 3 during apoptosis (198,199). There are currently three identified CIDE family proteins and all share a common CIDE domain at their N-terminus (200). Although originally thought to promote cell death (198,199,201), these proteins dually localize to LDs and the ER and promote lipid deposition with their expression (200,202). Their tissue distribution and functions will be detailed below.

Cidea

Murine Cidea is highly expressed in brown adipocytes, to a lesser extent in white adipocytes, and expressed at much lower levels in heart, brain, skeletal muscle, lymph nodes, thymus, appendix, and bone marrow (198,203). It is highly induced upon adipogenic differentiation (203) and its expression in human WAT is correlated with insulin sensitivity in obese humans (204,205). Although originally found to be localized to mitochondria (201,203), Cidea also localizes to LDs (204). In addition to its other tissue specificity, Cidea coats LDs in steatotic liver (206) and in the lactating mammary gland (207).

Cideb

Cideb is expressed in liver, kidney, and the small intestine (198). It localizes to the ER and LDs and is necessary for hepatocyte vLDL lipidation and cholesterol homeostasis (208-210). Cideb interacts with ApoB-100 to facilitate the TG-enrichment of vLDL particles (209). Cideb may also play a role in foam cell formation, as it is highly upregulated in lipid-laden macrophages (211).

Cidec/Fsp27

Fsp27 was identified as an mRNA whose expression is highly induced during adipogenic differentiation (212). It is specific to brown and white adipocytes (203,213), although its expression is massively induced in steatotic liver and lipid-filled macrophages (211,214). Similar to Cidea and Perilipin 1, its expression in WAT is also correlated with insulin sensitivity in obese humans (204). Fsp27 promotes the formation of unilocular adipocytes and Fsp27-deficient 3T3-L1 adipocytes display reduced TG content and LD number (215). Both Cidea and Fsp27 localize to LD-LD contact sites (LDCS), suggesting that they function in LD fusion (216,217). Interestingly, Fsp27 physically interacts with Perilipin 1 to promote LD fusion (218).

LD Proteins and Signaling

LD proteins are variable in their tissue-specificity and function and play integral parts in the dynamic signaling of the LD. Their diverse functions are still an active area of investigation and known functions range from inhibiting lipases to localizing LDs to microtubules. Some roles of specific LD proteins in LD signaling are detailed below.

Lipolysis

ATGL, HSL, and MGL are the three lipases that are demonstrated to be critical for TG breakdown at the adipocyte LD. Mouse knock out models

demonstrate the importance of LD proteins in regulation of lipolysis. Animals deficient in Perilipin 1 (177), Perilipin 5 (219), Cidea (203), and Fsp27 (220) all display increased lipolysis. Additionally, two LD-bound ATGL cofactors, Comparative gene identification 58 (Cgi-58)/α/β hydrolase domain-containing protein 5 (ABHD5) (an activator) (221) and G(0)/G(1) switch gene 2 (G0S2) (an inhibitor) (222) have been identified. Animals deficient in these proteins also demonstrate altered lipolysis (223-225). Although the mechanisms whereby these proteins inhibit lipolysis are often unclear, some mechanisms have been established by experimental evidence and will be detailed below.

Perilipin 1 was originally identified as a highly phosphorylated protein in the fat cake of isoproterenol (β-adrenergic agonist) -treated adipocytes (175) Rodent Perilipin A contains six PKA phosphorylation sites, which are phosphorylated during β-adrenergic stimulation (175,182,226,227). In unstimulated adipocytes, Perilipin 1 localizes to LDs and binds Cgi-58, sequestering it away from ATGL (228). Upon lipolytic stimulation, PKA phosphorylates both Perilipin 1 and HSL (229-231). HSL then translocates to the LD (232-234), where Perilipin 1 dissociates from Cgi-58 and docks and binds phosphorylated HSL to facilitate stimulated lipolysis (235-237) (Figure 4.1).

Perilipin 5 is the currently the sole PAT family member that inhibits lipolysis by directly interacting with both Cgi-58 and ATGL at the LD (238,239). This interaction is dependent upon the 64 C-terminal AAs of Perilipin 5 (238).

PKA also phosphorylates Perilipin 5 upon lipolytic stimulation, suggesting that it may function similarly to Perilipin 1, but in oxidative tissues (239). In human adipocytes, AA 120-220 of Fsp27 interact with ATGL, suggesting that Fsp27 may promote TG deposition by inhibiting lipase activity (240).

In an additional layer of lipolytic regulation, LD Proteins also function as substrates for chaperone-mediated autophagy (CMA), which is the lysosomal degradation of certain cellular protein components. CMA often takes place during nutrient deprivation. During starvation, both Perilipin 2 and 3 bind heat shock cognate protein of 70 kDa (Hsc70) and are degraded by CMA to facilitate the activation of lipolysis in mouse hepatocytes (241).

Figure 1.3 Lipolysis in the adipocyte

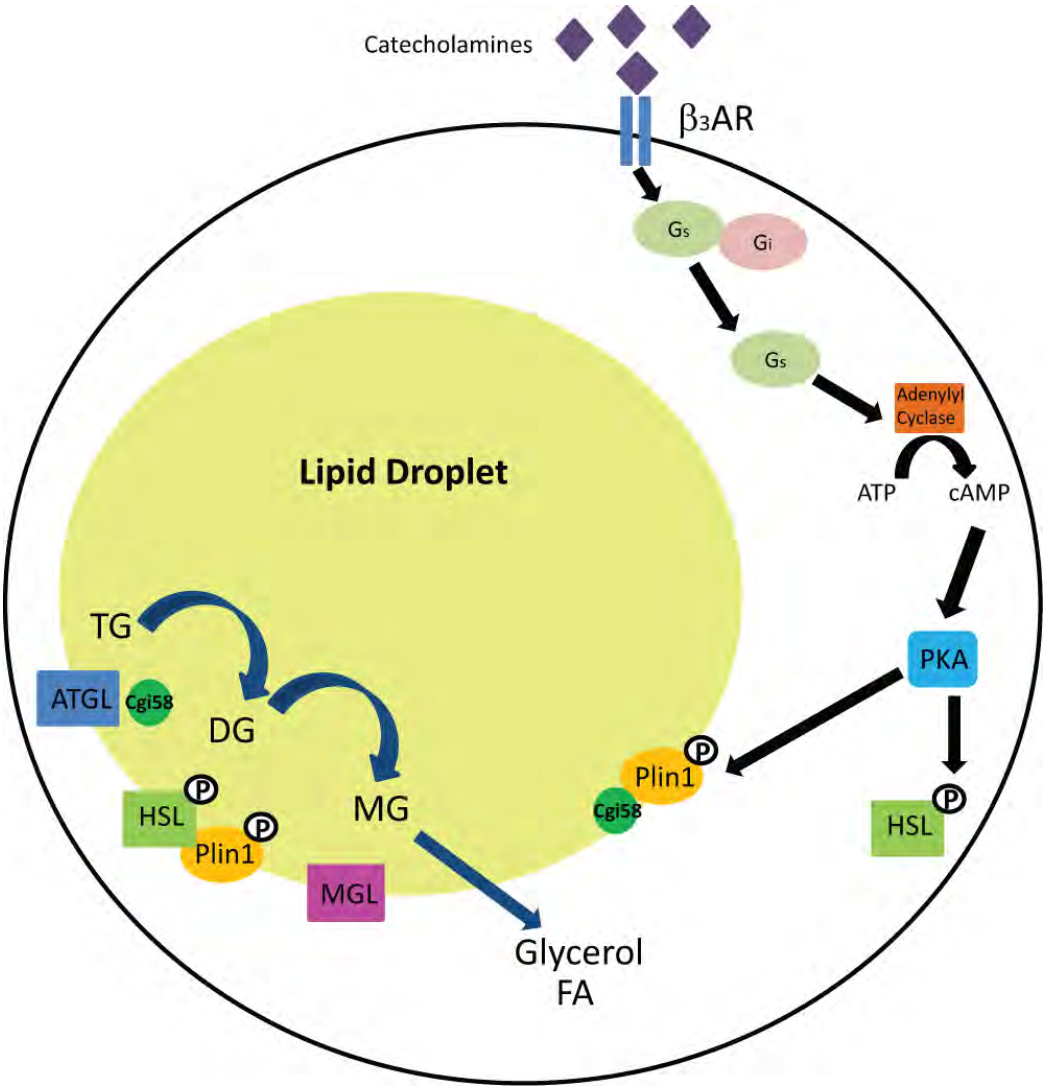

FIGURE 1.3 Lipolysis in the adipocyte. Catecholamines activate the β_3 adrenergic receptor (β_3AR), causing the stimulatory G protein (G_s) to dissociate from the inhibitory G protein (G_i). G_s activates adenylyl cyclase, which increases cAMP levels and activates protein kinase A (PKA). PKA phosphorylates Perilipin 1 (Plin1) and Hormone sensitive lipase (HSL), causing Plin1 to dissociate from Comparative gene identification 58 (Cgi58) and interact with HSL at the lipid droplet. Cgi58 binds and activates Adipose triglyceride lipase (ATGL), which breaks down triglyceride (TG) to diglyceride (DG). HSL breaks down DG to monoglyceride (MG) and Monoglyceride lipase (MGL) breaks down MG to fatty acid (FA) and glycerol.

LD Trafficking

The cellular trafficking of LDs is not well-understood, but recent data suggests that aqueous vesicle transportation machinery localizes to the LD during FA stimulation. Both Rab and SNARE proteins localize to LDs during oleate stimulation (167). Upon oleate loading in a cardiomyocyte cell line, SNARE complex proteins localized to LDs and physically interacted with Perilipin 2 (242). Additionally, microtubules are necessary for LD movement, as nocodozole treatment prevents LD fusion (243). In flies, dynein, a microtubule minus end motor, localizes to LDs and physically interacts with Perilipin 2 (243). Inhibiting dynein reduced LD formation, suggesting that it is necessary for LD formation and potentially LD fusion.

LDs and Human Disease

Insight from animal models

Animal models with PAT and CIDE protein deficiencies have been extensively characterized. These animals point toward critical functions for LD proteins in metabolic disease pathology. A brief summary of some of the published animal work is presented below and summarized in Table 1.1.

Perilipin 1

A Perilipin 1 null mouse was derived by targeted deletion of exons 4-6 (177). As Perilipin 1 is critical for LD deposition in adipocytes, Perilipin 1 null animals had greatly reduced adipose tissue weight and adipocyte size due to

increases in basal lipolysis. Interestingly, levels of stimulated lipolysis were vastly decreased in mutant adipocytes, suggesting that Perilipin 1 is required for stimulated-lipolysis. Knockouts were glucose intolerant and were resistant to diet-induced obesity, but not diet-induced glucose intolerance.

Perilipin 2

Perilipin 2 null mice were generated by two separate groups (244,245). Chang et al. generated Perilipin 2 null mice by targeted removal of exons 2 and 3, which was later shown to produce truncated, but functional Perilipin 2 in the murine mammary gland (246). To circumvent this problem, McManaman et al. generated new Perilipin 2 null mice by targeted removal of exon 5 (245). Perilipin 2 null animals from both groups demonstrated reduced hepatic steatosis. Additionally, the Perilipin 2 null mice generated by McManaman et al. (245) showed resistance to diet-induced obesity and improved glucose tolerance. Perilipin 2 null animals had reduced adipose tissue inflammation and increased Ucp1-positive beige/brite adipocytes in their iWAT. They also had increased activity and food consumption.

Perilipin 5

A Perilipin 5 null mouse was generated by targeted deletion of exons 1-4 (219). Although Perilipin 5 null animals displayed a beneficial reduction in myocardial lipids and an increase in oxidation, they also showed damaging increases in myocardial ROS. Despite this, streptozotocin-treated diabetic

Perilipin 5 null animals were protected from diabetes-induced heart malfunction (247).

Cidea

A Cidea null mouse was derived by targeted deletion of the part of the first intron and the second exon of the Cidea gene (203). Cidea null mice demonstrated reduced adipose tissue weight and increased BAT lipolysis. During cold exposure, null animals had increased metabolic rate and body temperature, which may stem from a physical interaction between Cidea and the mitochondrial uncoupler Ucp1 (203).

Cideb

A Cideb null mouse was generated by targeted removal of exons 3-5 (208). Cideb null animals were resistant to diet-induced obesity, glucose intolerance, and hepatic steatosis. They had reduced serum TGs, FFAs, concomitant with increased hepatic FA oxidation and increased serum adiponectin. Their overall metabolism was increased and lipogenic genes in the liver were decreased. Interestingly, Cideb mice had increased liver TGs in the chow-fed condition due to reduced hepatic secretion of vLDL particles (209). vLDL particles secreted by the livers of the Cideb null mice had normal levels of ApoB-100, but reduced TG levels, suggesting that Cideb is necessary for vLDL particle lipidation (209).

Cidec/Fsp27

Groups have generated global and tissue-specific Fsp27 null animals. Global Fsp27 null animals were created by targeted deletion of exons 1 and 2 (220). Fsp27 null animals demonstrated a very significant reduction in WAT weight. Adipocytes from these animals had multilocular LDs and had increased basal and stimulated lipolysis. Fsp27 null animals were resistant to diet-induced obesity and demonstrated improved glucose tolerance at 23°C. When Zhou et al. housed Fsp27 null animals at 30°C to remove thermogenic stress, they more closely phenocopied lipodystrophic humans and had both reduced weight gain, increased hepatic TG, and reduced glucose and insulin tolerance (248).

Animals with an adipose tissue-specific Fsp27 deficiency (Fsp27AtKO) were generated using Cre/loxP technology. Fsp27 fl/fl mice were crossed to an adipose tissue-specific AP2-cre (249). Similar to Fsp27 null animals, Fsp27AtKO animals also had reduced adipose tissue weight and multilocular adipocytes, with concomitant increases adipocyte lipolysis and hepatic steatosis. These animals were more glucose intolerant compared with controls in high fat-fed conditions. Additionally, liver-specific knockdown of Fsp27 in db/db mice reduced liver TGs, further cementing the idea that Fsp27 expression promotes lipid deposition (214).

Table 1.1 LD proteins of the PAT and CIDE families. Tissue specificity and some knock out animal models of the PAT and CIDE family LD proteins are briefly described below. Tissues listed in **bold text** are those with highest gene expression. Abbreviations: N/A, not applicable; BAT, brown adipose tissue; WAT, white adipose tissue; ROS, reactive oxygen species; ↑, increased; ↓, decreased. Numbers correspond to primary references of the animal model work.

Table 1.1 LD proteins of the PAT and CIDE families

Protein	Tissue Specificity	Mouse Model	Phenotype
Perilipin 1	**WAT**, **BAT**, steroidogenic tissues	Perilipin 1 Null (177,250)	↓AT weight ↓stimulated lipolysis ↓glucose tolerance
Perilipin 2	ubiquitous	A Perilipin 2 Null B Perilipin 2 Null A. (244) B.(245)	A ↓steatosis B ↓steatosis, ↓obesity ↑glucose tolerance
Perilipin 3	ubiquitous	N/A	N/A
Perilipin 4	**WAT**, **BAT**, muscle, heart	N/A	N/A
Perilipin 5	**muscle, heart,** liver, WAT, BAT, testis, adrenal gland	Perilipin 5 Null (219)	↓myocardial lipids ↑oxidation, ↑ROS ↓heart malfunction
Cidea	**BAT**, **steatotic liver**, WAT, heart, brain, skeletal muscle, lymph nodes, thymus, appendix, bone marrow	Cidea Null (203)	↓AT weight ↑BAT lipolysis
Cideb	liver, kidney, small intestine	Cideb Null (208)	↓steatosis, ↓obesity ↑glucose tolerance ↓vLDL secretion
Cidec/Fsp27	BAT, WAT, steatotic liver, foam cells	A Fsp27 Null (220)	A ↓obesity, ↑lipolysis ↑multilocular WAT ↑glucose tolerance RT
		B Adipose-Specific Fsp27 Deletion (249)	B ↑steatosis, ↓obesity ↑multilocular WAT ↓glucose tolerance

Human Mutations

Rare human mutations in LD proteins are associated with metabolic disease, thus promoting the idea that LD protein dysfunction can underlie metabolic disease pathology (142). Some of these mutations are detailed below and can be separated into a few different classes: 1) neutral lipid storage disease (NLSD), which results in lipid storage in locations other than adipose tissue, 2) familial partial lipodystrophy (FPL), which is a rare, inherited partial loss or redistribution of adipose tissue, or 3) congenital generalized lipodystrophy (CGL), which is a rare, inherited full loss of adipose tissue (142).

Perilipin 1

Perilipin 1 is the prominent LD protein in mature white adipocytes and functions to prevent unstimulated lipolysis and facilitate stimulated lipolysis (175,177,181). Thus, humans with reduced Perilipin 1 function manifested lipodystrophy, fatty liver, and metabolic syndrome. Two heterozygous frameshift mutations in the C-terminus of Perilipin 1 were identified in three separate families. These mutations resulted in autosomal dominant FPL, dyslipidemia, and diabetes, most likely due to Perilipin 1 haploinsufficiency (251). In all cases, mutated Perilipin 1 failed to sequester to Cgi-58/ABHD5, resulting in constitutively active ATGL and uncontrolled lipolysis (251).

Cidec

Cidec promotes unilocular LD formation and inhibit lipolysis in adipocytes. A patient with a homozygous nonsense mutation in Cidec has been metabolically characterized. This mutation resulted in a truncation of the C-terminus of Cidec and FPL with insulin-resistant diabetes (252). Strikingly, white adipocytes from the patient were characterized by small, multilocular LDs, much like adipocytes from Fsp27-deficient animals, and the mutated Cidec failed to localize to LDs (220,252).

Cgi-58/ABHD5 and ATGL

Cgi-58 is a LD-localized co-activator protein of the major TG-specific lipase ATGL (221). Mutations in Cgi-58 have been characterized and result in Chanarin-Dorfman Syndrome (CDS), an autosomal recessive NLSD characterized by TG deposition in non-adipose tissue and ichthyosis (253). Eight different mutations in Cgi-58 were characterized from nine different families with CDS (254). Mutated Cgi-58 was variable and contained insertions, deletions, splice and point mutations. Some mutants failed to localized to LDs and interact with Perilipin 1 (255), while other mutants were unable to activate ATGL (221).

Eight ATGL gene mutations have also been reported and they all resulted in premature stop codons (253). Patients with these mutations manifested NSLD with severe myopathy (NSLDM) and, although they did not have ichthyosis, they presented with muscle weakness and cardiomyopathy (95-97,256,257). Most

ATGL mutants were truncated in the C-terminal patatin domain and many failed to localize to LDs or were enzymatically inactive (95,98).

HSL

A mutation in the DG-specific lipase HSL also caused a milder form of NLSD characterized by fatty liver, dyslipidemia, and insulin-resistant diabetes (258). This was a frameshift mutation that added 86 AA to the C-terminus of the HSL, reducing its abundance and decreasing its lipase activity.

Seipin

Seipin has been suggested to function in LD biogenesis at the ER and Seipin mutations cause the autosomal recessive CGL Berardinelli-Seip congenital lipodystrophy type 2 (BSCL2) (259). This syndrome is characterized by an absence of adipose tissue, hypertriglyceridemia, hepatic steatosis, cardiomyopathy, T2D, and often intellectual impairment (260). Most characterized mutations resulted in severely truncated and non-functional Seipin protein (259,261). Further mutational analysis demonstrated that these mutants were mislocalized and mutant cells displayed reduced adipogenic and lipogenic gene expression, although the exact mechanism whereby Seipin mutation causes BSCL2 is still unknown (262).

Research has clarified the roles of certain members of the LD proteome in the pathology of human disease. Nonetheless, as the LD proteome is highly diverse, further characterization is necessary to pinpoint additional proteins that

are critical for proper lipid sequestration in humans. Thus, I strove to uncover additional uncharacterized candidate LD proteins in the literature. Hypoxia-inducible gene 2 (Hig2)/Hypoxia-inducible lipid droplet-associated protein (Hilpda) presented a promising target.

Hypoxia-inducible Gene 2

Overview

Hypoxia-Inducible Gene 2 (Hig2/Hilpda) is a little-studied 7kDa, 63 AA protein. It is a direct target of Hypoxia-Inducible Factor 1 alpha (Hif1α), but not Hif2α (263). Hig2 is induced in hypoxic and glucose-deprived conditions (264). As such, its expression is upregulated in cancers with dysregulated hypoxia signaling, such as renal clear cell carcinoma (RCC), and it was posed as a potential RCC biomarker (265). Early studies suggested that the protein was both secreted and activated by Wnt signaling (266), but these claims were later refuted (263).

In addition to its potential role in cancer, Hig2 may also play a role in lipid metabolism and LD dynamics. Ectopically expressed Hig2 localized to LDs in cancer cell lines and promoted LD deposition *in vitro* (263). It also localized to LDs in human liver histology sections (263). Work published while this thesis was in progress demonstrated that Hig2 is also a target of Pparα (267), similar to the LD proteins Perilipin 5, Cidea and Fsp27 (195-197,268,269). Additionally, microarray experiments from forskolin-treated primary mouse visceral adipocytes

demonstrate that its expression is highly induced upon lipolytic stimulation (270). Thus, we strove to explore the role of Hig2 as a potential LD protein in two metabolically critical tissues, liver and adipose tissue.

Project Goals

Proper adipose tissue lipid sequestration is critical for the prevention of lipotoxicity, dyslipidemia, and ectopic lipid deposition. Thus, our lab is particularly interested in novel regulators of lipid storage in adipocytes. Furthermore, elucidating hepatocyte-specific mechanisms that promote liver steatosis could provide therapeutic targets to prevent the initial and reversible stage of NAFLD. Therefore, experiments in this thesis are aimed at **dissecting the role of Hig2 in lipid deposition in liver and adipose tissue, determining the downstream signaling pathways by which Hig2 alters lipid deposition, and defining how the actions of Hig2 in these signaling pathways affect whole body metabolism.**

Two main questions are addressed in this thesis:

1) What is the role of Hig2 in lipid deposition hepatocytes and adipocytes? Does it function as a canonical LD protein and promote TG deposition by inhibition of lipolysis?
2) What is the contribution of hepatocyte and adipocyte-specific Hig2 to whole body metabolism? Does the expression of Hig2 promote tissue-specific lipid sequestration?

To answer these questions, experiments in this thesis use both *in vitro* and *in vivo* methods to elucidate the role of Hig2. In primary hepatocytes, I found that ectopically expressed Hig2 localized to LDs and promoted TG deposition and LD formation. Conversely, I found that Hig2-deficient hepatocytes had reduced TG content, LD size, and LD number. Animals with a hepatocyte-specific Hig2 deficiency demonstrated improved glucose tolerance and reduced liver weight and TG content in the chow-fed condition (Chapter 2). Although expression of many genes involved in lipid regulation was unchanged in Hig2-deficient hepatocytes, lipid flux was significantly altered. I found that Hig2-deficient hepatocytes had increased β-oxidation, lipolysis, and TG turnover (Chapter 2). As LD proteins in adipose tissue are critical for proper lipid storage and Hig2 is ubiquitously expressed, I sought to investigate the role of Hig2 in adipocytes. I found that Hig2 expression significantly increased with adipogenic differentiation in a human adipocyte cell line and was highly expressed in adipocytes in human tissue. Additionally, I found that Hig2 localized to LDs in human and mouse adipocyte cell lines (Chapter 3). Mice with an adipocyte-specific Hig2 deletion had reduced adipose tissue weight and improved glucose tolerance, but unchanged lipolysis measurements, excepting increased HSL phosphorylation. I found that these differences in fat pad weight, glucose tolerance, and HSL phosphorylation were all abrogated at thermoneutrality, a housing condition which poses no thermal stress. As thermoneutrality reduces catecholamine

levels and thus deactivates BAT, I hypothesized that BAT was the tissue responsible for the beneficial phenotypes in the adipocyte-specific Hig2 animals. Accordingly, animals with a brown adipocyte-specific deletion of Hig2 demonstrated improved glucose tolerance, suggesting that brown adipocytes do largely mediate the beneficial metabolic effects in adipocyte-deficient Hig2 animals (Chapter 3). Therefore, Hig2 acts as a LD protein in both hepatocytes and adipocytes and promotes lipid deposition and glucose intolerance. Thus, Hig2 presents a promising target for the treatment of NAFLD and T2D.

CHAPTER II: The Lipid Droplet Protein Hypoxia-inducible Gene 2 Promotes Hepatic Triglyceride Deposition by Inhibiting Lipolysis

This chapter is derived from the article with the same name published in the Journal of Biological Chemistry:

DiStefano, M. T., Danai, L. V., Roth Flach, R. J., Chawla, A., Pedersen, D. J., Guilherme, A., and Czech, M. P. (2015) J Biol Chem 290, 15175-15184.

Author Contributions

- **Figure 2.1B Cloning of GFP tagged constructs.** The synthesis and cloning of the GFP control, GFP-Hig2, and Truncated Hig2-GFP plasmids were performed by Anil Chawla, Czech Lab.
- **Figure 2.1C, D Animal handling and dissection.** The wild type animals were maintained on a high fat diet and dissected by Adilson Guilherme and David J. Pederson, Czech Lab.
- **Figure 2.2A, B Cloning of HA tagged constructs.** The synthesis and cloning of the HA control and Hig2-HA plasmids were performed by Anil Chawla, Czech Lab.
- The rest of the experiments in the chapter were performed by Marina T. DiStefano.
- The manuscript was written by Marina T. DiStefano with helpful suggestions by Joseph V. Virbasius, Rachel J. Roth Flach, and Michael P. Czech.

Summary:

The liver is a major site of glucose, fatty acid (FA), and triglyceride (TG) synthesis and serves as a major regulator of whole body nutrient homeostasis. Chronic exposure of humans or rodents to high-calorie diets promotes non-alcoholic fatty liver disease (NAFLD), characterized by neutral lipid accumulation in lipid droplets (LD) of hepatocytes. In this chapter, it is shown that the LD protein Hypoxia-inducible gene 2 (Hig2/Hilpda) functions to enhance lipid accumulation in hepatocytes by attenuating TG hydrolysis. Hig2 expression increased in livers of mice on a high fat diet (HFD) and during fasting, two states associated with enhanced hepatic TG content. Hig2 expressed in primary mouse hepatocytes localized to LDs and promoted LD TG deposition in the presence of oleate. Conversely, tamoxifen-inducible Hig2 deletion reduced both TG content and LD size in primary hepatocytes from mice harboring floxed alleles of Hig2 and a cre/ERT2 transgene controlled by the ubiquitin C promoter. Hepatic TG was also decreased by liver-specific deletion of Hig2 in mice with floxed Hig2 alleles expressing cre controlled by the albumin promoter. Importantly, this chapter demonstrates that Hig2-deficient hepatocytes exhibit increased TG lipolysis, TG turnover, and fatty acid oxidation compared with controls. Interestingly, mice with liver-specific Hig2 deletion also display improved glucose tolerance. Taken together, these data indicate that Hig2 plays a major role in

promoting lipid sequestration within LDs in mouse hepatocytes through a mechanism that impairs TG degradation.

Introduction:

The liver is a major site of glucose, TG, and FA synthesis and serves as a master regulator of whole body nutrient homeostasis (271). Chronic exposure of humans or rodents to high-calorie diets can lead to a disease spectrum known as NAFLD (272). This syndrome begins with simple neutral lipid accumulation in liver, progresses to liver inflammation, and can culminate in irreversible cirrhosis and hepatocellular carcinoma (273). Overabundance of liver lipids has also been associated with insulin resistance both in humans and rodents (274), although these conditions can also appear independently (130). Thus, understanding the molecular pathways that contribute to hepatic lipid accumulation is important in addressing therapeutic strategies for NAFLD and in understanding how it relates to metabolic disease.

In all cells including hepatocytes, neutral lipids are stored in organelles termed LDs (275). These LDs are highly dynamic and are regulated by the nutritional status of the organism (173). Two main families of LD-associated proteins are the PAT family (173), named for its three founding members Perilipin, Adipophilin, and Tip47 that have PAT domains, and the CIDE family (200). The PAT family has five members (Perilipin 1-5), while the CIDE family has three members (Cidea, Cideb, and Cidec/Fsp27). LDs are heterogeneous in

their coats and LD proteins generally demonstrate tissue-specific distribution patterns (276). In healthy murine liver, Perilipin 2 and Perilipin 3 promote LD formation (277), while Cideb promotes VLDL lipidation (209). Although deletion of Perilipin 3 has not yet been performed, genetic deletion of Perilipin 2 or Cideb ameliorates hepatic steatosis (208,245). However, in the context of diet-induced obesity and fatty liver, Fsp27 (Cidec in humans) and Cidea are critical for LD formation (200). Both are highly upregulated in murine liver upon diet-induced obesity and genetic deletion of either results in clearance of obesity-associated hepatic steatosis (200,206,214). Fsp27 is also relevant to human disease, as a patient with a homozygous nonsense mutation in CIDEC displays partial lipodystrophy, fatty liver, and metabolic syndrome (248,252). As the LD proteome may be quite extensive (278), identifying additional members will shed new light on the mechanisms for TG deposition and potentially the basis of human disease.

Hig2 was initially identified in a screen for genes induced by oxygen deprivation in human cervical cancer cells and encodes a 7 kDa protein with little apparent homology to known proteins (264). Its expression is also increased in many cancers, particularly RCC and it is a target gene of both Hif1α and PPARα (263-265,267,279). Gimm et al. demonstrated that Hig2 localized to LDs and promoted TG deposition in cancer cells *in vitro* (263). These authors also showed that Hig2 co-localized with Perilipins 2 and 3, two LD proteins that are essential

for neutral lipid deposition in healthy liver. Due to the importance of hepatic lipid homeostasis and deposition, the role of Hig2 in these processes was examined.

In this chapter, it is demonstrated that Hig2 localizes to LDs in primary mouse hepatocytes. Importantly, its deletion in hepatocytes *in vivo* causes depletion of hepatic TG, indicating that it plays a physiological role in regulating liver lipid abundance in mice. Furthermore, it is shown that the basis for its ability to promote LD formation and TG deposition in liver is through the inhibition of TG lipolysis.

Materials and Methods:

Animal Studies: All of the studies performed were approved by the Institutional Animal Care and Use Committee (IACUC) of the University of Massachusetts Medical School. Animals were maintained in a 12 hour light/dark cycle. Hig2$^{fl/fl}$ animals were purchased from Jackson Laboratories (Hilpdatm1.1Nat/J). For metabolic studies, the animals were backcrossed onto C57Bl/6J animals for at least 6 generations. Genomic DNA was extracted from the obtained mice and subjected to PCR for genotyping using Qiagen Fast Cycling PCR Kit (Hig2$^{fl/fl}$ primer 5'-CCGGCAGGGCCTCCTCTTGCTCCTG-3', 5' GTGTGTTGGCTAGCTGACCCCTCGTG-3'). Hig2$^{fl/fl}$ animals were crossed to a tamoxifen-inducible ubiquitous cre mouse line (B6.Cg-Tg(UBC-cre/ERT2)1Ejb/J, Jackson Laboratories). Hig2fl/fl animals were also crossed to an albumin cre

mouse line (C57BL/6-Tg(Alb-cre)21Mgn/J, Jackson). Cre genotyping was performed according to the method of Jackson Laboratories.

At 5-6 weeks of age, male C57Bl/6J, $Hig2^{fl/fl}$, or $Hig2^{fl/fl}$ albumin cre+ littermates animals were placed on a high fat diet (60% fat, D12492i Research Diets) or fed chow (Lab Diet 5P76) for 12 or 16 weeks.

Mice were fasted 16 hours for glucose tolerance tests and 4 hours for insulin tolerance tests. Mice were injected IP with 1g/kg of glucose or 1IU/kg of insulin, blood was drawn from the tail vein at the indicated times, and blood glucose levels were measured with a Breeze-2-glucose meter (Bayer). Mice were euthanized by CO_2 inhalation followed by bilateral thoracotomy.

Plasma and lipid analysis: Mice were fasted for 3 hours for plasma lipid analysis. Blood was taken via cardiac puncture, and EDTA-containing plasma was collected. Total serum cholesterol levels (ab65359, Abcam), serum triglyceride levels (Triglyceride Determination Kit, Sigma), serum NEFAs (Wako Diagnostics), and β-hydroxybutyrate (Sigma) were measured using calorimetric assays according to the manufacturer's instructions. Insulin levels were measured with an Insulin ELISA Kit (Millipore) according to the manufacturer's instructions.

Triglyceride and Cholesterol Extraction: Whole livers were isolated and flash frozen in liquid nitrogen. Lipids were extracted from livers or pelleted hepatocytes via the Folch method (280). Lipids were dissolved in isopropanol with 1% Triton-X100. Triglyceride (Triglyceride Determination Kit, Sigma) and cholesteryl ester (ab65359, Abcam) levels were measured using calorimetric assays according to the manufacturer's instructions and normalized to liver weight or hepatocyte protein content.

Hepatocyte isolation: Male or female 8-10 week old chow-fed animals were anesthetized with an IP injection of 1:1 ketamine:xylazine and perfused with HBSS supplemented with 0.5M EGTA. Livers were digested with a perfusion of 50mg/ml collagenase (Sigma, C6885) in HBSS supplemented with 1mM $CaCl_2$, physically dissociated, and filtered through a 100μm filter. Hepatocytes were washed, centrifuged at low speed, filtered through a 70μm filter, and plated at a density of 1 million cells/ml.

RNA Isolation and RT-qPCR: Total RNA was isolated from cells or tissues using TriPure isolation reagent (Roche) according to the manufacturer's protocol. The isolated RNA was DNase treated (DNA-free, Life Technologies), and cDNA was synthesized using iScript cDNA synthesis kit (BioRad). RT-qPCR was performed on the BioRad CFX96 using iQ SybrGreen supermix, and 36B4

served as the reference gene. Primer sequences are as follows: 36B4 (5'-TCCAGGCTTTGGGCATCA-3', 5'-CTTTATCAGCTGCACATCACTCAGA-3'); Hig2 (5'-CATGTTGACCCTGCTTTCCAT-3', 5'- GCTCTCCAGTAAGCCTCCCA-3'); Tnfα (5'-CCCTCACACTCAGATCATCTTCT-3', 5'-GCTACGACGTGGGCTACAG-3'); IL6 (5'-TAGTCCTTCCTACCCCAATTTCC-3', 5'-TTGGTCCTTAGCCACTCCTTC-3'); IL1β (5'-GCAACTGTTCCTGAACTCAACT-3', 5'-ATCTTTTGGGGTCCGTCAACT-3'); F4/80 (5'-CCCCAGTGTCCTTACAGAGTG-3', 5'-GTGCCCAGAGTGGATGTCT-3'); CD36 (5'-GAACCACTGCTTTCAAAAACTGG-3', 5'-TGCTGTTCTTTGCCACGTCA-3'); Cpt1a (5'-GCTGCTTCCCCTCACAAGTTCC-3', 5'-GCTTTGGCTGCCTGTGTCAGTATGC-3'); Mttfa (5'-AGTTCCCACGCTGGTAGTGT-3', 5'-GCGCACATCTCGACCC-3'); Pparγ (5'-GACTACCCTTTACTGAAATTACC-3', 5'-GTGGTCTTCCATCACGGAGA-3'); Srebp1c (5'-GGAGCCATGGATTGCACA-3', 5'-GGCCCGGGAAGTCACTGT-3'); Srebp2 (5'-GCAGCAACGGGACCATTCT-3', 5'-CCCCATGACTAAGTCCTTCAACT-3'); ApoB (5'-TGGCTCTGATCCCAAATCCCT-3', 5'-CCGTGCATTCATTGTCGATCTG-3'); Atgl (5'-CAGCACATTTATCCCGGTGTAC-3', 5'-AAATGCCGCCATCCACATAG-3'); Perilipin 2 (5'-GACCTTGTGTCCTCCGCTTAT-3', 5'-CAACCGCAATTTGTGGCTC-3'); Cidea (5'-TGACATTCATGGGATTGCAGAC-3'

5’-GGCCAGTTGTGATGACTAAGAC-3’); Fsp27 (5’-ATCAGAACAGCGCAAGAAGA-3’, 5’-CAGCTTGTACAGGTCGAAGG-3’)

Immunoblotting: Tissues and cells were lysed in a high-salt, high-SDS buffer (2% SDS, 150mM NaCl, 2mM EDTA) with 1x Halt protease and phosphatase inhibitors (Thermo Scientific). Lysates were resolved by 15% SDS-PAGE gel run in a 1x Tris-Tricine Buffer (National Diagnostics) and transferred to nitrocellulose membranes. Membranes were blotted with the following antibodies: β-Actin (A2228, Sigma), HA-Tag (2367, Cell Signaling Technology). The Hig2 antibody was directed against a 15 amino acid peptide (PPKGLPDHPSRGVGV) at the C terminus of murine Hig2 (Rockland Immunochemicals).

Cell Culture: Hepatocytes were isolated from male or female 8-10 week old $Hig2^{fl/fl}$ Ubc ERT2 Cre+ animals, plated in M199 adherence media (Life Technologies, 11150, supplemented with 2% FBS, 10% BSA, 1%Pen/Strep, 100nM Insulin, and 100nM Dexamethasone) for 3 hours, changed to M199 maintenance media (M199 supplemented with 1% Pen/Strep, 100nM Insulin, and 100nM Dexamethasone) and treated with ethanol vehicle or 2.5μM (Z)4-Hydroxytamoxifen (Sigma H7904) dissolved in filtered ethanol (5mg/ml) for 48 hours before experiments.

For imaging experiments, hepatocytes were plated on collagen-coated Millicell 4 chambered slides (Millipore) and transfected with GFP control, GFP-Hig2, or GFP-Hig2 truncated (missing residues 1-28) constructs using 1.5μg DNA, Optimem and Lipofectamine 2000 (Life Technologies) according to manufacturer's instructions 48 hours prior to experiments. GFP constructs were made using two unique restriction sites Not1 and BamH1 in a pShuttle plasmid (Clontech, Mountain View, CA). cDNA of full-length Hig2 or the PCR product of truncated Hig2 was inserted in frame at these two restriction sites. Hepatocytes were also infected with HA-tagged adenoviruses 48 hours prior to experiments. Adenoviruses were made as follows: The cDNA of the transgene of interest was first cloned into a pShuttle plasmid (Clontech, Mountain View, CA) and then subcloned into a molecular clone of E1-and E3-deleted human adenovirus serotype 5. This adenovirus plasmid backbone was modified from pAdX system (Clontech, Mountain View, CA) by introducing a green-white selection mechanism (281). The recombinant clones of adenovirus vector with the transgene of interest were selected through this green-white screening, confirmed by restriction enzyme analyses and rescued in 293 cells after restriction enzyme linearization and transfection. The recombinant virus is expanded and purified by standard CsCl gradient sedimentation followed by dialysis for desalting (282). The HA control construct was made by inserting 3HA at Not1 and BamH1 sites of the 4124 base pair plasmid pShuttle Adeno vector.

3HA Hig2 adenovirus plasmid DNA was made by inserting a full-length gene of Hig2 at restriction sites Blp1 (5') and BamH1 (3') of 3HA adeno viral plasmid DNA. Cells were loaded with the indicated concentration of oleic acid (Sigma) dissolved in ethanol and conjugated to 10% fatty acid-free BSA dissolved in 0.1M Tris pH 8. For radiation experiments, hepatocytes were plated on collagen-coated plates in William's E Medium Adherence Media (Life Technologies 12551, supplemented with 2% Fetal Bovine Serum, 10% BSA (Sigma A4503), 1% Pen/Strep, 100nM Insulin, and 100nM Dexamethasone). After three hours, media was changed to maintenance media (William's E Medium supplemented with 1% Pen/Strep, 100nM Insulin, and 100nM Dexamethasone).

Cell Imaging: Cells were fixed in 10% buffered formalin in PBS for 15 minutes, stained with Oil-Red-O, and mounted with Prolong Gold with DAPI (Life Technologies). Cells were imaged at room temperature with a Solamere Technology Group modified Yokogawa CSU10 Spinning Disk Confocal with a Nikon TE-2000E2 inverted microscope at 20x, 60x, and 100x. Images were acquired with MetaMorph Software, version 6.1 (Universal Imaging, Downington PA).

Lipid droplet analysis was performed on fixed, Oil-Red-O- and DAPI- stained cells with BioPix iQ Imaging Software (BioPix AB, Sweden). At least 90 cells were analyzed per condition.

Oleate Tracer Studies: Hepatocytes were isolated from male 8-10 week old $Hig2^{fl/fl}$ or $Hig2^{fl/fl}$ albumin cre+ animals. 24 hours after isolation, cells were loaded with 1μCi/ml [^{3}H] oleic acid mixed with 100μM oleic acid conjugated to 0.5% fatty acid-free BSA in William's E Medium. Assays were performed as previously described (214,283).

Oleate Uptake: Cells were loaded with 100μM [^{3}H] oleic acid overnight. The following day, media was removed, cells were washed, and lysed in 0.5ml of lysis buffer (1% Triton-X100 in PBS), and lysates were placed in vials with scintillation fluid and counted using a Beckman LS 6500 scintillation counter. Counts were normalized to length of incubation time and protein content.

Total β-Oxidation: Cells were loaded with 100μM [^{3}H] oleic acid overnight. The following day, media was collected, precipitated twice with perchloric acid and BSA, spun to pellet insoluble products, and the soluble fraction was removed, placed in vials with scintillation fluid, and counted. Counts were normalized to length of incubation time and protein content. Empty media was loaded with [^{3}H] oleic acid, precipitated, counted, and subtracted as a background reading.

Triglyceride Turnover: Cells were loaded with 100μM [^{3}H] Oleic Acid overnight. The following day, cells were washed 2x, and media was replaced with William's E Media with 0.6mM Triacsin C (Sigma). Cells were collected at indicated times, washed, and lysed in 0.5ml lysis buffer (1% Triton-X100 in PBS), placed in vials

with scintillation fluid, and counted. Counts are normalized to protein content and graphed as a percentage of time 0.

Lipolysis: Cells were loaded with 100μM [^{3}H] oleic acid overnight. The following day, cells were washed 2x and media was replaced with William's E Media with 0.6 mM Triacsin C (Sigma) and 100μM Etomoxir (Sigma). Media was collected at the indicated times, placed in vials with scintillation fluid, and counted. Counts are normalized to protein content.

Statistical Analysis: Data were analyzed in GraphPad Prism 6 (GraphPad Software, Inc.). A two-tailed student's t test with Welch's Correction was used to compare two groups of data. Where indicated, data were analyzed using a two-way ANOVA with repeated measures or a linear regression model. $P<.05$ was considered to be significant. The Grubb's test was used to determine if there were statistical outliers and if an outlier was determined, it was removed from the statistical analysis. Variance was estimated using standard error of the mean.

Results:

Hig2 is localized to LDs and its expression is modified by nutritional status.

To characterize Hig2 as a potential hepatic LD protein, its localization was first determined in primary mouse hepatocytes. Primary hepatocytes were isolated from C57Bl/6J animals and transfected with either GFP control or GFP-

tagged Hig2 constructs and incubated with oleic acid to induce LD formation. While the GFP control construct displayed a diffuse, cytoplasmic distribution in the cells, GFP-Hig2 clearly localized around the perimeter of Oil-Red-O positive LDs (Figure 2.1B). Gimm et al. used deletion analysis to determine that the 37 N-terminal amino acids of Hig2 are required for LD targeting in cancer cell lines (263), which was termed here as the “Putative Lipid Droplet Binding Domain” (Figure 2.1A). To confirm that this was also the targeting domain in hepatocytes, a Hig2 truncation mutant with a loss of amino acids 1-28 of this putative binding domain was created. When the Hig2 truncation mutant was transfected into primary hepatocytes, it also localized diffusely, similar to the GFP control, demonstrating that Hig2 localizes to LDs in hepatocytes through this putative LD binding domain (Figure 2.1B). As Gimm et al. determined by sequence analysis that an amphipathic helix is located in this domain (263), it is possible that Hig2 may interact with the lipid droplet directly via surface interaction (160).

Hepatic LD protein expression is highly sensitive to nutritional status. As both Fsp27 and Cidea, two bona fide liver LD proteins, are highly upregulated upon high fat diet (HFD) feeding in mice (200), Hig2 expression was measured in two situations of hepatic steatosis. Fasting, which liberates lipids from adipose tissue via lipolysis, causes a temporary increase in liver lipids (128). Indeed, a 24-hour fast caused a 2-fold increase in Hig2 mRNA expression in C57Bl/6J mouse livers (Figure 2.1C). Obesity-induced hepatic steatosis in C57Bl/6J mice

also caused a significant 2.7-fold increase in Hig2 mRNA expression in liver (Figure 2.1D), consistent with the concept that Hig2 expression is highly correlated with liver lipid levels.

Figure 2.1 Hig2 is localized to LDs and its expression is modified by nutritional status.

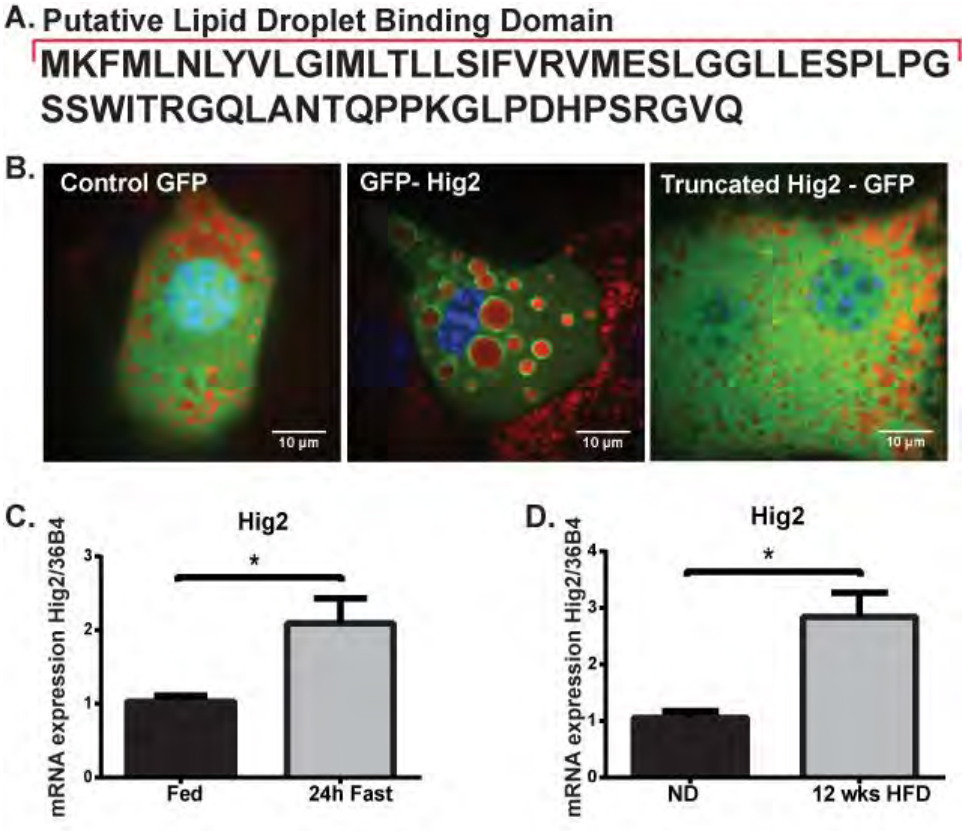

FIGURE 2.1 Hig2 is localized to LDs and its expression is modified by nutritional status. A, amino acid sequence of murine Hig2 with putative lipid droplet binding domain residues 1-37 indicated. B, hepatocytes were transfected with GFP-tagged constructs (*green*), loaded with 500μM oleic acid for 4 h, fixed, and stained with Oil Red O (*red*) and DAPI (*blue*). Truncated Hig2-GFP is missing residues 1-28. C and D, whole livers were isolated from C57Bl/6J animals, RNA was extracted, and qRT-PCR was performed for Hig2 and normalized to 36B4. C, animals were fasted for 24 h or fed. Data are represented as the mean ± S.E. (*, $p<0.05$, n=6). D, animals were fed ND or HFD for 12 weeks. (*, $p<0.05$, n=5-6). Data are represented as the mean ± S.E.

Ectopic expression of Hig2 promotes hepatocyte lipid deposition.

LD protein overexpression can also promote lipid deposition (173). For example, experimentally enhancing Fsp27 expression promotes TG accumulation in a variety of cell types, while Fsp27 deficiency reduces LD formation (215,220). Thus, it was tested whether Hig2 expression modifies TG accumulation in liver by manipulating Hig2 expression in primary mouse hepatocytes. First, primary hepatocytes were isolated from $Hig2^{fl/fl}$ animals and infected with either control adenovirus (AV) or an AV expressing HA-tagged Hig2. As expected, Hig2-HA AV- infected cells demonstrated increased Hig2-HA levels compared with controls as determined by Western blot (Figure 2.2B). The cells were incubated with 250μM oleic acid for 24 hours to induce LD formation, fixed, and then stained with Oil-Red-O to image LDs. Imaging revealed that Hig2-HA AV- infected hepatocytes had significantly more LDs compared with controls (Figure 2.2A). Though there was no significant difference in TG levels in BSA vehicle-treated hepatocytes, Hig2-infected cells demonstrated a 1.5-fold increase in TG content compared with control cells after oleate loading (Figure 2.2C). Taken together, these results demonstrate that high Hig2 expression is sufficient to promote lipid deposition in hepatocytes. These results confirmed those of a report published while these studies were in progress showing that overexpression of Hig2 in liver via adeno-associated virus (AAV) vector injection in mice resulted in increased hepatic lipid deposition *in vivo* (267).

Figure 2.2 Ectopic expression of Hig2 promotes hepatocyte lipid deposition.

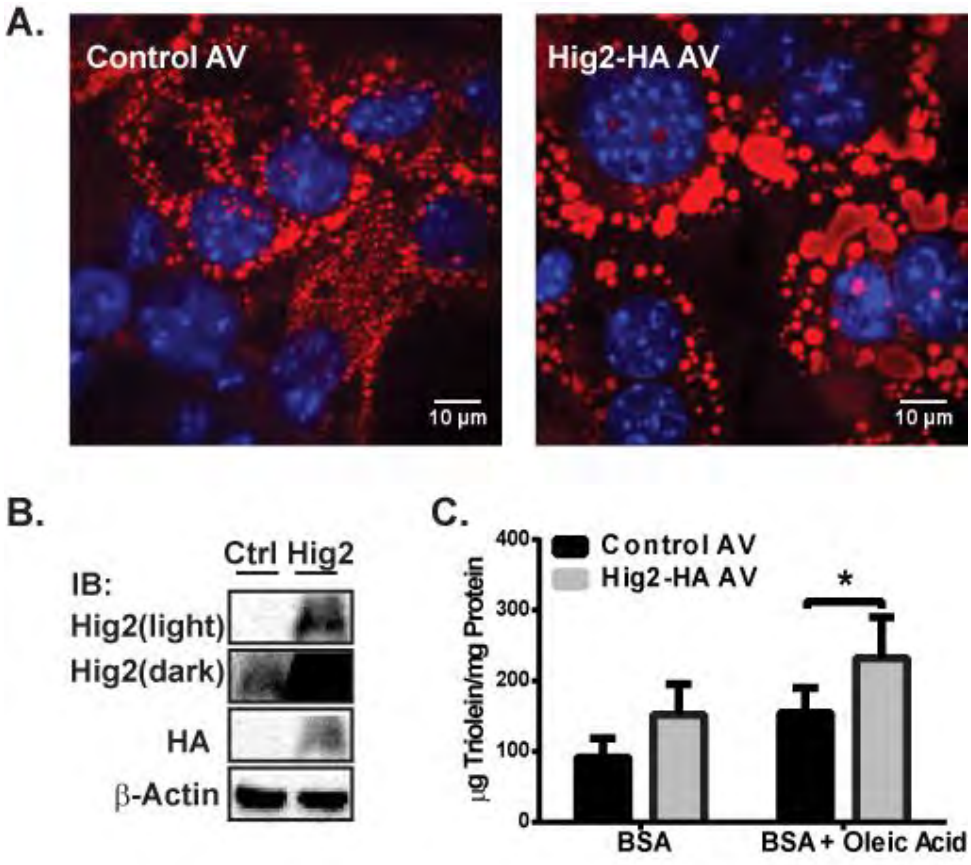

FIGURE 2.2 Ectopic expression of Hig2 promotes hepatocyte lipid deposition. Hepatocytes were isolated from Hig2fl/fl animals and infected with HA (control) or Hig2-HA (Hig2) adenovirus. A and C, hepatocytes were loaded with 250μM oleic acid for 24 h. A, cells were fixed and stained with Oil red O (red) and DAPI (blue). B, representative immunoblots (IB) of Hig2 (light and dark exposure), HA-Tag, and β-actin. Ctrl, control. C, triglyceride content from control and Hig2-HA infected cells. (*, $p<0.05$, $n=6$). Data are represented as the mean ± S.E.

Inducible Hig2 deficiency reduces LD triglyceride in hepatocytes.

Conversely, to determine whether Hig2 expression is necessary for lipid deposition in hepatocytes, Hig2 was genetically deleted in primary hepatocytes using a tamoxifen-inducible mouse model (Hig2iKO). Hig2$^{fl/fl}$ mice were crossed to Ubc ERT2 cre+ mice (Figure 2.3A), hepatocytes were isolated from these Hig2iKO animals, plated for 3 hours, and treated with either 2.5μM 4-OH-tamoxifen to induce deletion or ethanol vehicle as a control for 48 hours before analysis (Figure 2.3B). Tamoxifen treatment resulted in a 90% reduction in Hig2 mRNA and protein expression compared with ethanol vehicle- treated controls as assessed by qRT-PCR and Western blot, respectively (Figure 2.3C-D). When TG was extracted and quantified, it was found that ethanol vehicle-treated cells had 1.7-fold more TG after BSA treatment and 1.4-fold more TG after oleic acid loading compared with tamoxifen-treated cells (Figure 2.3E). These results demonstrate that Hig2 deficiency greatly reduced TG deposition in hepatocytes.

Figure 2.3 Inducible Hig2 deficiency reduces LD triglyceride in hepatocytes.

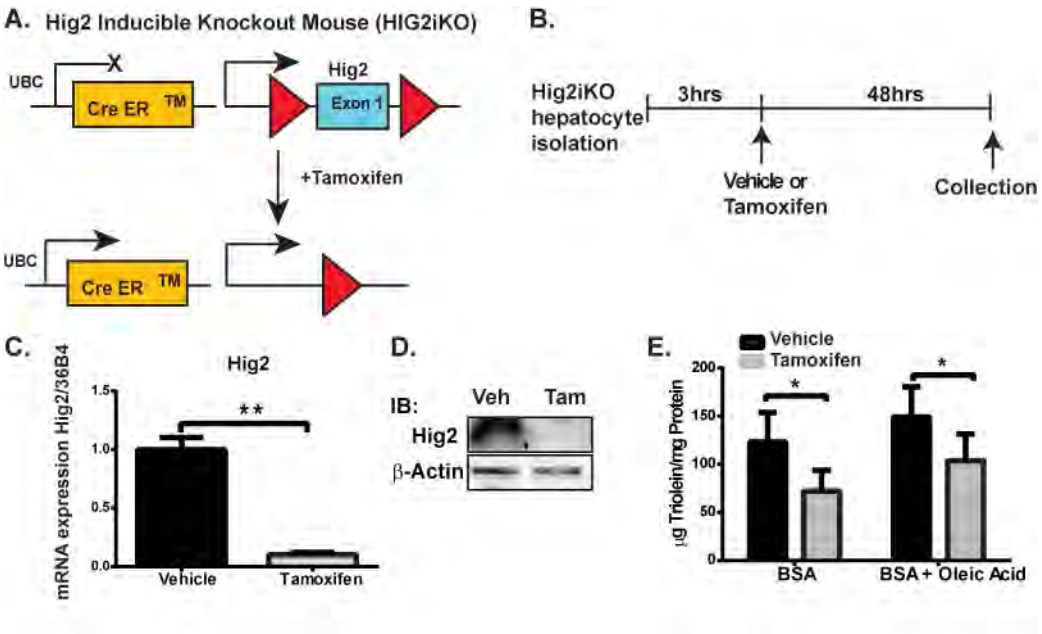

FIGURE 2.3 Inducible Hig2 deficiency reduces LD triglyceride in hepatocytes. A, schematic of Hig2 deletion with tamoxifen-inducible UbcERT2-cre. B, schematic of experimental design. Hepatocytes were isolated from Hig2iKO mice, plated for 3 h, and treated with ethanol vehicle or 2.5μM tamoxifen in ethanol for 48 h. C, qRT-PCR was performed for Hig2 and normalized to 36B4. (**, $p<0.01$, n=8). D, representative immunoblots (IB) of Hig2 and β-actin. Veh, vehicle; Tam, tamoxifen. E, triglyceride content from cells treated with 500μM oleic acid or BSA vehicle for 4h. (*, $p<0.05$, n=5).

Inducible Hig2 deficiency reduces LD size and number in hepatocytes.

Cells were fixed and stained with Oil-Red-O, and LDs were quantified. Strikingly, tamoxifen-treated hepatocytes had less Oil-Red-O-positive LD compared with ethanol vehicle-treated controls (Figure 2.4A). To confirm that this was not a side effect of tamoxifen treatment or the Ubc ERT2 cre transgene, Ubc ERT2 cre+ hepatocytes on a wild type background were treated with vehicle or tamoxifen and no alterations in lipid accumulation were observed (Figure 2.4D). The ethanol vehicle-treated hepatocytes demonstrated an average of 63 $\pm$ 8 LD per cell, while tamoxifen-treated hepatocytes displayed over a 67% reduction in LD content and had an average of only 18 $\pm$ 3 LD per cell (Figure 2.4B). Furthermore, the LDs in Hig2iKO hepatocytes were approximately 50% smaller than ethanol vehicle-treated controls and displayed an average size of 2.3 $\pm$ 0.6 μm^2 compared with 4.3 $\pm$ 0.6 μm^2 for ethanol vehicle-treated controls (Figure 2.4C). Interestingly, Hig2-deficient hepatocytes had significantly more LDs than controls after loading with 500μM oleic acid for 24 hours (41 $\pm$ 6 compared with 75 $\pm$ 11); however, these LDs were over 50% smaller than control LDs (4.0 $\pm$ .8 μm^2 vs. 9.3 $\pm$ 1.8 μm^2) (Figure 2.4B,C). This phenomenon is similar to the smaller LDs found in Fsp27-deficient adipocytes (220). These results demonstrate that Hig2 deficiency greatly reduced LD abundance deposition in hepatocytes. Taken together, these experiments in primary

hepatocytes suggest Hig2 expression is required for hepatocyte lipid deposition and LD growth *in vitro*.

Figure 2.4 Inducible Hig2 deficiency reduces LD size and number in hepatocytes.

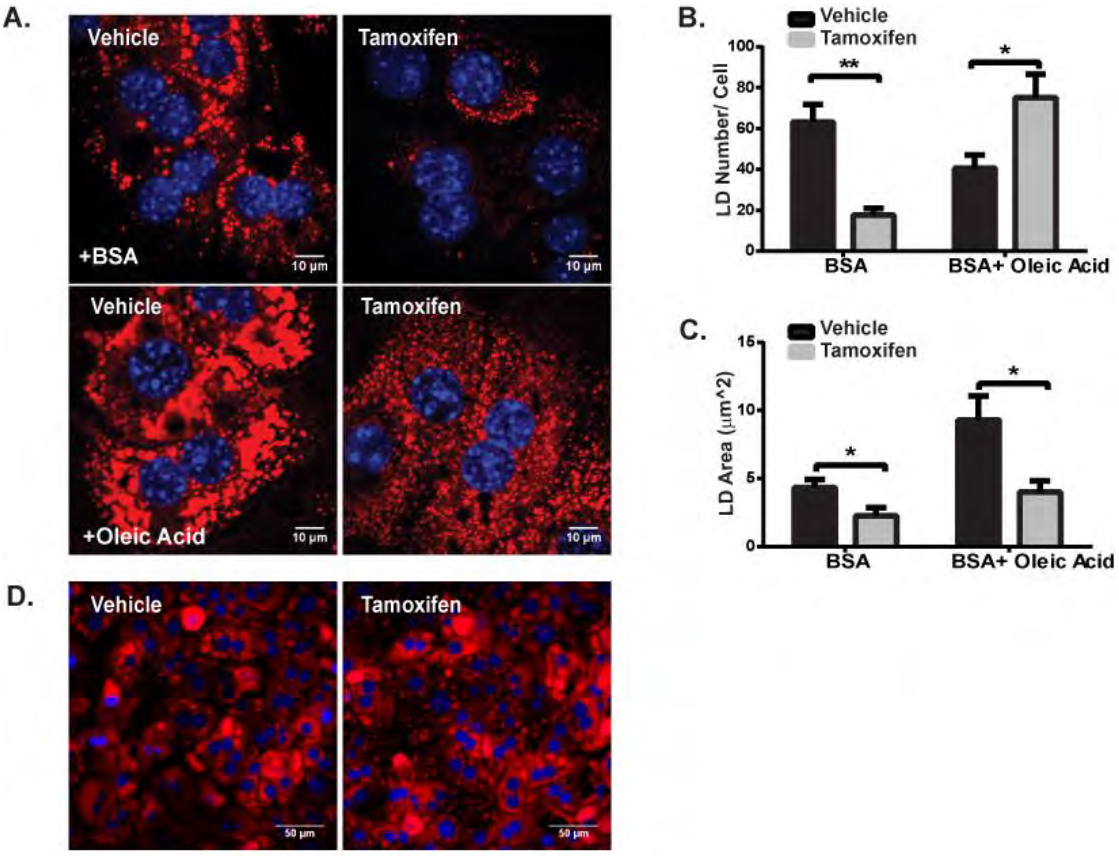

FIGURE 2.4 Inducible Hig2 deficiency reduces LD size and number in hepatocytes. A, hepatocytes were treated with BSA vehicle or 500µM oleic acid for 24 h, fixed, and stained with Oil-red-O (*red*) and DAPI (*blue*). B and C, hepatocytes were treated with 500µM oleic acid or BSA vehicle for 24 h. B, the number of lipid droplets per cell. C, total lipid droplet area per cell. (*, $p<0.05$, **, $p<0.01$, n=5-6). Data are represented as the mean $\pm$ S.E. D, C57Bl/6J Ubc ERT2 cre+ hepatocytes were isolated and treated as in Figure 2.3, treated with 500µM oleic acid for 24h, fixed, and stained with Oil-red-O (*red*) and DAPI (*blue*).

Liver-specific Hig2-deficient mice display hepatocyte-specific Hig2 deletion.

Excess accumulation of liver lipids is often associated with insulin resistance in obese mice and humans (274). Therefore, mice with liver-specific deletion of Hig2 were generated to address whether Hig2 deficiency could reduce hepatic steatosis and preserve glucose tolerance in a model of diet-induced obesity. The $Hig2^{fl/fl}$ mouse was crossed with mice expressing albumin cre to generate a mouse with liver-specific Hig2 deletion (Hig2LKO, Figure 2.5A). Hig2LKO mice demonstrated a significant, 89% reduction of Hig2 mRNA specifically in hepatocytes compared with fl/fl controls (Figure 2.5B) and a concomitant reduction in Hig2 protein levels as determined by Western blot (Figure 2.5C). Other tissues such as white adipose tissue (WAT), spleen, and kidney did not show significant reductions in Hig2 mRNA (Figure 2.5D), demonstrating that the deletion was specific for hepatocytes.

Figure 2.5 Liver-specific Hig2-deficient mice display hepatocyte-specific Hig2 deletion.

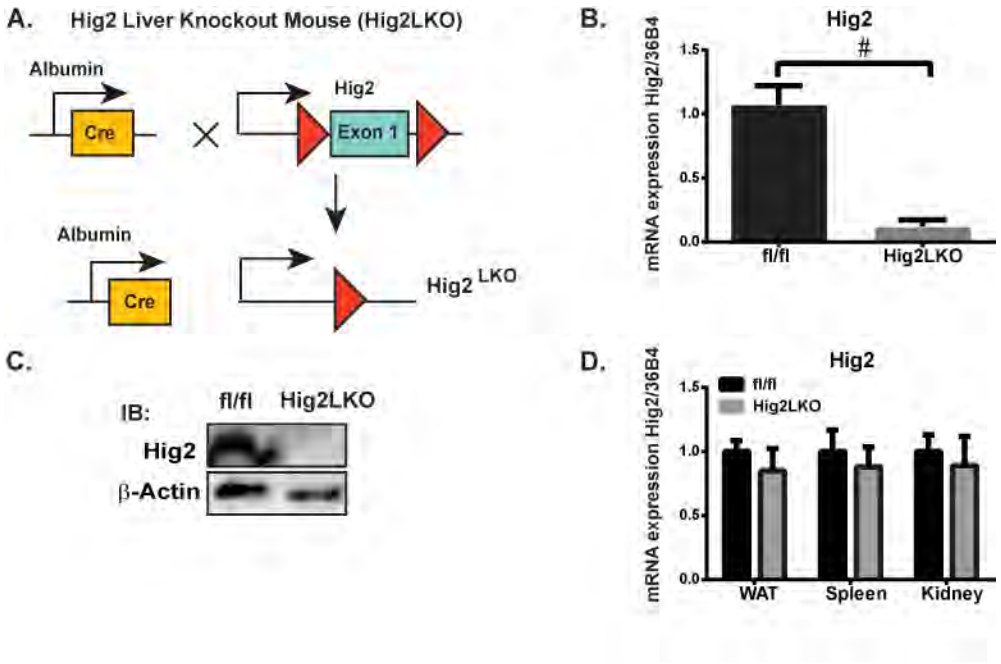

FIGURE 2.5 Liver-specific Hig2-deficient mice display hepatocyte-specific Hig2 deletion. A, schematic of albumin-cre-mediated Hig2 deletion. B and C, hepatocytes were isolated from fl/fl and Hig2LKO mice. B, qRT-PCR was performed for Hig2 and normalized to 36B4. (#, $p<.005$, n=5). Data are represented as the mean ± S.E. C, representative immunoblots (IB) of Hig2 and β-actin. D, white adipose tissue (WAT), kidney, and spleen were isolated from fl/fl and Hig2LKO mice. qRT-PCR was performed for Hig2 and normalized to 36B4. (n=8-9).Data are represented as the mean ± S.E.

Liver-specific Hig2-deficient mice display decreased liver triglyceride in normal diet conditions and improved glucose tolerance.

Fl/fl and Hig2LKO animals were placed on HFD or normal diet (ND) for 16 weeks and their body weight was measured weekly. Although there was no significant difference in the body weights of the Hig2LKO animals versus the fl/fl controls (Figure 2.6A), the Hig2LKO animals demonstrated significantly improved glucose tolerance as measured by a glucose tolerance test (GTT) in both the ND group and at early time points following glucose injection in the HFD-fed group (Figure 2.6B). However, no significant difference between genotypes was observed in an insulin tolerance test (ITT, Figure 2.6C).

Fasting circulating insulin levels, serum TGs, serum cholesterol, serum non-esterified fatty acids (NEFA), β-hydroxybutyrate and liver cholesterol were measured, but all were unchanged among the groups in both ND and HFD-fed conditions (Table 2.1). Because Hig2 deletion reduces TG content *in vitro*, the livers of the Hig2LKO animals fed ND or HFD for 16 weeks were examined. The gross liver weights were not significantly different in either diet condition, but in the ND condition, the Hig2LKO animals had lighter livers than the fl/fl controls (1.14 $\pm$ .04 vs. 1.23 $\pm$ .03g, p=.08) (Figure 2.6D). Though differences in H&E stained histology sections from fl/fl and Hig2LKO animals were unremarkable (Figure 2.6F), ND-fed Hig2LKO animals had 30% less liver TGs than fl/fl controls

(p=.08); however, this difference was abrogated in HFD-fed animals (Figure 2.6E).

Figure 2.6 Liver-specific Hig2-deficient mice display decreased liver triglyceride in normal diet conditions and improved glucose tolerance.

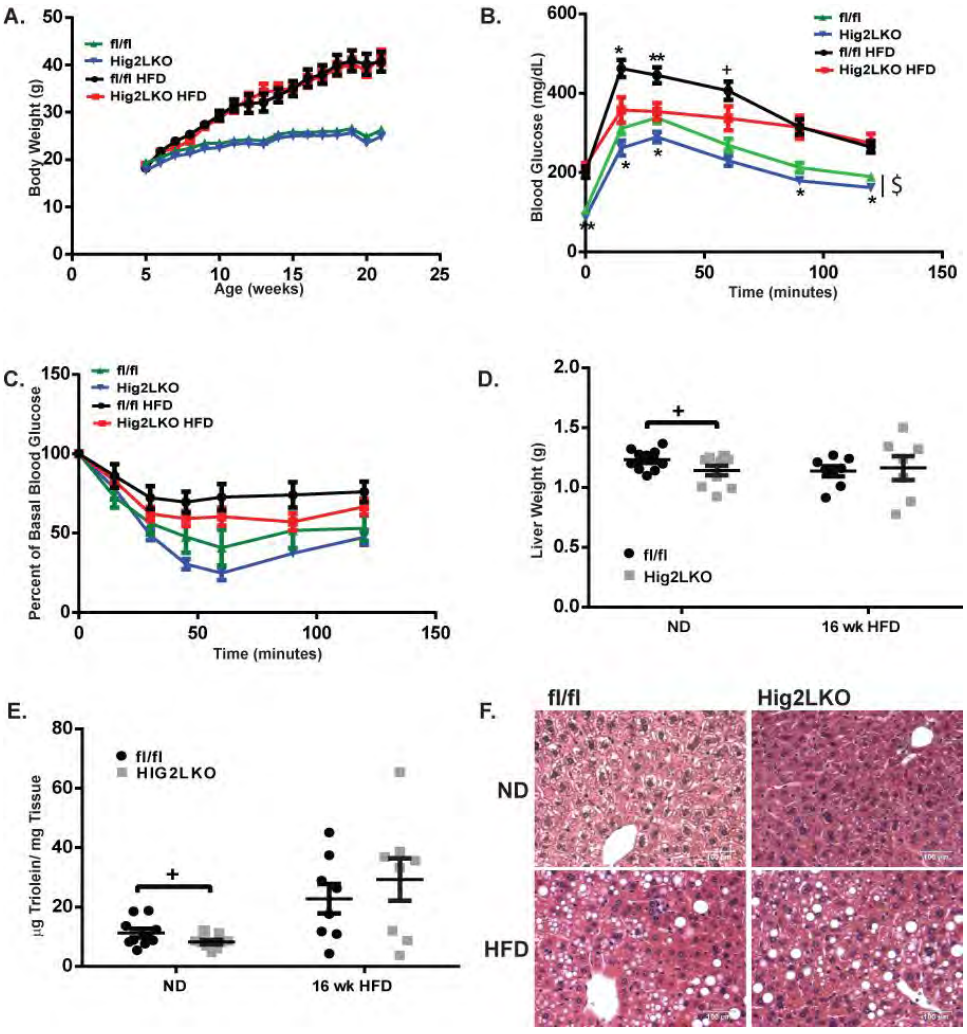

FIGURE 2.6 Liver-specific Hig2-deficient mice display decreased liver triglyceride in normal diet conditions and improved glucose tolerance. A-F, fl/fl or Hig2LKO animals were fed ND or HFD for 16 weeks. A, body weight curves. (n=10-13). B, glucose tolerance test. (+, p=0.08, *, p<0.05, **, p<0.01; $, p<0.05, two-way analysis of variance, n=7-11). C, insulin tolerance test. (n=9-17). Data are represented as the mean ± S.E. D, liver weights. (+, p=0.08, n=8-11). Data are represented as individual values ± S.E. E, lipids were extracted from livers, and triglyceride content was assessed. (+, p=0.08, n=8-11). Data are represented as individual values ± S.E. F, livers were sectioned and stained with H&E.

Table 2.1
Liver cholesterol and serum metabolites were assessed from fl/fl or Hig2LKO animals fed ND or HFD for 16 weeks. (*n*=5-13). Data are the mean ± S.E.
BD, below detection; NEFA, non-esterified fatty acids.

Parameters	**Normal Diet**		**16wks HFD**	
	Hig2 fl/fl	Hig2LKO	Hig2 fl/fl	Hig2LKO
Insulin (ng/ml)	BD	BD	2.831 ± 0.477	2.640 ± 0.268
Serum triglycerides (mg/dL)	64.283 ± 4.302	51.456 ± 5.113	107.384 ± 6.634	102.954 ± 10.707
Serum cholesterol (mg/dL)	64.401 ± 5.782	70.218 ± 5.929	127.834 ± 6.993	137.622 ± 6.255
Liver cholesterol (μg/mg)	1.745 ± 0.106	1.717 ± 0.071	1.804 ± 0.226	2.181 ± 0.082
NEFA (mmol/liter)	0.416 ± 0.028	0.348 ± 0.038	0.536 ± 0.068	0.476 ± 0.058
β-Hydroxybutyrate (mmol/liter)	0.469 ± 0.042	0.569 ± 0.078	0.373 ± 0.038	0.274 ± 0.017

Gene expression in inflammatory, lipid, and energy metabolism pathways is unchanged in liver-specific Hig2-deficient mice.

To assess liver inflammation, RNA was isolated from mice fed HFD for 16 weeks and qRT-PCR was performed to assess the expression of genes involved in inflammatory pathways. No changes in gene expression were observed in Hig2LKO mouse livers compared with fl/fl controls for TNFα, IL6, IL1β, and the macrophage marker F4/80 (Figure 2.7A).

It was critical to examine potential mechanisms by which Hig2 controls TG accumulation in hepatocytes. Hepatic TG accumulation is controlled by FA uptake and hepatic lipogenesis versus hepatic lipolysis (TG turnover) (11). First, qRT-PCR on RNA isolated from livers isolated from fl/fl and Hig2LKO mice on ND was performed and the expression was assessed of several genes that are critically involved in the aforementioned pathways. However, no changes in gene expression were observed in Hig2LKO mouse livers compared with fl/fl controls for CD36 (FA uptake), Cpt1a, Mttfa (mitochondrial oxidation), Pparγ, Fasn, Srebp1c (lipogenesis), Srebp2 (cholesterol synthesis), ApoB (lipid export), or Atgl (lipolysis) (Figure 2.7B). Hig2 deficiency could potentially reduce the expression of other LD proteins in liver to reduce the lipid content, thus the expression of Perilipin 2, Cidea, and Fsp27 by qRT-PCR was measured and the expression of these genes was also unchanged in Hig2LKO mouse livers compared with fl/fl livers (Figure 2.7C).

Figure 2.7 Gene expression in inflammatory, lipid, and energy metabolism pathways is unchanged in liver-specific Hig2-deficient mice.

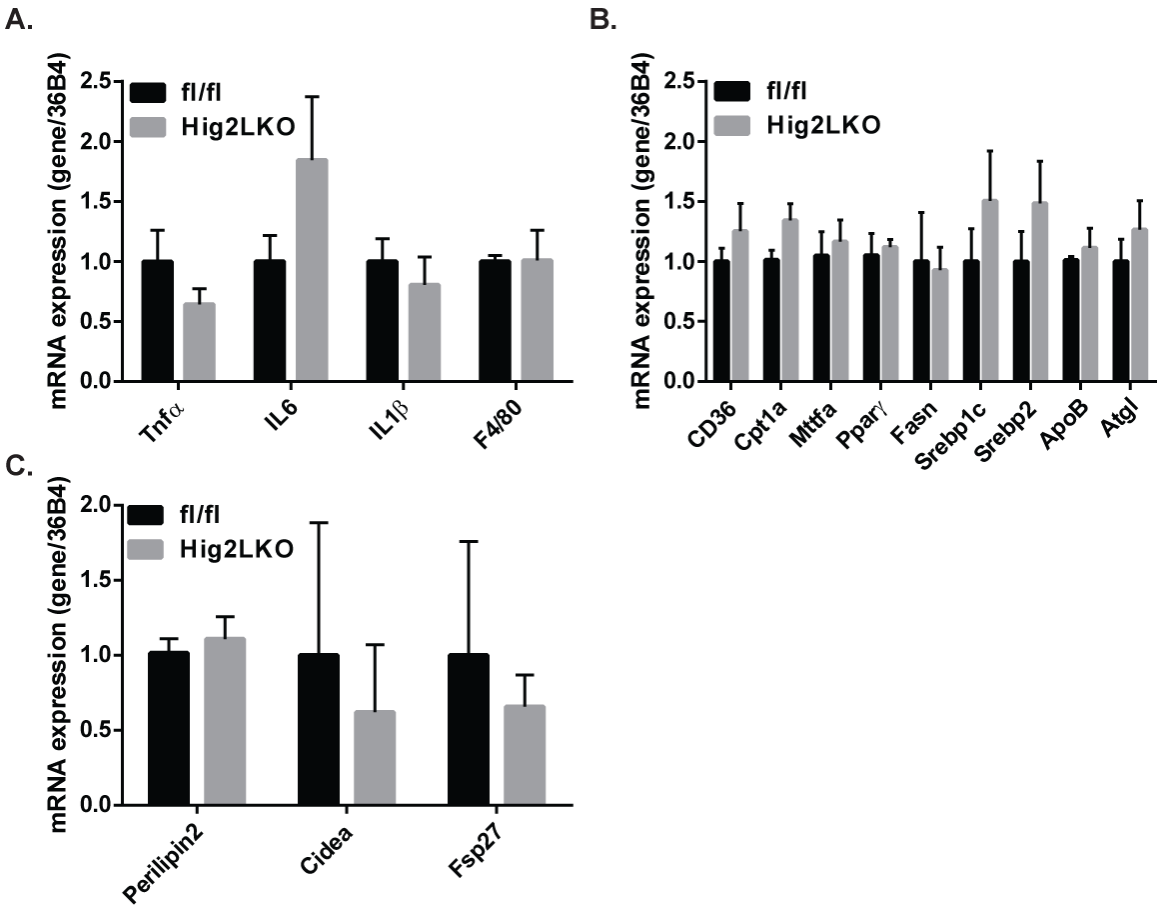

FIGURE 2.7 Gene expression in inflammatory, lipid, and energy metabolism pathways is unchanged in liver-specific Hig2-deficient mice. A-C, whole livers were isolated from fl/fl or Hig2LKO animals, RNA was extracted, and qRT-PCR was performed for the indicated genes and normalized to 36B4. A, animals were fed HFD for 16 weeks. Data are represented as the mean ± S.E. (n=4-9). B, C animals were fed ND for 16 weeks. (n=3-4). Data are represented as the mean ± S.E.

Hig2 deficiency increases hepatocyte lipolysis, β-oxidation, and triglyceride turnover.

Because there were no transcriptional changes in the targets examined, it was hypothesized that Hig2 was promoting hepatic lipid deposition in a post-transcriptional manner. Thus, lipid flux in Hig2LKO hepatocytes was assessed to determine whether they demonstrated a difference in lipid handling. Hepatocytes were isolated from ND-fed fl/fl and Hig2LKO hepatocytes, the cells were incubated with [^{3}H] oleic acid and then the total amount of radiation was measured in Hig2LKO and fl/fl controls after overnight [^{3}H] oleic acid loading. As expected, the Hig2LKO hepatocytes displayed a 45% reduction in lipid uptake compared with controls (p=.07; Figure 2.8A), confirming results obtained in Figure 2.3 with the Hig2iKO hepatocytes.

Genetic deletion of LD proteins such as Fsp27, Perilipin1, and Cidea in mice, has demonstrated a role for LD proteins in TG turnover and β-oxidation (177,203,220,284). Hepatic TG turnover has been experimentally determined to be on the timescale of 10-30 hours *in vivo* (285). Thus, parameters were assessed by loading the ND-fed Hig2LKO or fl/fl hepatocytes with [^{3}H] oleic acid overnight and then TG turnover, lipolysis, and β-oxidation were measured. Strikingly, despite the absence of changes in gene expression, Hig2LKO hepatocytes had significantly increased TG turnover compared with fl/fl controls as determined by linear regression analysis (Figure 2.8C). Hig2LKO hepatocytes

also exhibited double the amount of lipolysis at two hours as compared with controls (Figure 2.8D). Similar to Fsp27-deficient animals, Hig2LKO hepatocytes also displayed 3.3-fold higher degree of FA oxidation compared with control fl/fl hepatocytes as detected by accumulation of soluble [^{3}H] oleic acid oxidation products (Figure 2.8B). Taken together, these results suggest that Hig2 promotes lipid deposition in a healthy liver, at least in part, by localizing to LDs in hepatocytes and inhibiting TG lipolysis.

Figure 2.8 Hig2 deficiency increases hepatocyte lipolysis, β-oxidation, and triglyceride turnover.

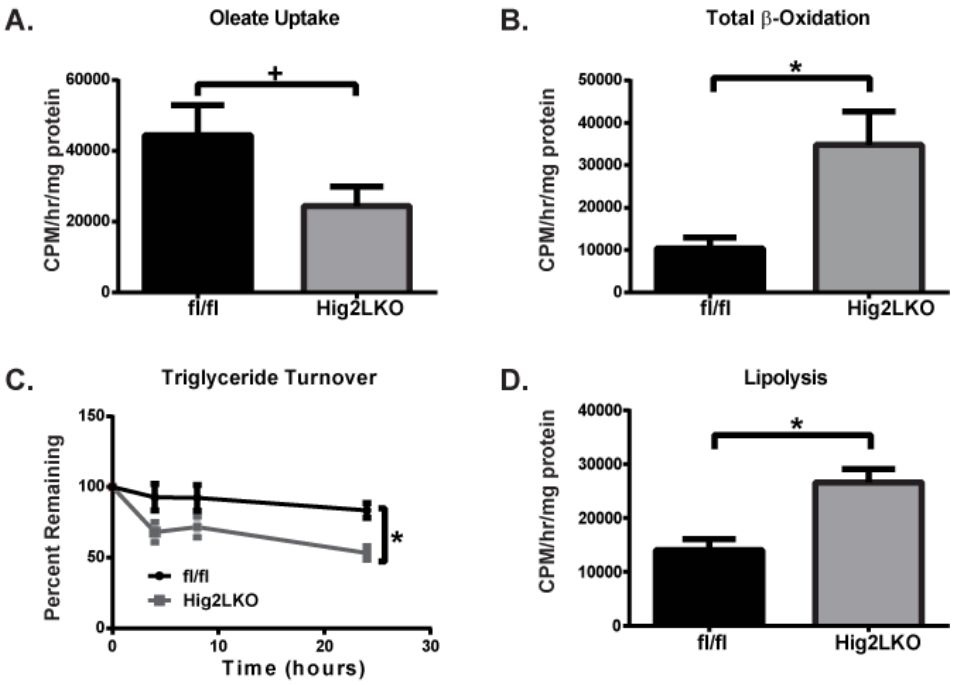

FIGURE 2.8 Hig2 deficiency increases hepatocyte lipolysis, β-oxidation, and triglyceride turnover. A-D, hepatocytes were isolated from fl/fl or Hig2LKO animals, plated, and loaded with 100μM [^{3}H]oleic acid overnight. A, oleate uptake. (+, p=0.07, n=8). B, total β-oxidation. (*, p<0.05, n=6). C, triglyceride turnover. (*, p<0.05 via linear regression analysis of the slope, n=8-10). D, lipolysis. (*, p<0.05, *n*=3) Data are represented as the mean ± S.E.

Discussion:

The findings presented in this chapter define Hig2 as a physiologically important LD-associated protein that functions to promote TG accumulation in liver *in vivo*. It is demonstrated that GFP-tagged Hig2 localizes specifically to hepatocyte LDs in a manner that was dependent on its putative lipid binding domain (Figure 2.1). While ectopic expression of Hig2 promoted LD abundance and TG deposition (Figure 2.2), Hig2 deletion in hepatocytes *in vitro* reduced TG accumulation (Figure 2.3) and LD number (Figure 2.4). Liver-specific Hig2 deletion (Figure 2.5) reduced hepatic TGs in ND-fed mice and improved glucose tolerance in both ND and HFD-fed conditions (Figure 2.6). Hepatocytes isolated from these animals, despite showing no discernable gene expression changes (Figure 2.7), showed increased TG turnover and FA oxidation, suggesting that Hig2 promotes TG deposition by inhibiting lipolysis (Figure 2.8). Indeed, direct measurement of TG hydrolysis in hepatocytes deficient in Hig2 revealed increased lipolytic rates over controls, analogous to what has been reported for other LD proteins, such as Fsp27 (214).

As the data in Figure 2.5 indicate, Hig2 may not be nearly as crucial for hepatic lipid deposition in HFD-fed liver as it is in the ND-fed condition. No decrease was found in total liver TG in the Hig2LKO mice compared with fl/fl controls when both groups of mice were on a HFD. This contrasts with a decrease in liver TG observed in these Hig2LKO mice on ND (Figure 2.5). One

likely possibility to explain this result is other proteins that are redundant in function to Hig2.

Many LD proteins in the PAT family and the CIDE family alter lipid deposition by inhibiting lipolysis (173,180,200). Some of these are upregulated under HFD conditions and could replace Hig2 action on lipolysis. For example, the expression of the LD protein Fsp27 is highly upregulated by the fatty liver conditions we have examined here (286). Fsp27 inhibits lipolysis in adipocytes (215), similar to the present findings on Hig2 and hepatocytes. Taken together, it seems likely that compensation by other upregulated LD proteins explains the failure of Hig2 depletion to lower liver TG under HFD conditions.

These findings complement the recent findings of Mattijssen et al. (267) which were published while these studies were in progress. The authors demonstrated that overexpression of Hig2 in mouse livers driven by AAV results in hepatic steatosis, similar to our results using AV as an expression vector for Hig2 (Figure 2.2). Consistent with their findings, increased lipid product export was also observed in hepatocytes from Hig2LKO mice compared with controls (Figure 2.8), but this export consists almost entirely of FA oxidation products rather than lipoproteins. It has been shown that increases in lipolysis can shunt FAs to the mitochondria, leading to increases in β-oxidation (287). It was also observed that Hig2LKO hepatocytes had increased lipolysis and TG turnover, which is phenotypically similar to what is observed after loss of LD proteins and

further suggests that Hig2 acts similarly to other proteins in this class. Thus, the increased β-oxidation products observed in Hig2-deficient hepatocytes most likely reflect the higher levels of lipolysis and free FA availability for oxidation observed in the Hig2-deficient hepatocytes.

The increased lipolysis in Hig2LKO hepatocytes does not appear to be the result of altered expression of Atgl (Figure 2.7B), the rate-limiting TG lipase in adipose tissue. However, Atgl activity is inhibited by G0/G1 Switch Protein 2 (G0S2) (222,288). Hig2 could function similarly to negatively regulate lipolysis by interacting with and inhibiting Atgl or other lipases in liver. The lipolysis pathway in liver is not well studied, but liver-specific Atgl depletion in mice increases liver TG, while overexpression reduces liver TGs and increases β-oxidation independent of changes in hepatic gene expression or serum TGs, much like we observe in the Hig2LKO mouse (289-291). Sequence alignments of Hig2 and G0S2 show 13.5% sequence identity, mostly located in the area where G0S2 is known to bind and inhibit Atgl (Figure 2.9) (222,292,293). Another target of Hig2 regulation could be Adiponutrin, a lipase from the patatin-like phospholipase domain containing (PNPLA) family that contains the most sequence similarity to Atgl (287). If Hig2 physically interacts with a lipase, it could either inhibit its activity or restrict its access to LDs. The exact mechanism by which Hig2 inhibits lipolysis will be assessed in future studies.

A remarkable finding in this study was the significant improvement in glucose tolerance observed in liver-specific Hig2 deficiency, even under HFD conditions in which liver TG was unchanged (Figure 2.6). Although in obese animals and humans liver TG accumulation generally correlates with insulin resistance, many experimental models show dissociation of liver lipid accumulation from glucose tolerance, and the precise mechanistic connections between liver fat and metabolism and insulin sensitivity are far from clear (294). The mechanism by which Hig2 improves glucose tolerance in HFD animals, primarily in early time points following glucose injection is also unclear at this point. Hig2LKO animals trend toward enhanced insulin sensitivity in an ITT (Fig. 2.6), although the differences did not reach statistical significance, and the basis of improved glucose clearance in these animals is under further investigation.

Although this work on Hig2 has been performed in murine cells and tissues, mutations in other LD proteins such as Fsp27 and Perilipin 1 are associated with human disease (251,252). It will therefore be of interest to investigate whether Hig2 plays an important role in human biology. Tissue expression analysis of Hig2 shows that it is ubiquitously expressed (Figure 2.10). This expression pattern parallels that of Perilipin 2, which can be found coating LDs in most tissues. This raises the question of whether Hig2 is required for lipid deposition in other tissues, particularly metabolically active tissues such as adipose tissue and muscle or for macrophage foam cell formation. The full range

of Hig2 functions in diverse cell types in human biology is a key question for future research.

Figure 2.9 Hig2 and G0S2 share sequence homology.

```
G0S2_MOUSE  MESVQELIPLAKEMMAQKPRGKLVKLYVLGSVLALFGVVLGLVETVC----SPFTAASRL 56
Hig2_MOUSE  ------------------MKFMLNLYVLGIMLTLLSIFVRVMESLGGLLESPLPGSSWI 41

G0S2_MOUSE  RDQEAAVVELREACEQQSLHKQALLAGGKAQEATLCSRALSLRQHAS---- 103
Hig2_MOUSE  TRGQLANTQPPK----------------------------GLPDHPSRGVQ 64

Identical Positions: 15
Similar Positions: 24
Sequence Identity: 13.5%
```

FIGURE 2.9 Hig2 and G0S2 share sequence homology. Protein sequences for mouse G0S2 and Hig2 were aligned, and sequence identity was calculated using the uniProt KB database with the default parameters of the program Clustal Omega (292,293). Amino acid color coding is as follows: red=identical, blue=very similar, green=similar. Residues 27-42 of G0S2 are sufficient for ATGL binding and are highlighted in yellow.

Figure 2.10 Hig2 is ubiquitously expressed in mouse tissue.

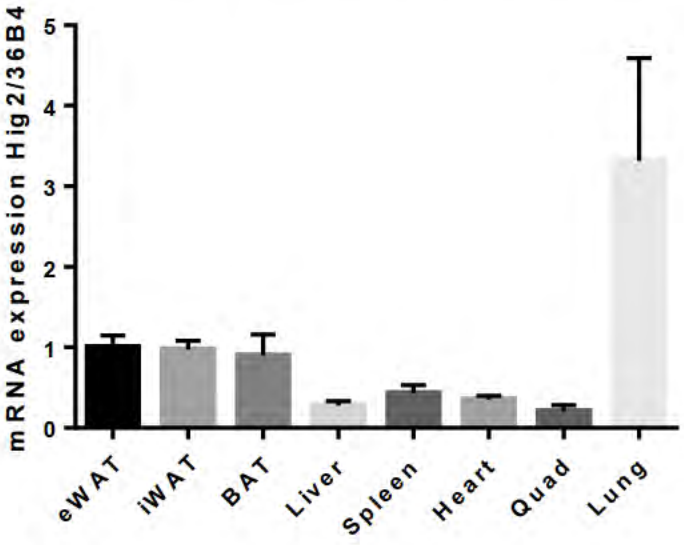

FIGURE 2.10 Hig2 is ubiquitously expressed in mouse tissue. The indicated tissues were isolated from C57BL/6J mice, RNA was extracted, and qRT-PCR was performed for Hig2 and normalized to 36B4. (n=3-4) Data are represented as the mean ± S.E.

CHAPTER III: Adipocyte-specific Hig2 promotes fat deposition and diet-induced glucose intolerance

Author Contributions

- **Figure 3.1 B Tissue acquisition and preparation.** The acquisition of the bariatric surgery fat samples was performed by Olga Hardy, Czech lab. The isolation and preparation of RNA for microarray analysis were performed by Sarah Nicoloro, Czech Lab.
- **Figure 3.1 F SGBS culture.** The culture, differentiation, and RNA isolation of SGBS cells was performed by Ozlem Senol-Cosar, Czech Lab.
- **Figure 3.4 Metabolic cage measurements.** The metabolic cage measurements were performed by the UMass Mouse Metabolic Phenotyping Center.
- The rest of the experiments in the chapter were performed by Marina T. DiStefano
- The SGBS cells were donated by the lab of Martin Wabitsch.
- The manuscript was written by Marina T. DiStefano with helpful suggestions by Joseph V. Virbasius, Rachel J. Roth Flach, and Michael P. Czech.

Summary:

Adipose tissue is a dynamic organ with inputs into whole body metabolism. Proper lipid storage in adipocyte-specific lipid droplets (LDs) is critical for metabolic health; one hypothesis suggests that in chronic states of over nutrition, adipocytes can no longer buffer the influx of calories, resulting in dyslipidemia, which is often associated with metabolic disease. In this chapter, it is shown that the LD protein Hypoxia-inducible Gene 2 (Hig2/Hilpda) functions to enhance lipid accumulation in adipose tissue. Hig2 expression increased in epididymal white adipose tissue (eWAT) of obese mice and differentiating human SGBS adipocytes, two states associated with increasing adipocyte TG content. Hig2 localized to LDs in mature human SGBS and 3T3-L1 adipocytes. eWAT weight and brown adipose tissue (BAT) lipid content were decreased by adipocyte-specific deletion of Hig2 in mice with floxed Hig2 alleles expressing cre controlled by the adiponectin promoter. *Ex vivo* lipolysis measurements and circulating NEFAs were unchanged in Hig2-deficient animals, suggesting that adipocyte-specific Hig2 deficiency may not reduce eWAT weight by increasing lipolysis. Interestingly, HFD-fed mice with adipocyte-specific Hig2 deletion also displayed improved glucose tolerance. These improvements were abrogated by thermoneutrality (30°C), a temperature with no thermal stress and little BAT activation, suggesting that active BAT may play a role. Consistent with this idea, brown adipocyte-specific deletion of Hig2 in mice with floxed Hig2 alleles

expressing cre controlled by the ucp1 promoter also resulted in improved glucose tolerance in obesity. Taken together, these data indicate that Hig2 plays a role in promoting lipid sequestration within LDs in mouse adipocytes and in promoting obesity-induced glucose intolerance.

Introduction:

Once considered an inert storage organ, adipose tissue is a dynamic tissue with inputs into whole body metabolism (122). Adipose tissue contains fat cells, termed adipocytes, and preadipocytes, immune cells, and endothelial cells (295). When digested and separated from the adipocytes, these cells are collectively known as the SVF (31). Adipose tissue stores the majority of caloric energy in the form of neutral lipids in organelles termed LDs in adipocytes (296). LDs are highly dynamic organelles and are regulated by tissue-specific proteins embedded in or associated with the droplet termed LD proteins. These proteins can regulate the size of the LD by inhibiting or facilitating lipolysis, the breakdown of TGs into glycerol and FFAs (297). LD proteins are relevant to human disease, as humans with mutations in these proteins manifest lipodystrophy, fatty liver, and metabolic syndrome (142).

Two main families of LD-associated proteins are the PAT family (173), named for its three founding members Perilipin, Adipophilin, and Tip47 that have PAT domains, and the CIDE family (200). The PAT family has five members (Perilipin 1-5), while the CIDE family has three members (Cidea, Cideb, and

Cidec/Fsp27). LDs are heterogeneous in their coats and LD proteins generally demonstrate tissue-specific distribution patterns (276). Perilipins 1, 2, 3, and 4, Cidea, and Fsp27 are expressed in adipose tissue and localize to LDs in adipocytes (Table 1.1). I*n vitro* and *in vivo* studies suggest that Perilipin 1 and Fsp27 are two LD proteins that are critical for lipid storage in adipocytes (175,177,180,215,220); these experiments were confirmed by the discovery of lipodystrophic humans with Perilipin 1 and Fsp27 mutations (252,298).

Proper lipid storage in WAT is critical for metabolic health (295). In a lean individual, calories are stored as lipid in adipocytes. One hypothesis suggests that in chronic states of over nutrition, adipocytes can no longer buffer the influx of calories, resulting in dyslipidemia and ectopic fat deposition in other organs, such as liver and muscle, which can lead to insulin resistance, cardiovascular disease, inflammation, and cancer (136). Increasing the storage capacity of the adipose tissue poses a unique solution to this problem. Thus, further investigating the LD proteome for key players in lipid storage could be beneficial for human health.

Brown adipose tissue (BAT) generates heat through nonshivering thermogenesis, an uncoupling of the proton gradient of the electron transport chain mediated by UCP1. This differs from shivering thermogenesis, a temporary involuntary muscle movement that generates heat (299). Thus, brown adipocytes are characterized by high mitochondrial number, high UCP1 expression, and

small, numerous (multilocular) LDs (295). Until recently, BAT was thought to be present solely for warmth in human infants and hibernating mammals, but 2FDG-PET scans have revealed that adult humans retain some functional BAT (50).

As BAT metabolism is energetically expensive, human BAT activation presents a unique anti-obesity therapeutic potential. BAT thermogenesis can be activated by many means, but one of the most prominent stimuli is increased beta-adrenergic activation in response to cold temperatures (47). For example, when rodents are housed at room temperature (23°C), a mild cold stress, their metabolic rate can increase up to 50% due to BAT energy consumption (60). As housing mice at room temperature (23°C) poses such a thermal stress, it can be informative to subject mouse models to thermoneutrality, the temperature at which they are not subject to any external cold stress, (30°C for mice) to eliminate the contribution of nonshivering thermogenesis to whole body metabolism (300).

Hypoxia-inducible gene 2 (Hig2) is a little-studied 63 amino acid protein that was found in microarray analyses to be highly expressed in the adipocyte fraction of adipose tissue samples collected from bariatric surgery patients (Figure 3.1B). As Hig2 is ubiquitously expressed, promotes lipid deposition, and was highly expressed in adipocytes in human patients, its role in adipose tissue was examined.

In this chapter, it is demonstrated that Hig2 localizes to LDs in adipocytes. Its expression is increased with both adipogenic differentiation and fat deposition. Mice harboring an adipocyte-specific deletion of Hig2 demonstrate reduced epididymal fat pad weight and improved glucose tolerance on HFD. These effects are abrogated by thermoneutral housing, suggesting that BAT may play a role in the improvements. This is supported by the fact that mice harboring a brown adipocyte-specific deletion of Hig2 also display improved glucose tolerance. Interestingly, *ex vivo* glycerol release, serum NEFAs and phosphorylation of PKA substrates are unchanged in adipocyte-specific Hig2-deficient animals compared with fl/fl controls, suggesting that Hig2 may not inhibit lipolysis to promote lipid deposition in adipocytes. Taken together, these results suggest that adipocyte-specific Hig2 promotes lipid deposition and glucose intolerance, which may be entirely due to its expression in brown adipocytes.

Materials and Methods:

Animal Studies: All of the studies performed were approved by the Institutional Animal Care and Use Committee (IACUC) of the University of Massachusetts Medical School. Animals were maintained in a 12 hour light/dark cycle. Hig2$^{fl/fl}$ animals were purchased from Jackson Laboratories (Hilpdatm1.1Nat/J). For metabolic studies, the animals were backcrossed onto C57Bl/6J animals for at least 6 generations. Genomic DNA was extracted from the obtained mice and subjected to PCR for genotyping using Qiagen Fast Cycling PCR Kit (Hig2$^{fl/fl}$

primer 5'-CCGGCAGGGCCTCCTCTTGCTCCTG-3', 5' GTGTGTTGGCTAGCTGACCCCTCGTG-3'). Hig2$^{fl/fl}$ animals were crossed to an adiponectin cre mouse line (B6;FVB-Tg(Adipoq-cre)1Evdr/J, Jackson Laboratories). Hig2fl/fl animals were also crossed to a ucp1 cre mouse line (B6.FVB-Tg(Ucp1-cre)1Evdr/J, Jackson Laboratories). Cre genotyping was performed according to the method of Jackson Laboratories.

At 4-6 weeks of age, male C57Bl/6J, Hig2$^{fl/fl}$, Hig2$^{fl/fl}$ adiponectin cre+, or Hig2$^{fl/fl}$ ucp1 cre+ littermates animals were placed on a high fat diet (60% fat, D12492i or 45% fat, D12451 (Fig 3.1 only), Research Diets) or fed chow (Lab Diet 5P76) for 8,12,16 or 20 weeks. Animals were switched to thermoneutral housing (30°C, 12 hour light/dark cycle) for 4 weeks and retained on the same diet they were previously fed.

Mice were fasted 16 hours for glucose tolerance tests and 4 hours for insulin tolerance tests. Mice were injected IP with 1g/kg of glucose or 1IU/kg of insulin, blood was drawn from the tail vein at the indicated times, and blood glucose levels were measured with a Breeze-2-glucose meter (Bayer). Mice were euthanized by CO_2 inhalation followed by bilateral thoracotomy.

The metabolic cage studies were performed at the UMass Mouse Metabolic Phenotyping Center. Mice were fed HFD for 16 weeks and the metabolic cages were used to measure food intake, RER, VO_2 consumption, CO_2 production,

energy expenditure and physical activity over a 3-day period, and an average for each parameter was calculated (TSE Systems).

Ex Vivo Lipolysis: Mice were fasted for 16 hours and euthanized by CO_2 inhalation followed by bilateral thoracotomy. Epididymal adipose tissue was removed and cut into 80-100mg pieces, placed in 0.5ml Krebs-Ringer-Hepes Buffer pH 7.4, supplemented with 2.5% fatty acid-free BSA and 1mM sodium pyruvate. Samples were incubated in a 37°C shaking water bath with or without 10μM isoproterenol (Sigma, I5627) for 2 hours and glycerol release into KRH was measured using a calorimetric assay (Sigma) according to the manufacturer's instructions and normalized to the fat pad weight.

Adipose tissue fractionation: Whole fat pads were isolated, minced, and placed in 5 ml Hanks Balanced Salt Solution (ThermoFisher, 14170120), pH 7.4, supplemented with 5% fatty acid-free BSA and 1mg/ml collagenase. Samples were incubated in a 37°C shaking water bath for 45 minutes, and the digestion reaction was terminated with 5 ml of HBSS and BSA. Tissue was filtered through a 200μM filter, spun at 200 g for 5 minutes, and adipocyte and stromal vascular fractions (SVF) were separated. Both were washed with HBSS 2x and then placed in TriPure for RNA isolation.

Plasma and lipid analysis: Mice were fasted for 16 hours for plasma lipid analysis. Blood was taken via cardiac puncture, and EDTA-containing plasma was collected. Total serum cholesterol levels (ab65359 Abcam), serum triglyceride levels (Triglyceride Determination Kit, Sigma), serum NEFAs (Wako Diagnostics), and serum Glycerol (Free Glycerol Determination Kit, Sigma) were measured using calorimetric assays according to the manufacturer's instructions. Insulin and adiponectin levels (Millipore) were measured by ELISA according to manufacturer's instructions.

Triglyceride and Cholesterol Extraction: Whole livers were isolated and flash frozen in liquid nitrogen. Lipids were extracted from livers via the Folch method (280). Lipids were dissolved in isopropanol with 1% Triton-X100. Triglyceride (Triglyceride Determination Kit, Sigma) and cholesteryl ester (ab65359 Abcam) levels were measured using calorimetric assays according to the manufacturer's instructions and normalized to liver weight.

Human samples: Human adipose tissue samples were collected from morbidly obese patients who underwent gastric bypass surgery between 2005 and 2009 at the University of Massachusetts Medical School (301). Samples used for microarray analysis were from BMI-matched female patients, whereas qRT-PCR validations were performed in samples from both males and females. Adipose

tissue samples were obtained from lower abdominal wall (for subcutaneous) and omentum (for visceral) during the surgery. Informed consent was given by the patients and the study was approved by University of Massachusetts Medical School Institutional Review Board.

RNA Isolation and RT-qPCR: Total RNA was isolated from cells or tissues using TriPure isolation reagent (Roche) according to the manufacturer's protocol. The isolated RNA was DNase treated (DNA-free, Life Technologies), and cDNA was synthesized using iScript cDNA synthesis kit (BioRad). RT-qPCR was performed on the BioRad CFX96 using iQ SybrGreen supermix and 36B4 served as the reference gene. Primer sequences are as follows: 36B4 (5'-TCCAGGCTTTGGGCATCA-3', 5'-CTTTATCAGCTGCACATCACTCAGA-3'); Hig2 (5'-CATGTTGACCCTGCTTTCCAT-3', 5'- GCTCTCCAGTAAGCCTCCCA-3'); Atgl (5'-CAGCACATTTATCCCGGTGTAC-3', 5'-AAATGCCGCCATCCACATAG-3'); Hsl (5'-GATTTACGCACGATGACACAGT-3', 5'-GCCATATTGTCTTCTGCGAGTG-3'); Cgi-58 (5'-GGTTAAGTCTAGTGCAGC-3', 5'- AAGCTGTCTCACCACTTG-3', 5'-AAGCTGTCTCACCACTTG-3'); G0S2 (5'- GTGAAGCTATACGTGCTGGG-3', 5'-CCGTCTCAACTAGGCCGAG-3'); Perilipin1 (5'- CTGTGTGCAATGCCTATGAGA-3', 5'-CTGGAGGGTATTGAAGAGCCG-3'); Fsp27 (5'-ATCAGAACAGCGCAAGAAGA-3', 5'-CAGCTTGTACAGGTCGAAGG-3'); Ucp1 (5'-

ACTGCCACACCTCCAGTCATT-3', 5'-CTTTGCCTCACTCAGGATTGG-3'); Prdm16 (5'-CAGCACGGTGAAGCCATTC-3', 5'-GCGTGCATCCGCTTGTG-3') Human Primers: RPLP0 (5'-CAGATTGGCTACCCAACTGTT-3', 5'-GGGAAGGTGTAATCCGTCTCC-3'); HIG2 (5'-AAGCATGTGTTGAACCTCTACC-3', 5'-GATGGAGAGTAGGGTCAGTACC-3')

Immunoblotting: Tissues and cells were lysed in a high-salt, Tris-HCl buffer (50mM Tris, pH 8, 150mM NaCl, 1mM EDTA, 1% Triton X-100) with 1x Halt protease and phosphatase inhibitors (Thermo Scientific). Lysates were resolved by SDS-PAGE gel and transferred to nitrocellulose membranes. Membranes were blotted with the following antibodies: α-Tubulin (T5168, Sigma), β-Actin (A5136, Sigma), HSL (4107, Cell Signaling), pHSL(ser563) (4139, Cell Signaling), ATGL (2138, Cell Signaling).

Cell Culture: 3T3-L1 fibroblasts were grown and differentiated into adipocytes as previously described (302). Briefly, 3T3-L1 fibroblasts were grown to confluence in complete medium (high glucose (25mM) DMEM containing 10% fetal bovine serum, 50units/ml penicillin, and 50µg/ml of streptomycin). Two days after confluence, differentiation medium (0.25µM dexamethasone, 0.5mM 1-methyl-3-isobutylxanthine, and 10^{-7}M insulin) was added. Cells were considered fully mature 7 days post-differentiation.

Simpson Golabi Behmel Syndrome (SGBS) cells were obtained from Dr. Martin Wabitsch's laboratory. SGBS fibroblasts were grown and differentiated into adipocytes as previously described with modifications (303). Briefly, SGBS fibroblasts were grown to confluence in DMEM/F12 containing 10% fetal bovine serum, 33μM biotin, 17μM pantothenic acid, 50units/ml penicillin, and 50μg/ml streptomycin. Two days after confluence, serum-free differentiation medium (25nM dexamethasone, 250μM 1-methyl-3-isobutylxanthine, 0.01mg/ml transferrin, 0.2nM triiodothyronine, 20nM human insulin, 2μM rosiglitazone, and 100nM cortisol) was added. Four days later, the differentiation cocktail was replaced with maintenance medium (DMEM/F12, biotin, pantothenic acid, transferrin, insulin and cortisol). Cells were considered fully mature 14 days post-differentiation. Adenoviruses were made as follows: The cDNA of the transgene of interest was first cloned into a pShuttle plasmid (Clontech, Mountain View, CA) and then subcloned into a molecular clone of E1-and E3-deleted human adenovirus serotype 5. This adenovirus plasmid backbone was modified from pAdX system (Clontech, Mountain View, CA) by introducing a green-white selection mechanism (281). The recombinant clones of adenovirus vector with the transgene of interest were selected through this green-white screening, confirmed by restriction enzyme analyses and rescued in 293 cells after restriction enzyme linearization and transfection. The recombinant virus is expanded and purified by standard CsCl gradient sedimentation followed by

dialysis for desalting (282). The HA control construct was made by inserting 3HA at Not1 and BamH1 sites of the 4124 base pair plasmid pShuttle Adeno vector. 3HA Hig2 adenovirus plasmid DNA was made by inserting a full-length gene of Hig2 at restriction sites Blp1 (5') and BamH1 (3') of 3HA adeno viral plasmid DNA.

Cell Imaging: Cells were fixed in 10% buffered formalin in PBS for 1 hour, blocked in 1% normal goat serum in PBS for 1hour at room temperature, incubated with Hig2 (1:100, Rockland Immunochemicals, (304)) for 2 hours at room temperature, incubated with fluorescent secondary 1:1000 for 1 hour, treated with Bodipy 493/503 (ThermoFisher, D-3922) at 1:10,000 for 15 minutes, and mounted with Prolong Gold with DAPI (Life Technologies). Cells were imaged at room temperature with a Solamere Technology Group modified Yokogawa CSU10 Spinning Disk Confocal with a Nikon TE-2000E2 inverted microscope at 60x.

Histology: Tissues were isolated and fixed in 10% formalin, embedded in paraffin, sectioned, and stained with hematoxylin and eosin (H&E). The UMass Morphology Core performed the embedding and sectioning.

Statistical Analysis: Data were analyzed in GraphPad Prism 6 (GraphPad Software, Inc.). A two-tailed student's t test with Welch's Correction was used to compare two groups of data. Where indicated, data were analyzed using a one-way ANOVA or a two-way ANOVA with repeated measures. $P<.05$ was considered to be significant. The Grubb's test was used to determine if there were statistical outliers and if an outlier was determined, it was removed from the statistical analysis. Variance was estimated using standard error of the mean.

Results:

Hig2 expression increases with adipogenesis and obesity.

To elucidate critical genes for human adipocyte biology, microarray analyses were performed on omental adipose tissue from human patients undergoing bariatric surgery after fractionation into adipocytes and SVF (301) and genes were sorted by adipocyte specificity. One of the top gene hits that displayed 10-fold enrichment in signal in the adipocyte fraction compared with SVF was Hig2 (Figure 3.1B). To validate this result, qRT-PCR was performed, and Hig2 expression 28-fold higher in human epididymal adipocytes (Figure 3.1C) and 12-fold higher in human subcutaneous adipocytes (Figure 3.1D) compared with respective SVFs. Hig2 expression increased with lipid deposition in liver (304). To investigate whether this was also the case in adipose tissue, wild type animals were placed on a HFD for 20 weeks, and Hig2 expression in

epididymal white adipose tissue (eWAT) was measured by qRT-PCR. Hig2 expression in eWAT of wild type animals doubled with high-fat-feeding (Figure 3.1A).

As LD proteins often display increases in expression with adipogenic differentiation (176,183,185,193,212), Hig2 expression was also measured by qRT-PCR in two adipocyte cell lines upon adipogenic stimulation. In the murine 3T3-L1 adipocyte cell line, Hig2 expression was unchanged with differentiation (Figure 3.1E); however, its expression was increased by 10-fold after 14 days of adipogenic differentiation in the human Simpson-Golabi-Behmel syndrome (SGBS) adipocyte cell line (Figure 3.1F).

Figure 3.1 Hig2 expression increases with adipogenesis and obesity.

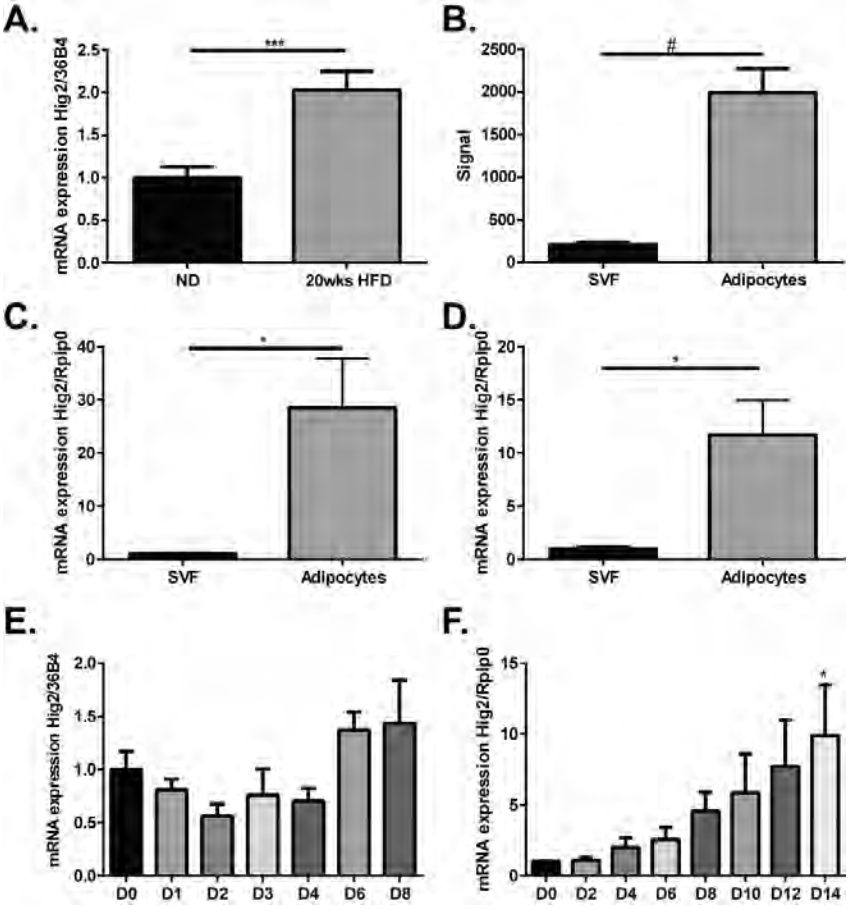

FIGURE 3.1 Hig2 expression increases with adipogenesis and obesity. A, C57BL/6J animals were fed HFD for 20 weeks, eWAT was isolated, RNA was extracted, and qRT-PCR was performed for Hig2 and normalized to 36B4. (***, p<.005, n=7-8). Data are represented as the mean ± S.E. B-D Adipose tissue was isolated from patients undergoing bariatric surgery. B, microarray from omental adipose tissue. (#, p<.0001, n=6). C, D qRT-PCR was performed on indicated tissues for Hig2 and normalized to Rplp0. C, fractionated omental adipose tissue. (*, p<0.05, n=6-7). D, fractionated subcutaneous adipose tissue. (*, p<0.05, n=7-8). Data are represented as the mean ± S.E. E, 3T3-L1 cells were differentiated, RNA was extracted on the indicated day, and qRT-PCR was performed for Hig2 and normalized to 36B4. (n=3-7). Data are represented as the mean ± S.E. F, SGBS cells were differentiated, RNA was extracted on the indicated day, and qRT-PCR was performed for Hig2 and normalized to Rplp0. (*, p<0.05, one-way analysis of variance, n=3-7). Data are represented as the mean ± S.E.

Hig2 localizes to LDs in human and mouse cultured adipocytes.

As Hig2 expression significantly increased with differentiation in SGBS cells, immunofluorescence for endogenous Hig2 was performed in SGBS cells on day 10, post-differentiation. Interestingly, Hig2 (*green)* localized around cellular structures (Figure 3.2A); staining confirmed that these structures were indeed LDs and that Hig2 (*red*) localized to Bodipy-positive (*green*) LDs, much like it did in primary hepatocytes, demonstrating that Hig2 is also a LD protein in human adipocytes (Figure 3.2B). To investigate whether this was the case in mouse adipocytes, mature 3T3-L1 adipocytes were infected with either HA control or HA-tagged Hig2 adenovirus and imaged. While the HA control adenovirus displayed a diffuse localization pattern, ectopically expressed Hig2 appeared to localize to LDs in cultured mouse adipocytes (Figure 3.2C), demonstrating that Hig2 is a LD protein in mouse adipocytes.

FIGURE 3.2 Hig2 localizes to LDs in human and mouse cultured adipocytes. A-B, SGBS cells were fixed Day 10 post-differentiation. A, Cells were stained with Hig2 (*green*) and DAPI (blue). The two panels are two different representative fields. B, Cells were stained with Hig2 (*red*), Bodipy (*green*), and DAPI (*blue*). Left, merge of Hig2 and DAPI, right, merge of Hig2, Bodipy, and DAPI. C, Mature 3T3-L1 adipocytes were infected with HA control or HIG2-HA adenovirus, stimulated with 500μM oleic acid complexed to fatty acid-free BSA for 30 minutes, fixed, and stained with HA (*green*) and DAPI (*blue*). Left, HA control-infected cells; right, HIG2-HA infected cells.

Figure 3.2 Hig2 localizes to LDs in human and mouse cultured adipocytes.

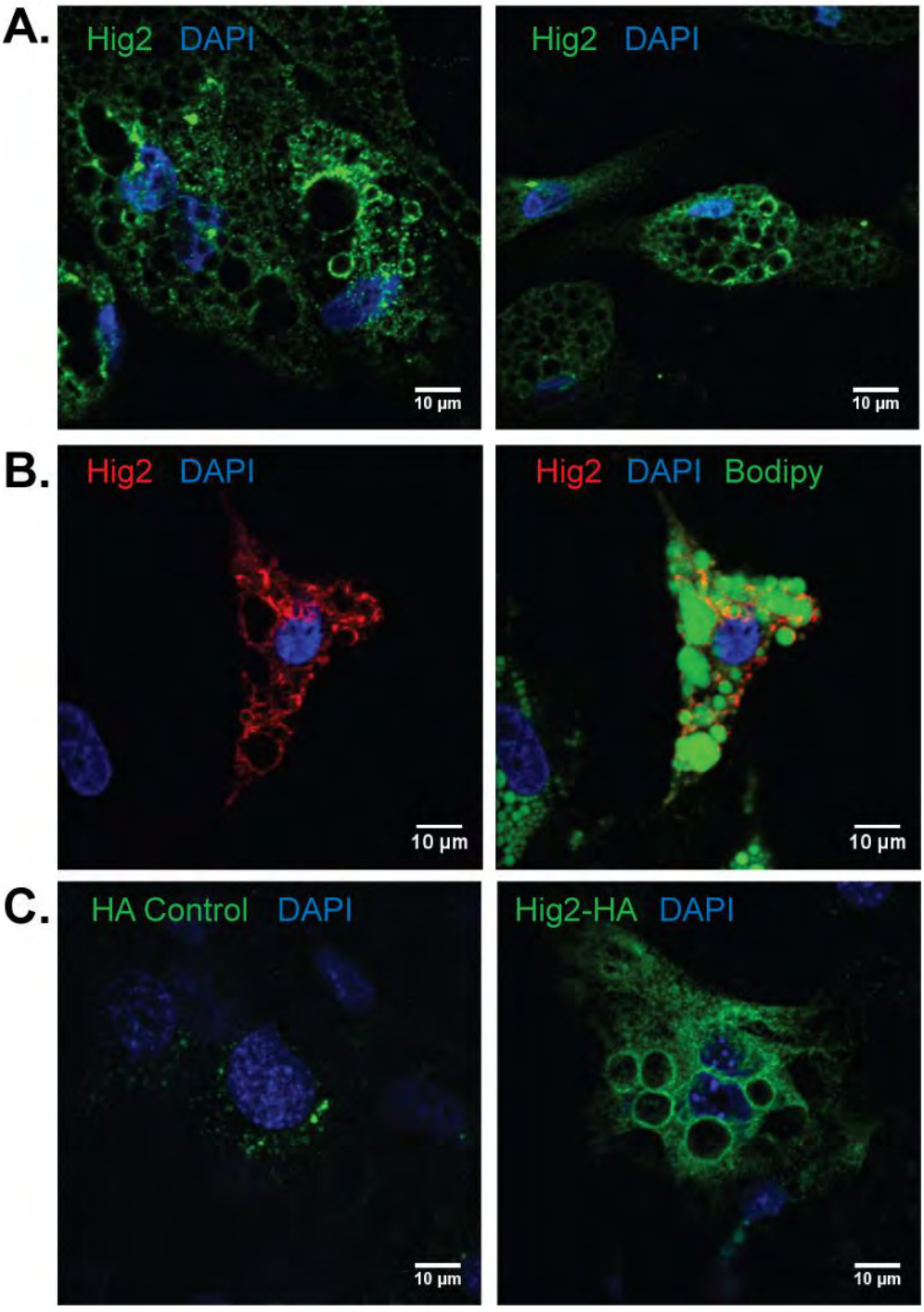

Adipocyte-specific Hig2-deficient mice display adipocyte-specific deletion.

To further investigate the role of adipocyte-specific Hig2, mice with an adipocyte-specific Hig2 deficiency (Hig2AdKO) were generated by crossing a $Hig2^{fl/fl}$ mouse with an Adiponectin Cre+ mouse (Figure 3.3A). To determine whether the deletion was adipocyte-specific, eWAT and inguinal WAT (iWAT) were fractionated, adipocytes were isolated, and qRT-PCR was performed for Hig2. As expected, there was a significant 60% reduction in Hig2 mRNA expression in eWAT and 70% reduction in iWAT in Hig2AdKO animals compared with fl/fl littermate controls (Figure 3.3B). There was also a significant 50% reduction in Hig2 expression in whole BAT but no change in non-adipose tissues such as kidney and spleen, demonstrating that the deletion is specific to adipocytes (Figure 3.3C,D).

Figure 3.3 Adipocyte-specific Hig2-deficient mice display adipocyte-specific Hig2 deletion.

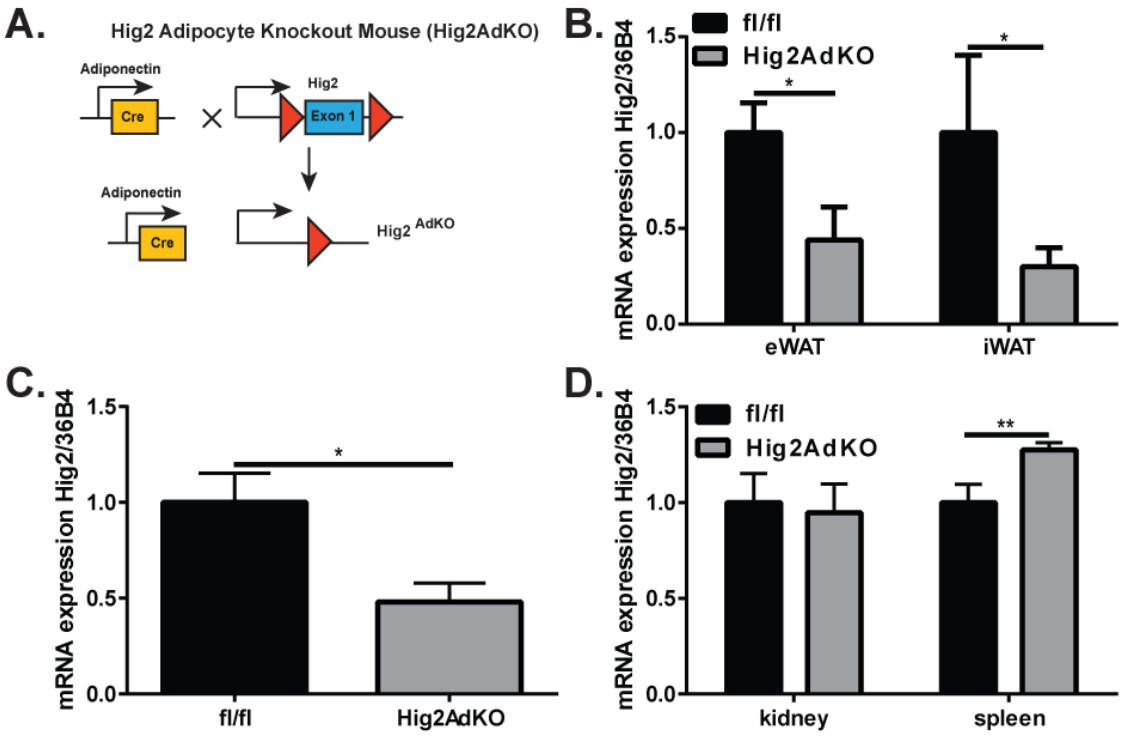

FIGURE 3.3 Adipocyte-specific Hig2-deficient mice display adipocyte-specific deletion. A, schematic of adiponectin-cre-mediated Hig2 deletion. B-D, indicated tissues were isolated from fl/fl and Hig2AdKO mice, RNA was extracted, and qRT-PCR was performed for Hig2 and normalized to 36B4. B, isolated epididymal and inguinal adipocytes. (*, $p=0.05$, n=3-9). C, brown adipose tissue. (*, $p<0.05$, n=5-8). D, kidney and spleen. (**, $p<.01$, n=4-10). Data are represented as the mean $\pm$ S.E.

Adipocyte-specific Hig2-deficient mice display improved glucose tolerance after HFD at 23°C.

To determine the role of adipocyte-specific Hig2 deficiency on whole body metabolism, Hig2AdKO and fl/fl animals were subjected to normal diet (ND) or high fat diet (HFD) for 16 weeks. There were no significant differences in body weight or insulin tolerance as measured by an insulin tolerance test (ITT) between genotypes in either feeding condition (Figure 3.4A,C), but Hig2AdKO animals had significantly improved glucose tolerance in the high-fat-fed condition as measured by a glucose tolerance test (GTT) (Figure 3.4B), suggesting that adipocyte Hig2 promotes glucose intolerance in diet-induced obesity.

Serum metabolites and liver triglyceride levels were measured in both ND and HFD conditions and, although there was a significant increase in fasted insulin in Hig2AdKO animals compared with fl/fl controls (2.7 $\pm$ 0.4 ng/ml vs 1.4 $\pm$ 0.3 ng/ml) in the HFD-fed condition, there were no changes in serum adiponectin levels, serum TGs, serum NEFAs, serum glycerol or liver TGs (Table 3.4). Differences in the ND condition were also unremarkable, except for an increase in liver TGs in Hig2AdKO animals compared with controls (9.02 $\pm$ 2.65μg/ml vs 17.9 $\pm$ 2.05μg/ml), (Table 3.1). It is unlikely that the increased fasting insulin in the 16 week HFD Hig2AdKO animals accounts for the improvements in glucose tolerance, as Hig2AdKO animals that were high-fat fed for 8 weeks display

improved glucose tolerance compared to fl/fl controls (Figure 3.4D), but no change in insulin levels during a GTT (Figure 3.4E).

Figure 3.4 Adipocyte-specific Hig2-deficient mice display improved glucose tolerance after HFD at 23°C.

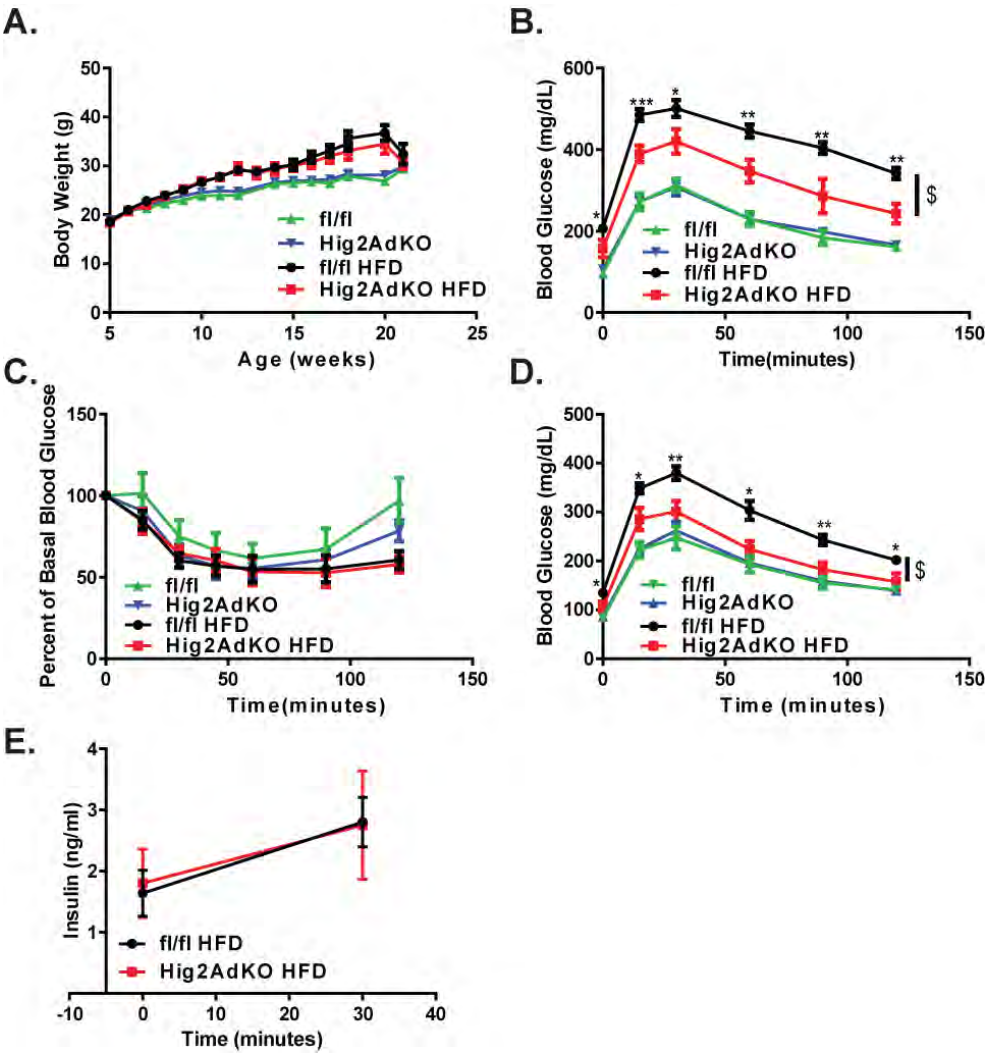

FIGURE 3.4 Adipocyte-specific Hig2-deficient mice display improved glucose tolerance after HFD at 23°C. A-C, fl/fl or Hig2AdKO animals were fed ND or HFD for 16 weeks. A, body weight curves. (n=8-20). B, glucose tolerance test. (*, p<0.05, **, p<.01, ***, p<.001, $, p<.005, two-way analysis of variance, n=5-13). C, insulin tolerance test. (n=4-13). Data are represented as the mean ± S.E. D-E, fl/fl or Hig2AdKO animals were fed HFD for 8 weeks. D, glucose tolerance test. (*, p<0.05, **, p<.01, ***, p<.001, $, p<.005, two-way analysis of variance, n=8-13). E, insulin was measured 0 and 30 minutes-post glucose injection. (n=3-6). Data are represented as the mean ± the S.E.

Table 3.1

Liver cholesterol and serum metabolites were assessed from fl/fl or Hig2AdKO animals fed ND or HFD for 16 weeks at 23°C. (*, p<0.05, *n*=5-13). Data are the mean ± S.E.

Parameters	**Normal Diet**		**16wks HFD**	
	Hig2 fl/fl	Hig2AdKO	Hig2 fl/fl	Hig2AdKO
Insulin (ng/ml)	1.441 ± 0.486	0.794 ± 0.271	1.436 ± 0.258	2.743 ± 0.395*
Adiponectin (μg/ml)	7.209 ± 0.225	7.456 ± 0.263	8.315 ± 0.708	9.052 ± 0.684
Serum triglycerides (mg/dL)	77.05 ± 4.176	75.94 ± 5.418	92.42 ± 8.409	88.64 ± 5.818
Serum cholesterol (mg/dL)	303.1 ± 21.11	314.7 ± 29.15	401.1 ± 34.42	330.9 ± 53.42
NEFA (mmol/liter)	0.690 ± 0.074	0.690 ± 0.048	0.553 ± 0.032	0.622 ± 0.037
Serum glycerol (mg/ml)	0.056 ± 0.003	0.053 ± 0.03	0.054 ± 0.004	0.056 ± 0.004
Liver triglycerides (μg/mg)	9.018 ± 2.652	17.89 ± 2.054*	42.43 ± 5.831	41.20 ± 6.384

Metabolic Cage parameters are unchanged in adipocyte-specific Hig2-deficient animals at 23°C.

As high fat-fed Hig2AdKO animals displayed improved glucose tolerance compared with fl/fl controls at 23°C, individually-housed obese animals were subjected to three days of metabolic cage analysis. Food intake was measured and found to be unchanged between the genotypes (Figure 3.5A). Furthermore, there were no differences between genotypes in daytime or nighttime physical activity (Figure 3.5B), oxygen consumption (Figure 3.5C), or carbon dioxide production (Figure 3.5D). Finally, respiratory exchange ratio (RER) and energy expenditure were calculated and found to be unchanged (Figure 3.5E, F).

Figure 3.5 Metabolic cage parameters are unchanged in adipocyte-specific Hig2-deficient animals at 23°C.

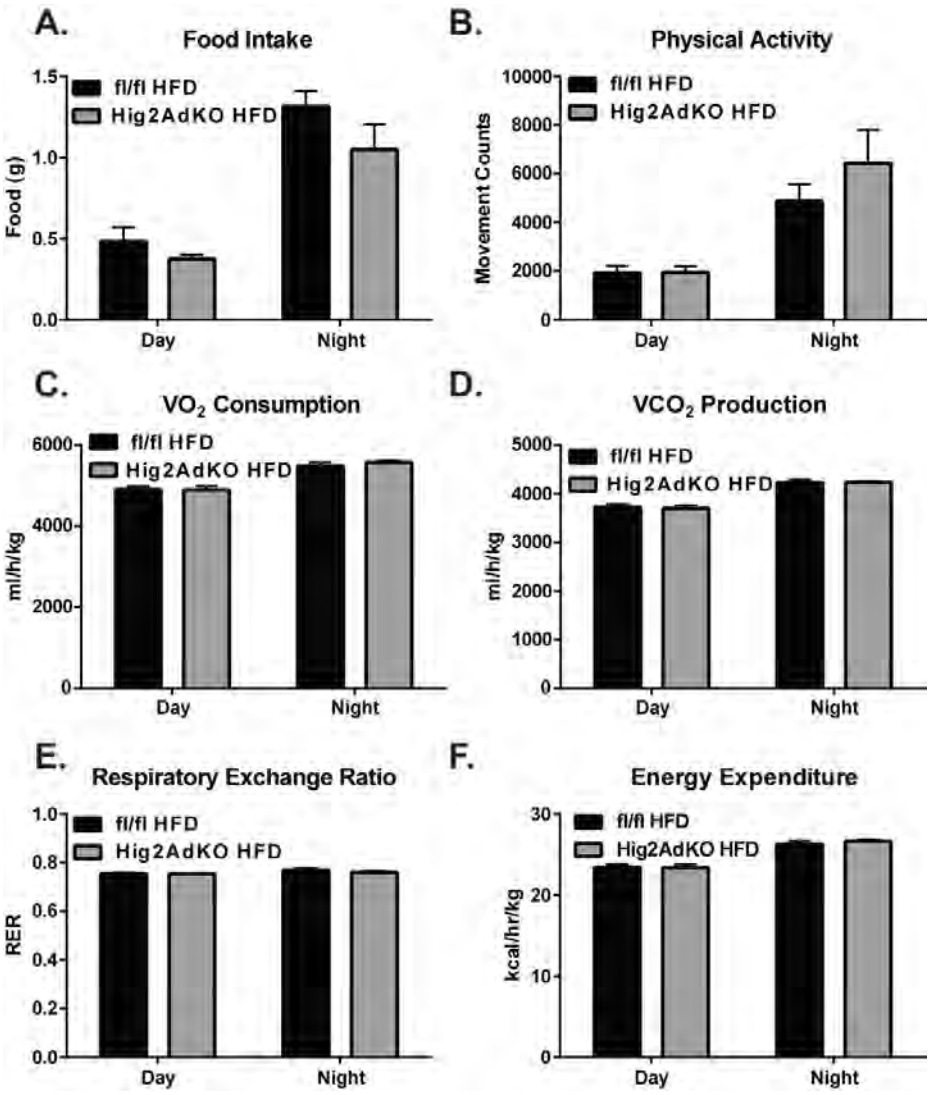

FIGURE 3.5 Metabolic cage parameters are unchanged in adipocyte-specific Hig2-deficient animals at 23°C. A-D, Metabolic cage analysis was performed over 3 days in fl/fl and Hig2AdKO mice that had been fed with HFD for 16 weeks. A, food intake. B, physical activity. C, average VO_2 consumption. D, average CO_2 production. E, respiratory exchange ratio (RER). F, energy expenditure normalized to lean body mass. Data are represented as the mean $\pm$ S.E. (n=4-6). Day (7am-7pm); Night, (7pm-7am).

Adipocyte-specific Hig2 deficiency alters adipose tissue distribution in HFD-fed mice at 23°C.

LD protein deficiencies alter lipid deposition *in vivo* (177,203,219,220,223,245). Thus, fat pad and liver weights of fl/fl and Hig2AdKO animals were examined. In chow-fed mice, eWAT and iWAT fat pad weights were unchanged between genotypes (Figure 3.6 A,B). However, upon HFD-feeding, Hig2AdKO animals had significantly less eWAT weight compared with fl/fl controls (3.9 $\pm$ .42% vs 5.7 $\pm$ .24%), while iWAT weight was unchanged (Figure 3.6A,B). This reduction corresponded to a concomitant increase in liver weight from 2.7 $\pm$ .07% of body weight in controls to 3.1 $\pm$ .11% in Hig2AdKO animals (Figure 3.6D). Chow-fed Hig2AdKO animals also had significantly increased liver weight compared with fl/fl littermates (Figure 3.6C).

The reduction in eWAT weight suggests that Hig2 deficiency reduces adipocyte-specific fat deposition. Thus, H&E-stained histology from HFD animals was examined to determine whether there were visible alterations in AT and liver to complement the weight differences. While eWAT, iWAT, and liver histology appeared unchanged between the genotypes (Figure 3.6E,F,H), there was a striking visible reduction in lipids in BAT of Hig2AdKO animals compared with fl/fl controls (Figure 3.6G). There were no differences in BAT weight between genotypes in the ND or HFD- fed mice (Figure 3.6D). Taken together, these

results suggest that adipocyte-specific Hig2 deficiency alters adipose tissue distribution in obesity.

Figure 3.6 Adipocyte-specific Hig2 deficiency alters adipose tissue distribution in HFD-fed mice at 23°C.

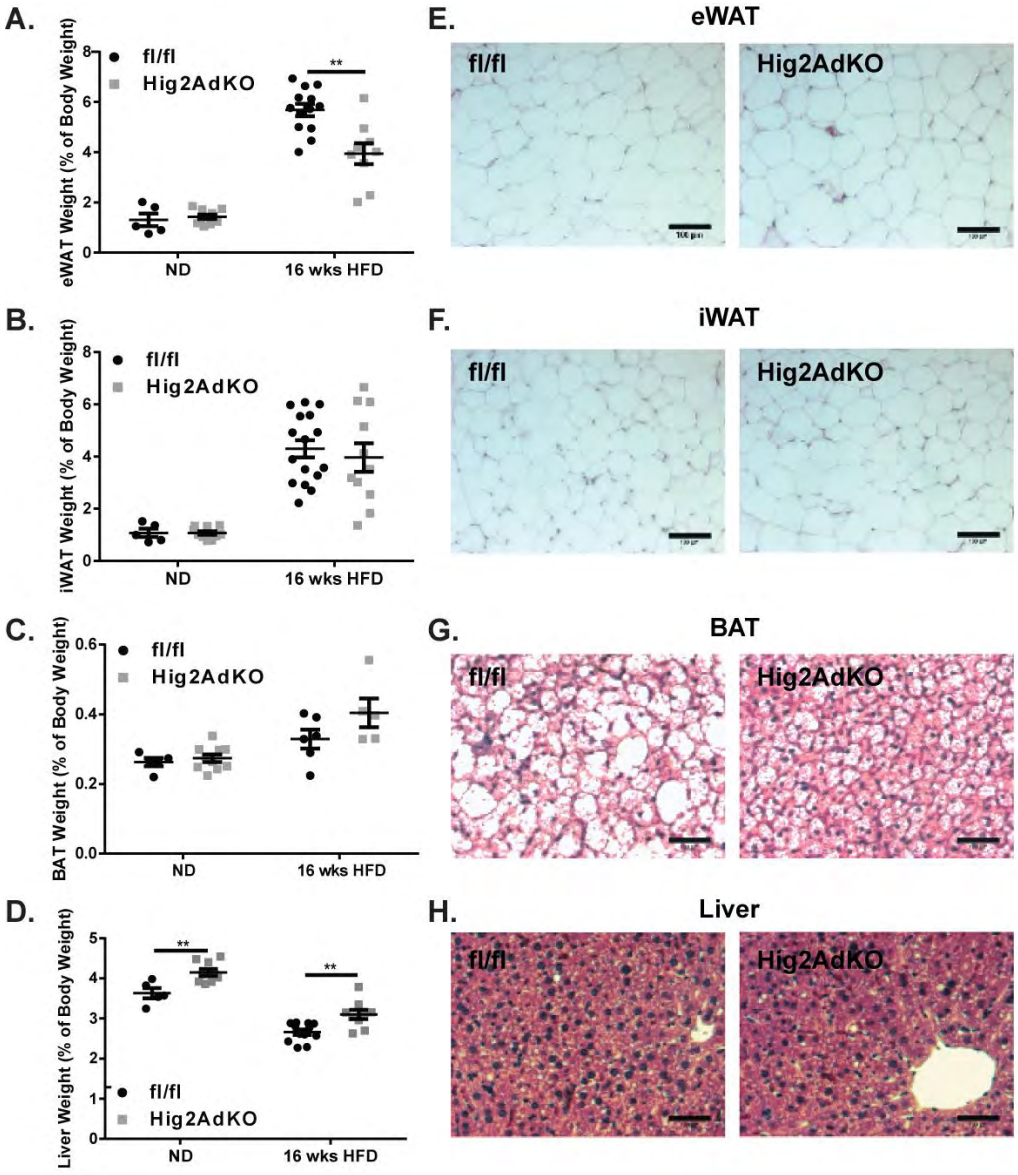

FIGURE 3.6 Adipocyte-specific Hig2 deficiency alters adipose tissue distribution in HFD-fed mice at 23°. A-H, fl/fl or Hig2AdKO animals were fed ND or HFD for 16 weeks. A-D, Tissues were weighed and normalized to body weight. A, eWAT. (**, $p<0.01$, n=5-13). B, iWAT. (n=5-14). C, BAT. (n=5-10). D, liver. (**, $p<0.01$, n=5-12). Data are represented as individual values $\pm$ S.E. E-H, HFD tissues were sectioned and stained with H&E. E, eWAT. F, iWAT. G, BAT. H, Liver.

Thermoneutrality abrogates the improved glucose tolerance in adipocyte-specific Hig2-deficient mice.

Mice are often housed at 23°C, which presents a cold stress and persistent activation of thermogenic pathways. Cold stress increases catecholamine levels, thereby activating nonshivering thermogenesis in BAT and substantially increasing food intake and metabolic rate (60). Thus, it is critical to characterize mice at thermoneutrality (30°C), a temperature which poses no thermal stress and little BAT activation (105,300,305). Recently, it has been demonstrated that mice with LD protein deficiencies placed at thermoneutrality more closely phenocopy lipodystrophic syndromes in humans with mutations in LD protein genes (248). For these reasons, Hig2AdKO animals were fed chow or HFD for 8 weeks at 23°C, then moved to 30°C for four weeks, and metabolic parameters were assessed.

While there were no differences in body weight or ITTs between genotypes when placed in thermoneutrality (Figure 3.7A,C), Hig2AdKO animals surprisingly had a significantly worsened glucose tolerance compared with fl/fl controls on a HFD (Figure 3.7B). This represented a marked reversal in glucose tolerance that was dependent on housing temperature, which is similar to the phenotype of Fsp27-deficient animals (248).

Figure 3.7 Thermoneutrality abrogates the improved glucose tolerance in adipocyte-specific Hig2-deficient mice.

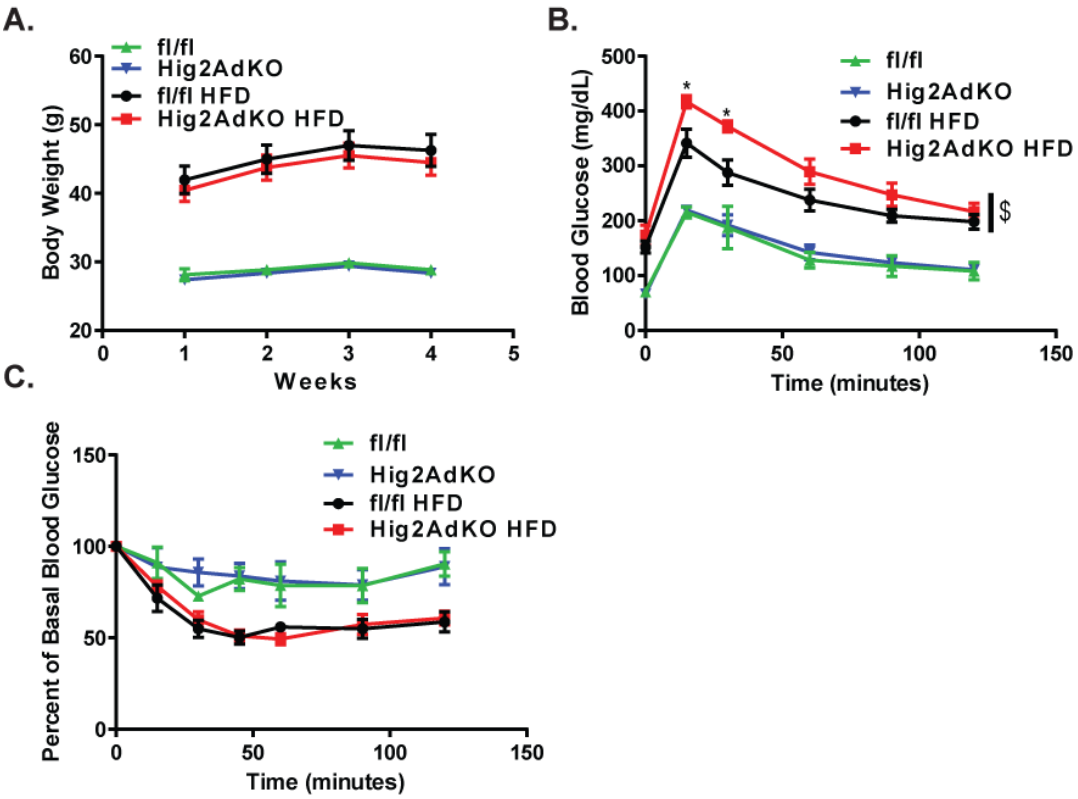

FIGURE 3.7 Thermoneutrality abrogates the improved glucose tolerance in adipocyte-specific Hig2-deficient mice. A-C, fl/fl or Hig2AdKO animals were fed ND or HFD for 8 weeks, then moved to 30°C for 4 weeks. A, body weight curves at 30°C. (n=3-9). B, glucose tolerance test. (*, $p<0.05$, $, $p<0.05$, two-way analysis of variance, n=3-10). C, insulin tolerance test. (n=3-5). Data are represented as the mean ± S.E.

Thermoneutrality abrogates the altered fat distribution in Adipocyte-specific Hig2-deficient mice.

As glucose tolerance on HFD was worsened with thermoneutral housing, alterations in fat distribution were also assessed. Indeed, the reduction in eWAT weight that was observed in Hig2AdKO animals at 23°C was abrogated when the animals were placed at thermoneutrality (Figure 3.8A). Furthermore, the increase in liver weight that was observed in Hig2AdKO animals at 23°C was also suppressed (Figure 3.8D); however, there continued to be no difference in iWAT or BAT weight between genotypes (3.8B,C). Additionally, H&E-stained histology sections of eWAT, iWAT, BAT, and liver were examined and no visual differences were observed between fl/fl and Hig2AdKO animals (Figure 3.8E-H), a striking contrast from 23°C, at which temperature the Hig2AdKO mouse BAT was cleared of lipids (Figure 3.8G). Serum and liver biochemical analyses were additionally examined in thermoneutrality and no differences were found between genotypes for all measured parameters (Table 3.2).Thus, all phenotypic differences in fl/fl vs. Hig2AdKO mice were abrogated at thermoneutrality (glucose tolerance, eWAT weight, liver weight, BAT lipid content), which suggests that these parameters may be mediated by BAT function that is dependent on activation of BAT by cold stress.

Figure 3.8 Thermoneutrality abrogates the altered fat distribution in Adipocyte-specific Hig2-deficient mice.

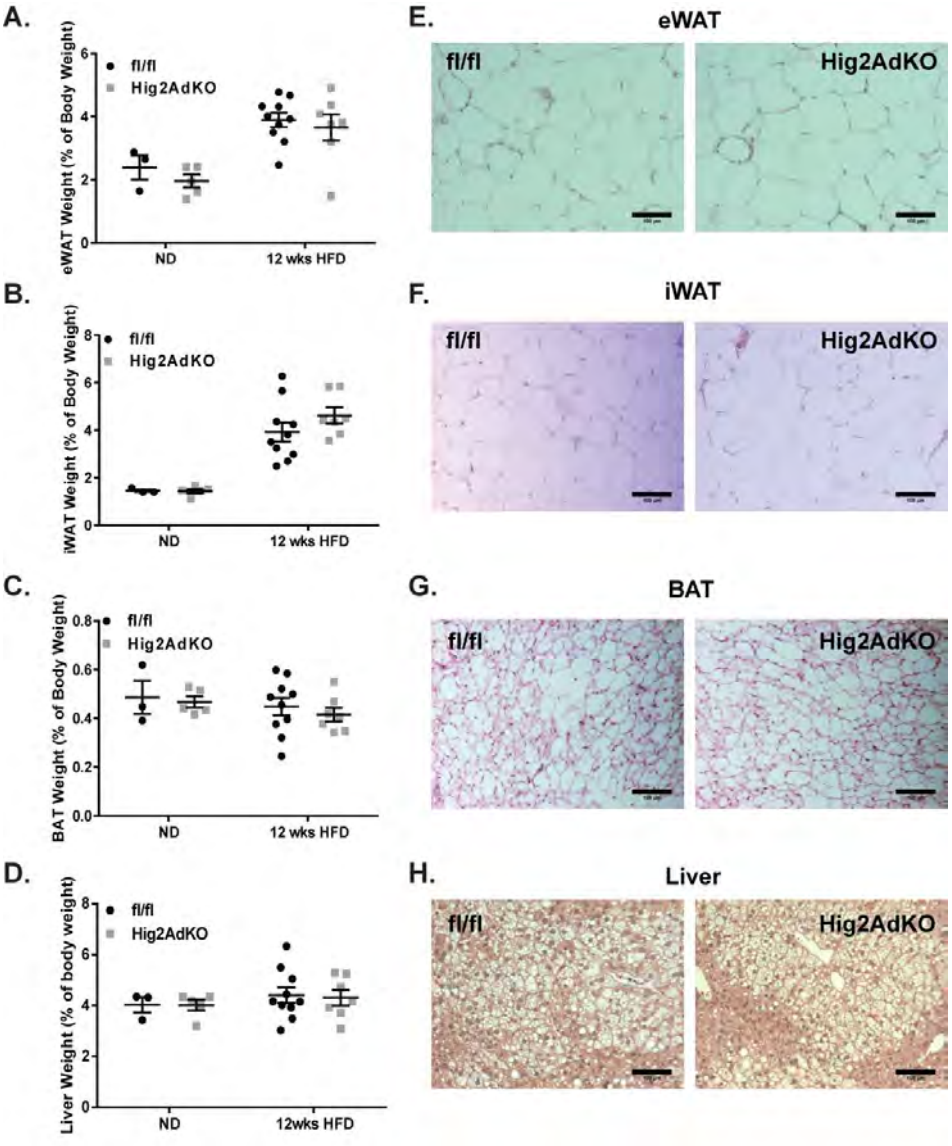

FIGURE 3.8 Thermoneutrality abrogates the altered fat distribution in Adipocyte-specific Hig2-deficient mice. A-H, fl/fl or Hig2AdKO animals were fed ND or HFD for 8 weeks, then moved to 30°C for 4 weeks. A-D, Tissues were weighed and normalized to body weight. A, eWAT. (n=3-10). B, iWAT. (n=3-10). C, BAT. (n=3-10). D, Liver. (n=3-10). Data are represented as individual values ± S.E. E-H, the indicated tissues were sectioned and stained with H&E. E, eWAT. F, iWAT. G, BAT. H, Liver.

Table 3.2

Liver cholesterol and serum metabolites were assessed from fl/fl or Hig2AdKO animals fed ND or HFD for 8 weeks then moved to 30°C for 4 weeks. (*n*=3-11). Data are the mean ± S.E. ND, not determined.

Parameters	**Normal Diet**		**12wks HFD**	
	Hig2 fl/fl	Hig2AdKO	Hig2 fl/fl	Hig2AdKO
Insulin (ng/ml)	ND	ND	2.956 ± 0.577	3.607 ± 0.304
Serum triglycerides (mg/dL)	101.1 ± 42.67	128.3 ± 23.05	89.03 ± 10.72	89.99 ± 8.815
Serum cholesterol (mg/dL)	678.3 ± 68.31	685.9 ± 75.38	1059 ± 57.95	1152 ± 22.41
NEFA (mmol/liter)	0.2132 ± 0.071	0.211 ± 0.032	0.312 ± 0.046	0.309 ± 0.051
Serum Glycerol (mg/ml)	0.021 ± 0.001	0.032 + 0.006	0.054 + 0.005	0.056 ± 0.006
Liver triglycerides (μg/mg)	7.277 ± 0.4573	8.222 ± 1.544	97.23 ± 8.578	88.36 ± 4.505
Liver cholesterol (μg/mg)	0.899 ± 0.191	0.868 ± 0.087	0.820 ± 0.093	0.720 ± 0.078

Adipocyte-specific Hig2 deficiency increases phosphorylated HSL, but does not alter ex vivo *glycerol release at 23°C.*

Hig2 deficiency was shown in Chapter II to increase lipolysis and β-oxidation in hepatocytes (304); thus, the role of Hig2 deficiency in adipocytes to control these parameters was investigated. *Ex vivo* glycerol release was measured from eWAT explants of fl/fl and Hig2AdKO animals in basal and isoproterenol-stimulated conditions, and no difference was found between genotypes (Figure 3.9A). Although there was no change in *ex vivo* basal or isoproterenol-stimulated glycerol release (Figure 3.9A), lipolytic gene expression was measured in eWAT to determine whether adipocyte-specific Hig2 deficiency altered lipolytic gene expression *in vivo*. There were significant approximately 2-fold expression increases in the lipase ATGL, as well as the LD protein Fsp27, both of which are responsive to increases in lipolysis (Figure 3.9B) (93,306,307). Furthermore, the LD protein Perilipin 1 was increased by 2-fold (Figure 3.9B), there was a non-significant trend to increased expression of the lipase HSL, and the two modulators of ATGL activity, Cgi58 and G0s2 were unchanged (Figure 3.8B). When immunoblots were performed on eWAT lysates from fl/fl and Hig2AdKO animals, phosphorylated HSL (pHsl) exhibited an approximately 5-fold increase in the Hig2AdKO mice compared with controls. This phosphorylation increase was specific to HSL, as the phosphorylation of other PKA substrates was unchanged between genotypes (Figure 3.9E). ATGL and total HSL (tHsl)

protein levels were also unchanged (Figure 3.9E,F), suggesting that adipocyte-specific Hig2 enhances some aspects of lipolytic signaling *in vivo*, independent of increases in glycerol release *ex vivo*.

To further probe these gene expression changes and because of the striking BAT lipid clearance observed in Hig2AdKO animals at 23°C, Ucp1, a gene critical for BAT function and Prdm16, a transcription factor essential for BAT identity (48), were measured in BAT by qRT-PCR; however, their expression was unchanged between genotypes (Figure 3.9D). Furthermore, the same genes, as indication of a BAT-like gene expression program (48), were assessed in iWAT but were also unchanged (Figure 3.9C).

These data suggest that adipocyte-specific Hig2 deficiency selectively increased phosphorylated HSL in eWAT *in vivo*, thus, it was assessed whether thermoneutrality, which abrogates the improvement in glucose tolerance in the Hig2AdKO animals (Figure 3.7) would also abrogate this increase.

Figure 3.9 Adipocyte-specific Hig2 deficiency increases phosphorylated HSL, but does not alter *ex vivo* glycerol release at 23°C.

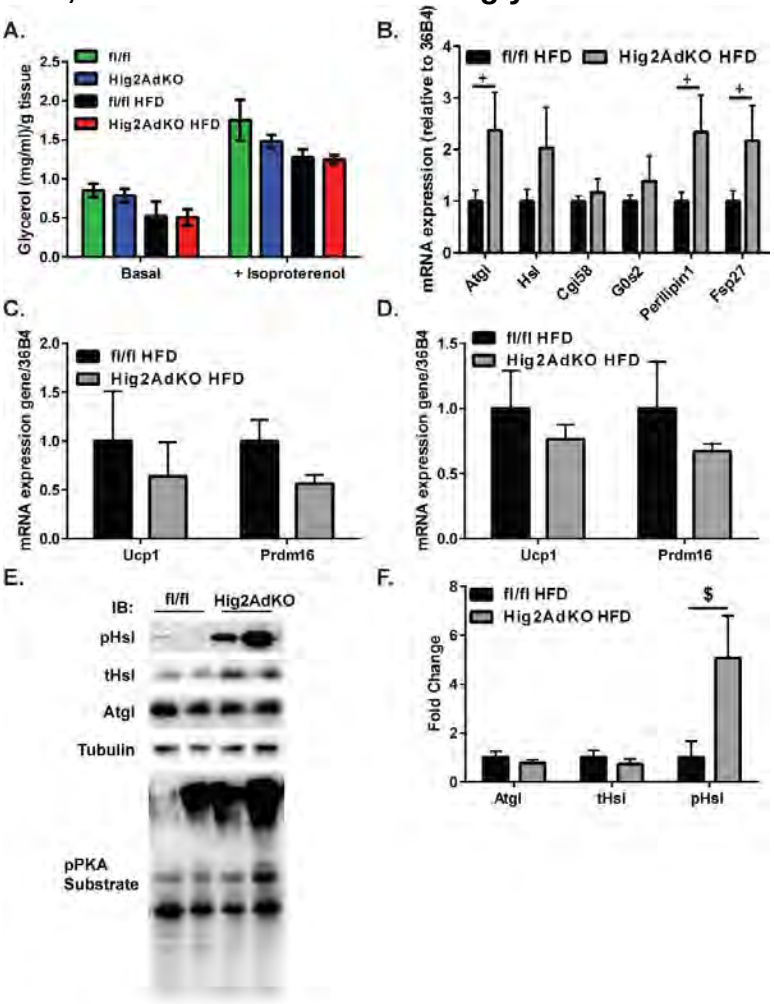

FIGURE 3.9 Adipocyte-specific Hig2 deficiency increases phosphorylated HSL, but does not alter *ex vivo* glycerol release at 23°C. A-G, fl/fl or Hig2AdKO animals were fed ND or HFD for 16 weeks. A, ex vivo lipolysis of eWAT. (n=3-5). Data are represented as the mean ± S.E. B-D, indicated tissues were isolated, RNA was extracted, and qRT-PCR was performed for the indicated genes and normalized to 36B4. B, HFD eWAT. (+, $p<0.09$, n=5-8). C, HFD iWAT. (n=4-10). D, HFD BAT. (n=4-8). Data are represented as the mean ± S.E. E, representative immunoblots from eWAT of phospho Hsl, total Hsl, Atgl, Tubulin, and phospho PKA substrate. IB, immunoblot; pHsl, phospho Hsl; tHsl, total Hsl. F, quantification of immunoblots from E, normalized to total HSL or Tubulin and fl/fl controls. ($, $p=0.08$, n=5). Data are represented as the mean ± S.E.

Thermoneutrality abrogates the increase in phosphorylated HSL in adipocyte-specific Hig2-deficient mice.

To determine whether thermoneutrality abrogated the differences that were observed in Hig2AdKO eWAT (Figure 3.9), an *ex vivo* lipolysis assay, qRT-PCR and immunoblots of lipolytic signaling genes were performed on eWAT from fl/fl and Hig2AdKO HFD animals housed at 30°C for 4 weeks. Similar to 23°C, there were no differences between genotypes in *ex vivo* glycerol release of eWAT explants (Figure 3.10A). The increases in ATGL, Perilipin1, and Fsp27 gene expression that were observed in Hig2AdKO eWAT at 23°C were all blunted at thermoneutrality, and expression levels of HSL, Cgi58, and G0s2 also remained unchanged (Figure 3.10B). Strikingly, the increase in pHSL that was observed at 23°C in Hig2AdKO mice was also suppressed in eWAT after thermoneutrality (Figure 3.10C,D), and tHSL, ATGL, and pPKA substrate protein levels remained unchanged (Figure 3.10B,C). These data suggest that thermoneutrality abrogates the increase in phosphorylated HSL in Hig2AdKO animals, which may partially explain the worsened glucose tolerance of these animals at thermoneutrality (Figure 3.7B).

Figure 3.10 Thermoneutrality abrogates the increase in phosphorylated HSL in adipocyte-specific Hig2-deficient mice.

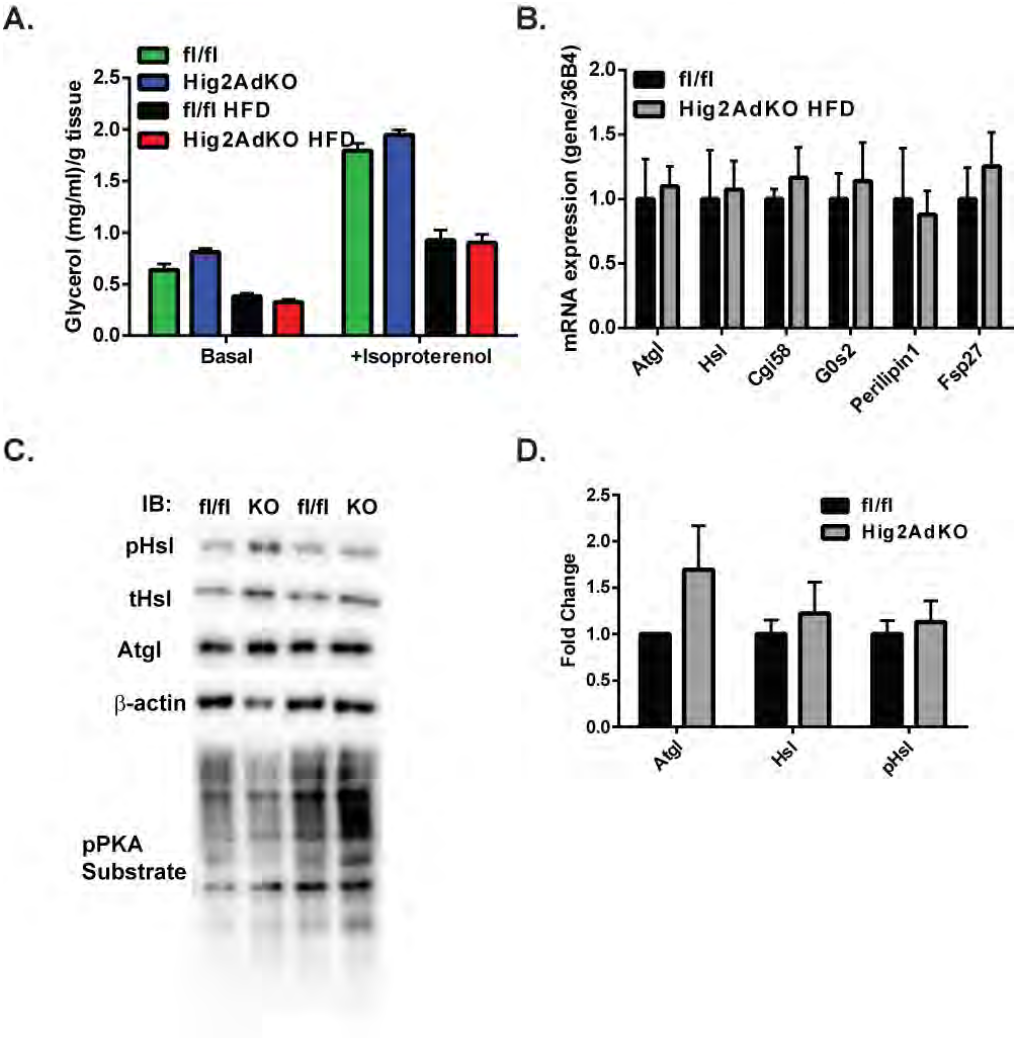

FIGURE 3.10 Thermoneutrality abrogates the increase in phosphorylated HSL in adipocyte-specific Hig2-deficient mice. A-G, fl/fl or Hig2AdKO animals were fed ND or HFD for 8 weeks, and then moved to 30°C for 4 weeks. A, ex vivo lipolysis of eWAT. (n=3-10). Data are represented as the mean ± S.E. B, eWAT was isolated from HFD animals, RNA was extracted, and qRT-PCR was performed for the indicated genes and normalized to 36B4. (n=4). Data are represented as the mean ± S.E. C, representative immunoblots (IB) from eWAT of phospho Hsl (pHsl), total Hsl (tHsl), Atgl, Tubulin, and phospho PKA substrate. IB, immunoblot; Ctl, control; KO, Hig2AdKO. D, quantification of immunoblots from E, normalized to total HSL or Tubulin and fl/fl controls. (n=4-5). Data are represented as the mean ± S.E.

Brown adipocyte-specific Hig2-deficient mice display brown adipocyte-specific deletion.

Thermoneutrality abrogated the improvement in glucose tolerance mediated by adipocyte-specific Hig2 deficiency and thermoneutrality reduces both lipolysis and brown fat activity (48). Furthermore, thermoneutrality abrogated the increase in phosphorylated HSL mediated by Hig2 deficiency (Figure 3.10). Thus, to elucidate the role of Hig2 specifically in the brown adipocyte, $Hig2^{fl/fl}$ animals were crossed to brown and beige/brite adipocyte-specific Ucp1 Cre+ animals to generate Hig2 brown adipocyte-specific knockout animals (Hig2BATKO) (Figure 3.11A).

Tissues were isolated from fl/fl and Hig2BATKO animals to assess deletion specificity. There was a significant reduction in Hig2 mRNA in whole BAT as measured by qRT-PCR (Figure 3.11B), but no reduction in other tissues such as white adipocytes, spleen, or kidney (Figure 3.11C,D), demonstrating that the deletion is specific. Interestingly, Hig2 expression was upregulated by approximately 7-fold in eWAT adipocytes of Hig2BATKO animals compared with floxed controls (3.11C).

Figure 3.11 Brown adipocyte-specific Hig2 deficient mice display brown adipocyte-specific deletion.

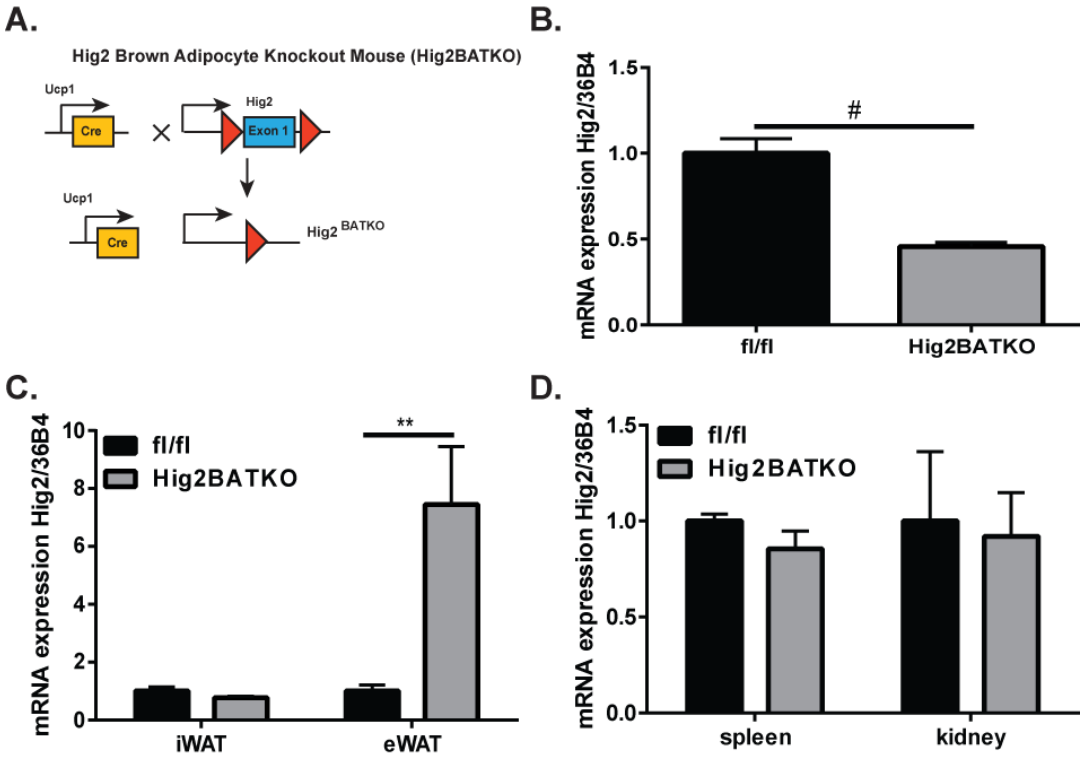

FIGURE 3.11 Brown adipocyte-specific Hig2-deficient mice display brown adipocyte-specific deletion. A, schematic of ucp1-cre-mediated Hig2 deletion. B-D indicated tissues were isolated from fl/fl and Hig2BATKO mice, RNA was extracted, and qRT-PCR was performed for Hig2 and normalized to 36B4. B, brown adipose tissue. (#, p<.001, n=7). C, isolated epididymal and inguinal adipocytes. (**, p<.01, n=3-7). D, kidney and spleen. (n=3-8). Data are represented as the mean ± S.E.

Brown adipocyte-specific Hig2 deficiency improves glucose tolerance under high fat-fed conditions at 23°C.

To evaluate the role of brown adipocyte-specific Hig2 deficiency on whole body metabolism at 23°C, fl/fl and Hig2BATKO animals were placed on HFD for 8 weeks and metabolic parameters were assessed. There were no differences in body weight or insulin tolerance between the genotypes (Figure 3.12A,C). However, when challenged with a GTT, Hig2BATKO animals were significantly more glucose tolerant compared to their fl/fl control littermates (Figure 3.12B), similar to the Hig2AdKO animals (Figure 3.4). Finally, no changes in *ex vivo* glycerol release from eWAT explants of fl/fl and Hig2BATKO animals were observed (Figure 3.12D). Taken together, these data suggest that the improvement in glucose tolerance in Hig2AdKO animals can be attributed to brown adipocyte-specific Hig2 deficiency.

Figure 3.12 Brown adipocyte-specific Hig2 deficiency improves glucose tolerance under high fat-fed conditions at 23°C.

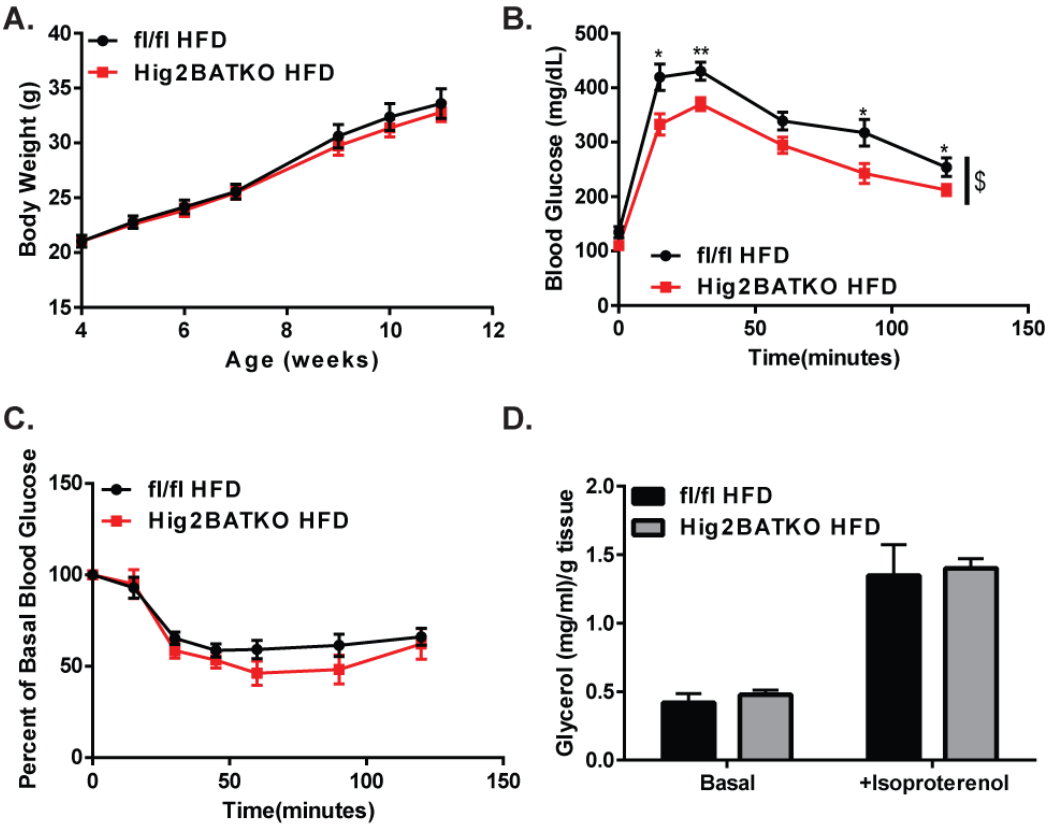

FIGURE 3.12 Brown adipocyte-specific Hig2 deficiency improves glucose tolerance under high-fat-fed conditions. A-D, fl/fl or Hig2BATKO animals were fed HFD for 8 weeks. A, body weight curves. (n=8-10). B, glucose tolerance test. (*, p<0.05, **, p<.01, $, p<.05, two-way analysis of variance, n=8-10). C, insulin tolerance test. (n=8-10). D, ex vivo lipolysis of eWAT. (n=3-8). Data are represented as the mean ± S.E.

Brown adipocyte-specific Hig2 deficiency does not alter adipose tissue distribution at 23°C.

To determine if Hig2 deficiency in brown adipocytes was responsible for the reduced eWAT weight and increased liver weight in Hig2AdKO animals, liver and fat pads were weighed from fl/fl and Hig2BATKO animals after 8 weeks of HFD at 23°C. eWAT, iWAT, BAT and liver weights were unchanged between genotypes (Figure 3.13A-D).

In accordance with these results, H&E-stained histological sections of eWAT, iWAT, BAT, and liver appeared to be unchanged between Hig2BATKO animals and fl/fl controls (Figure 3.13E-H). Serum biochemical analyses were also measured and displayed no remarkable differences between genotypes (Table 3.3). Taken together, these results demonstrate that brown adipocyte-specific Hig2 deficiency alone is not sufficient to redistribute fat deposition in WAT as observed in the Hig2AdKO animals.

Figure 3.13 Brown adipocyte-specific Hig2 deficiency does not alter adipose tissue weight after HFD at 23°C.

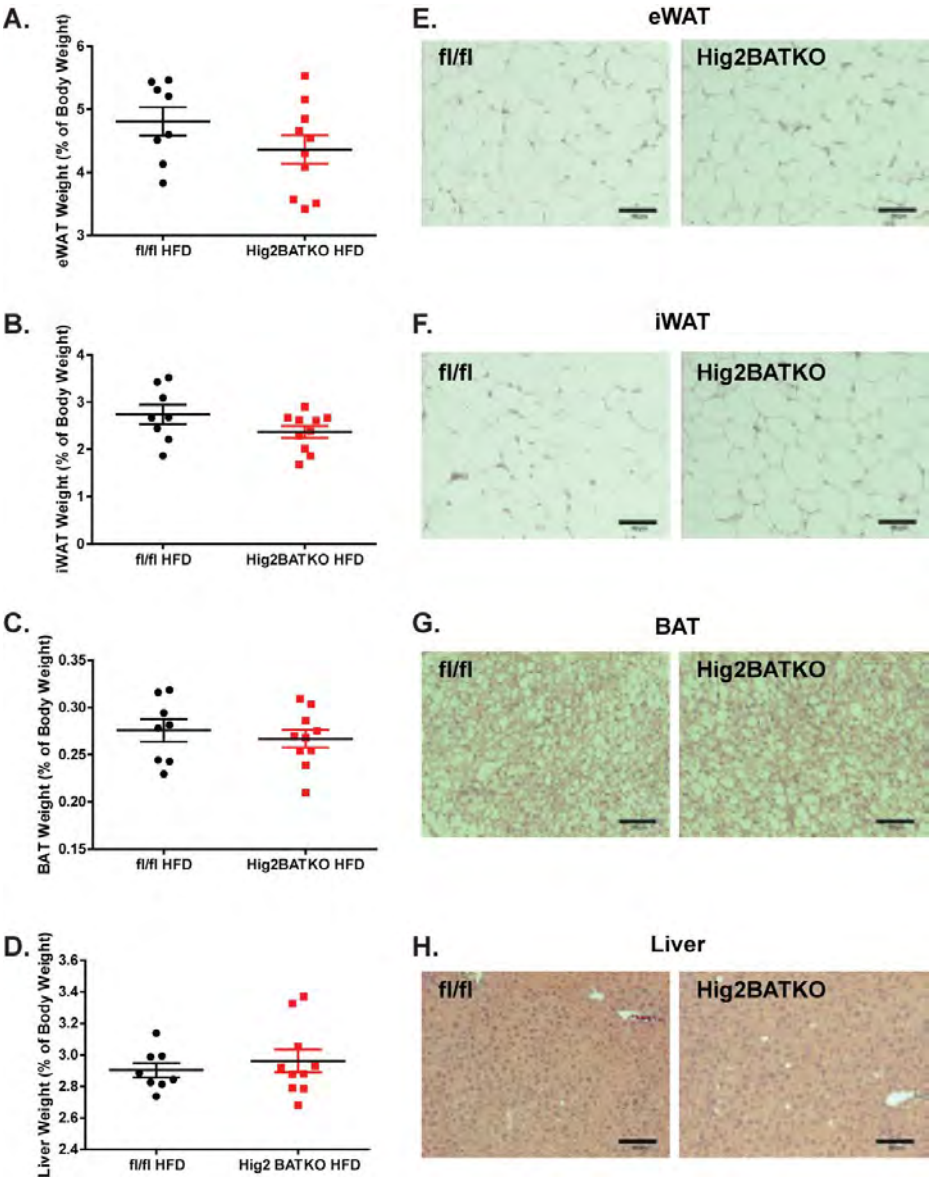

FIGURE 3.13 Brown adipocyte-specific Hig2 deficiency does not alter adipose tissue weight after HFD at 23°C. A-H, fl/fl or Hig2BATKO animals were fed HFD for 8 weeks. A-D, Tissues were weighed and normalized to body weight. A, eWAT. (n=8-10). B, iWAT. (n=8-10). C, BAT. (n=8-10). D, liver. (n=8-10). Data are represented as individual values ± S.E. E-H, the indicated tissues were sectioned and stained with H&E. E, eWAT. F, iWAT. G, BAT. H, Liver.

Table 3.3

Liver cholesterol and serum metabolites were assessed from fl/fl or Hig2BATKO animals fed HFD for 8 weeks at 23°C. (*n*=3-8). Data are the mean ± S.E.

Parameters	**8wks HFD**	
	Hig2 fl/fl	Hig2BATKO
Serum triglycerides (mg/dL)	114.7 ± 17.81	83.83 ± 8.038
NEFA (mmol/liter)	0.688 ± 0.054	0.599 ± 0.064
Serum Glycerol (mg/ml)	0.044 + 0.003	0.050 ± 0.004
Liver triglycerides (μg/mg)	31.97 ± 4.869	31.40 ± 2.539

Discussion:

The results in this chapter show that Hig2 localized to LDs (Figure 3.2) and its expression increased with adipogenic differentiation in the human SGBS adipocyte cell line, and that it is a highly expressed gene in isolated adipocytes from human patients (Figure 3.1). Hig2 deficiency in adipocytes (Figure 3.3) of mice reduced eWAT mass, largely cleared BAT of lipids, and improved HFD-mediated glucose intolerance *in vivo* (Figure 3.4, 3.6, Table 3.1). Interestingly, these improvements were abrogated when the animals were placed at thermoneutrality for 4 weeks (Figure 3.7, 3.8, Table 3.2), suggesting that brown fat activity or other physiological responses to cold stress mediated these effects.

To test that hypothesis, lipolytic signaling and *ex vivo* glycerol release were measured in eWAT from animals housed at room temperature and thermoneutrality. Although glycerol release was unchanged between genotypes, strikingly, phosphorylation of HSL was significantly increased in eWAT of Hig2AdKO animals compared with controls (Figure 3.9). This increase in pHSL was abolished at thermoneutrality (Figure 3.10); thus, the increase in pHSL in Hig2AdKO animals is associated with fat redistribution (Figure 3.6) and improvement in glucose tolerance (Figure 3.4) at room temperature, but a causative connection is not clear. Although insulin levels are significantly increased in Hig2AdKO animals with 16 week high-fat feeding (Table 3.1), they are likely not the cause of the improved glucose tolerance in these animals, as

glucose tolerance is also improved in Hig2AdKO animals fed HFD for 8 weeks, a time point when insulin levels are unchanged (Figure 3.4).

Finally, to examine the role of brown-adipocyte-specific Hig2, Hig2BATKO animals were generated and metabolically characterized. These animals displayed no improvements in serum parameters, histology, or adipose tissue distribution, but had significantly improved glucose tolerance, suggesting that brown adipocytes alone have little role to regulate the altered lipid deposition in eWAT or clearing of BAT lipids in Hig2AdKO animals, but play a significant role in the metabolic improvements that were observed (Figure 3.12, 3.13, Table 3.3). The mechanism whereby brown adipocyte-specific Hig2-deficiency prevents obesity-associated glucose intolerance is currently unclear. Unchanged food intake, oxygen consumption, energy expenditure, and RER in the Hig2AdKO animals (Figure 3.5) suggest that improvements may be mediated independent of BAT thermogenesis. One possibility points to the putative endocrine function of BAT. Recent experiments suggest that, in addition to its thermogenic properties, activated BAT may function as an endocrine organ and can secrete beneficial molecules that improve overall metabolic health (308-312). For instance, transplanting BAT into WAT of diabetic mice promoted adipogenesis and restored euglycemia (313). Taken together, these data suggest that Hig2 localizes to LD in human and mouse adipocytes that adipocyte-specific Hig2 promotes glucose intolerance in mice.

Although some of these data point towards inhibition of adipose tissue lipolysis as a potential mechanism for Hig2-mediated lipid deposition, much like the hepatocyte-specific mechanism, the exact mechanistic details need to be discerned and are still an area of active investigation. As the most striking change is the induction of pHSL, Hig2 could somehow be acting directly on HSL to prevent that activation. Interestingly, although pHSL is significantly increased in the eWAT of Hig2AdKO animals, other readouts of lipolytic stimulation, such as pPKA substrate proteins, *ex vivo* glycerol release, serum NEFAs, and serum glycerol are all unchanged (Figure 3.9, Table 3.1). These perplexing results raise several possibilities. First, the unchanged *ex vivo* glycerol release suggests that there may be crosstalk between multiple tissues *in vivo* and that this crosstalk is necessary for increased lipolysis in the eWAT as manifested by a reduction in its pad weight. This is underscored by the fact that adipocyte-specific Hig2 deficiency increases liver weight and clears lipids in BAT and thus redistributes lipids throughout tissues *in vivo*. Second, the lack of change in lipolysis readouts in serum suggests that Hig2 may regulate lipolysis locally; thus, these alterations are not substantial enough to be detected systemically. Third, Hig2 could be promoting lipid deposition by an entirely different mechanism than lipolytic inhibition.

Metabolic characterization of the Hig2BATKO animals suggests that brown adipocyte-specific deficiency of Hig2 is not sufficient to alter fat distribution

of WAT, but improves diet-mediated glucose intolerance. Future experiments targeting Hig2 specifically in white adipocytes would be useful to determine its true contribution to the phenotype of Hig2AdKO animals. As crosstalk has already been suggested, it might be true that Hig2 deletion in both brown and white adipocytes is necessary to mediate the fat redistribution, but the improvements observed in glucose tolerance are solely mediated by brown adipocytes.

Thermoneutrality experiments, which more accurately represent human clothing conditions, demonstrate that adipocyte-specific Hig2 deletion is detrimental to metabolic health (Figure 3.7). As Hig2 is localized to LDs in human adipocytes and is highly expressed in adipocytes of human patients (Figure 3.1,3.2), it will be interesting to investigate whether there are human mutations in Hig2, much like the canonical LD proteins Perilipin 1, and Fsp27/Cidec (251,252,298), and if these mutations cause partial lipodystrophy and metabolic dysregulation. Future experiments to challenge the Hig2AdKO animals with cold exposure to evaluate glucose tolerance would be insightful due to hyper-activation of lipolysis and BAT at these temperatures (48).

In summary, Chapters II and III demonstrated that Hig2 is a ubiquitously expressed gene and its expression promotes lipid deposition and diet-induced glucose intolerance in adipose tissue and liver. Thus, it will be of interest to investigate the role of Hig2 in other tissues. LDs are relevant in a large variety of

cells; thus, the role of Hig2 in lipid deposition in other tissues is still largely unanswered and is an active area of investigation.

CHAPTER IV: Final summary, conclusions, and future directions

Proper adipose tissue lipid sequestration is critical for the prevention of lipotoxicity, dyslipidemia, and ectopic lipid deposition. Thus, our lab is particularly interested in novel regulators of lipid storage in adipocytes (204,215). Furthermore, elucidating hepatocyte-specific mechanisms that promote liver steatosis could provide therapeutic targets to prevent the initial and reversible stage of NAFLD. One potential regulator of adipocyte lipid storage and hepatic steatosis is the LD protein Hig2. Work presented here was aimed at answering the following two questions:

1) **Does Hig2 function as a canonical LD protein in adipose tissue or liver and promote TG deposition by inhibition of lipolysis?**
2) **What is the contribution of hepatocyte and adipocyte-specific Hig2 to whole body metabolism?**

To answer those questions in liver, I first ectopically expressed a GFP-tagged Hig2 in primary hepatocytes and determined that GFP-Hig2 localized to Oil Red-O positive LDs (Figure 2.1). This localization was dependent upon its previously identified “LD-targeting domain” (Figure 2.1) (263), as a truncated mutant no longer localized to LDs when ectopically expressed in hepatocytes (Figure 2.1). To determine if Hig2 expression promoted lipid deposition, I overexpressed Hig2 in primary murine hepatocytes, extracted TGs, and determined that Hig2 overexpression increased TG levels (Figure 2.2). Conversely, using a tamoxifen-inducible cre model, I inducibly deleted Hig2 from

hepatocytes in culture and determined that Hig2-deficient hepatocytes displayed reduced LD size, LD number, and TG content (Figure 2.3,2.4). To elucidate the role of hepatocyte-specific Hig2 in whole body metabolism, I used an albumin promoter-driven cre recombinase to delete Hig2 specifically in hepatocytes (Figure 2.5). By the standard measures of metabolic characterization (insulin tolerance test, glucose tolerance test, plasma and liver biochemistry, organ weights, histology), I determined that hepatocyte-specific Hig2 deletion improved glucose tolerance in chow-fed and HFD-fed mice and reduced liver weight and liver TGs in chow-fed mice (Figure 2.6). Furthermore, to elucidate the mechanism whereby Hig2 promoted lipid deposition, I measured expression of lipid handling genes in chow-fed control and Hig2-deficient livers and found to them be unchanged (Figure 2.7). This suggested that Hig2 deficiency may alter lipid flux, independent of gene expression changes. To investigate lipid flux, I performed tracer experiments with [^{3}H] oleic acid and found that Hig2-deficient hepatocytes had decreased uptake of tracer lipids, increased production of acid-soluble oxidation products and increased turnover of tracer lipids, suggesting that Hig2 deficiency increases lipolysis and β-oxidation (Figure 2.8). Thus, my data suggest the answers to the two questions above in liver are: First, Hig2 does function as a canonical LD protein in hepatocytes and promotes TG deposition by inhibiting lipolysis. Second, hepatocyte-specific Hig2 promotes hepatic lipid deposition and glucose intolerance.

To answer the two questions in adipose tissue, I first imaged endogenous Hig2 in the human SGBS adipocyte cell line and determined that Hig2 localized to Bodipy-positive LDs (Figure 3.2). Its expression in SGBS also increased with adipogenic differentiation, similar to other canonical LD proteins (Figure 3.1). To elucidate the role of adipocyte-specific Hig2 and determine if adipocyte-specific Hig2 deficiency altered lipolysis, I used an adiponectin promoter-driven cre to delete Hig2 specifically in adipocytes (Figure 3.3). By the standard measures of metabolic characterization (insulin tolerance test, glucose tolerance test, plasma and liver biochemistry, organ weights, histology), I determined that adipocyte-specific Hig2 deficient animals had improved glucose tolerance, reduced eWAT weight, and BAT that was largely cleared of lipids upon HFD feeding (Figure 3.4, 3.6). An increase in phosphorylated HSL was present in the adipocyte-specific Hig2-deficient animals (Figure 3.9), although serum NEFAs and ex vivo glycerol release were unchanged (Table 3.1, Figure 3.9), suggesting that adipocyte-specific Hig2 deficiency may not alter lipolysis. Metabolic improvements and the increase in pHSL were largely abrogated when adipocyte-specific Hig2-deficient animals were moved to 30°C thermoneutrality, a temperature with minimal thermal stress and little BAT activation (Figure 3.7, 3.8, 3.10). To assess the role of brown adipocyte-specific Hig2 in whole body metabolism, I used a UCP1 promoter-driven cre to delete Hig2 specifically in brown adipocytes (Figure 3.11). I determined that brown adipocyte-specific Hig2 deficient animals had improved

glucose tolerance, but no changes in fat pad distribution, suggesting that brown adipocyte-specific Hig2 deficiency may specifically mediate the glucose tolerance improvements in adipocyte-specific Hig2-deficient animals (Figure 3.12, 3.13). Thus, my data suggest the answers to the two questions above in adipose tissue are: First, Hig2 does function as a LD protein in adipocytes, but may not promote TG deposition by inhibiting lipolysis. Second, adipocyte-specific Hig2 promotes adipose tissue lipid deposition and glucose intolerance.

In summary, the data in this thesis confirm that Hig2 is indeed a LD-localized protein in adipocytes and hepatocytes. Furthermore, the studies advance our understanding of the role of Hig2 as a LD protein that promotes lipid deposition and diet-induced glucose intolerance in two highly metabolically active tissues, liver and adipose tissue (Table 4.1), suggesting that Hig2 is a promising therapeutic target for the prevention of obesity and hepatic steatosis in NAFLD.

Table 4.1

	Hig2LKO	Hig2AdKO	Hig2BATKO
Cre Promoter	**Albumin**	**Adiponectin**	**Ucp1**
Tissue Deleted	Hepatocytes	Adipocytes	Brown and Beige/Brite Adipocytes
23°C			
Chow Fed	Improved GTT	Increased liver weight	No change
	Reduced liver weight		
	Reduced liver TG		
HFD-Fed	Improved GTT	Improved GTT	Improved GTT
	No change liver weight	Increased liver weight	No change liver weight
	No change liver TG	Decreased eWAT weight	No change eWAT weight
		BAT cleared of lipids	No change BAT lipids
		No change RER, energy expenditure	
30°C			
Chow Fed	N/A	No change	N/A
HFD-Fed	N/A	Worsened GTT	N/A
		No change liver weight	
		No change eWAT weight	
		No change BAT	

The phenotypes for all metabolically characterized Hig2 knockout animal models are summarized above. N/A; not applicable, HFD; high fat diet, GTT; glucose tolerance test, TG; triglyceride, eWAT; epididymal white adipose tissue, BAT; brown adipose tissue, RER; respiratory exchange ratio.

A role for Hig2 as a LD protein in hepatocytes

This section will discuss my interpretations, potential pitfalls, and future directions for the studies presented in Chapter II. Hig2 localized to LDs in the HeLa and Huh7 human cancer cell lines (263); thus, I hypothesized that Hig2 could act as a LD protein in metabolically active tissues if it were expressed there. I performed expression profiling of murine Hig2 and found that Hig2 was indeed expressed in a variety of mouse tissues (Figure 2.10), including liver, thus I decided to evaluate the role of Hig2 in hepatic lipid deposition as a potential therapeutic target for NAFLD. One caveat of this experiment is that I profiled the mRNA expression of Hig2, which could differ from Hig2 protein levels. To more accurately characterize tissue-specific Hig2 levels, western blots should be performed in the future. As Hig2 was expressed in liver, I hypothesized that Hig2 may act as a LD protein in hepatocytes and promote lipid deposition.

To begin to address my hypothesis, I ectopically expressed a GFP-tagged Hig2 in primary mouse hepatocytes and determined that Hig2 localized to Oil-Red-O positive LDs (Figure 2.1B). The concerns with this experiment are one, the ectopic expression of Hig2 and two, that a 7kDa protein (Hig2) is tagged with a 27kDa protein (GFP), both of which may alter its localization. To begin to address these concerns, I GFP tagged Hig2 on its N and C terminus and expressed both GFP-Hig2 (Figure 2.1B) and Hig2-GFP (not shown) in primary hepatocytes and found that they both localize to LDs, while GFP alone did not

(Figure 2.1B). The ideal experiment would be to image endogenous Hig2 in primary mouse hepatocytes, but both commercial antibodies and the antibody we synthesized in conjunction with Rockland Immunochemicals are not sufficiently sensitive for immunofluorescence in hepatocytes. Additionally, biochemical analyses, such as cell fractionation and western blotting should be performed to confirm the LD localization of Hig2. I was able to confirm that the 28 N-terminal AA are required for LD localization of Hig2 (Figure 2.1A) (263), as when I ectopically expressed a truncated Hig2-GFP mutant and imaged by microscopy, it no longer localized to LDs (Figure 2.1B). As I determined that Hig2 localized to LDs in hepatocytes dependent upon its N terminal LD-targeting domain, I proceeded to characterize it as a LD protein in hepatocytes.

Expression of liver-specific LD proteins, such as Fsp27 and Cidea are highly induced upon lipid deposition in liver (200). Thus, I measured the expression of Hig2 in fasting and diet-induced obesity, two models of increased liver lipid content, and found its expression to be significantly increased in both conditions (Figure 2.1C,D). As fasting increases hepatic PPARα expression (314) and Hig2 has been shown to be regulated by PPARα (267), PPARα likely mediates the increase in Hig2 expression in fasted mouse liver. The upstream regulator of hepatic Hig2 expression in obesity is currently unknown. I then hypothesized that modifying Hig2 expression would alter lipid deposition in hepatocytes. To answer this question, I infected primary mouse hepatocytes with

an HA-tagged Hig2 adenovirus and found that Hig2 was indeed overexpressed (Figure 2.2B) and that this overexpression increased TG content (Figure 2.2C). One can argue that overexpression experiments are highly artificial, although the result was additionally confirmed by another group that found that AAV-mediated hepatic Hig2 overexpression promoted steatosis in mice (267). To address overexpression concerns, I also wanted to delete Hig2 in isolated hepatocytes and evaluate TG levels and LDs. Thus, I deleted Hig2 using a tamoxifen-inducible ubiquitously expressed cre recombinase (Figure 2.3A) and confirmed that Hig2 was successfully deleted (Figure 2.3C,D). Using imaging analysis and TG extraction, I found that Hig2-deficient hepatocytes had less TGs (Figure 2.3E), fewer LDs (Figure 2.4A,B) and that the remaining LDs were smaller (Figure 2.4 C). These results were opposite of the overexpression results, further validating the hypothesis that hepatocyte-specific Hig2 expression promotes lipid deposition. As tamoxifen treatment can have side effects, I treated control hepatocytes with tamoxifen and imaged them to determine that tamoxifen treatment alone does not reduce TG content (Figure 2.4D). Additionally, I obtained the same results by using a hepatocyte-specific constitutively-expressed albumin cre recombinase to delete Hig2 (Figure 2.8A).

As Hig2 localized to LDs in hepatocytes and promoted lipid deposition, I strove to assess if Hig2 inhibited lipolysis and the role of hepatocyte-specific Hig2 deficiency on whole body metabolism. Considering Hig2-deficient hepatocytes

displayed reduced TG levels and LD number, I hypothesized that liver-specific Hig2 deficient animals would have reduced liver lipids and improved metabolic parameters when challenged with HFD, as hepatic steatosis is often correlated with insulin resistance and metabolic disease (274). To address this hypothesis, I derived hepatocyte-specific Hig2-deficient (Hig2LKO) mice using a hepatocyte specific albumin cre recombinase (Figure 2.5A) and confirmed that these animals displayed hepatocyte-specific Hig2 deletion (Figure 2.5 B,C,D). I challenged these mice with HFD and assessed their metabolic parameters (glucose tolerance test, insulin tolerance test, serum and liver biochemistry) and found that Hig2LKO animals displayed improved glucose tolerance when fed normal chow and HFD (Figure 2.6B), as I had hypothesized. I was surprised to find that this improvement in glucose tolerance was only associated with reduced liver weight and liver TGs in chow-fed animals (Figure 2.6D,E,F), while HFD-fed Hig2LKO animals displayed no alterations in liver TGs, liver weight, serum TGs, serum cholesterol, or serum NEFAs (Figure 2.6D,E,F, Table 2.1). One possible explanation for this is that other proteins may compensate for Hig2-deficiency in obesity-induced steatosis. For example, LD proteins such as Cidea and Fsp27 are not expressed in healthy liver, but are highly induced with development of hepatic steatosis (200). It is likely that their expression promotes obesity-induced steatosis independent of Hig2 deletion. To test this hypothesis, Hig2LKO animals could be injected with a lentivirus containing shCidea and shFsp27 constructs to

silence Cidea and FSP27 gene expression in liver and then liver biochemistry could be analyzed. Additionally, the mechanism by which Hig2 deficiency improves glucose tolerance in chow-fed animals and prevents obesity-associated glucose intolerance in HFD-fed animals is currently unknown. Chow-fed Hig2LKO animals displayed reduced liver lipids, a condition that has been correlated with improvements in insulin sensitivity (274), although this is not always the case (130). As HFD-fed Hig2LKO do not display reductions in liver lipids, the glucose tolerance improvement must be mediated by another means. For example, Hig2 deficiency could be altering the composition of liver lipids; the deficiency could increase the ratio of mono unsaturated FAs (MUFAs), the "benign FAs", to harmful saturated FAs (SFAs) to improve metabolic health (315), although this is highly speculative and expression of inflammatory markers such as TNFα, IL1β, IL6, and F4/80 is unchanged (Figure 2.7A). Lipidomic analysis of fl/fl and Hig2LKO livers will have to be completed in the future to determine if Hig2 deficiency alters hepatic lipid composition; currently, the mechanism for the Hig2 deficiency-mediated improvement in glucose tolerance is still under investigation.

To probe the mechanism of the reduced liver lipids in Hig2LKO chow-fed animals, I assessed gene expression of a range of genes known to control lipid handling and found them to be unchanged in Hig2LKO livers as compared with controls (Figure 2.7B,C). I interpreted this result to mean that Hig2 deficiency

reduced lipid deposition independent of gene expression changes. The caveat with this conclusion is that this gene expression analysis is specifically targeted; thus, changes in genes I did not measure could be responsible for the reduction in liver lipids. To form a broader picture of gene expression changes in Hig2LKO animals, whole-genome microarray or RNA-seq analysis should be performed on control and Hig2LKO chow-fed livers. As I could not discern any expression differences in lipid handling genes in Hig2LKO livers, I hypothesized that Hig2 deficiency may be altering lipid flux (enzyme activity, protein localization) independent of gene expression changes. To address this hypothesis, I performed tracer experiments with radioactive FAs, specifically [^{3}H] oleic acid, in Hig2-deficient hepatocytes. I determined that Hig2-deficient hepatocytes contained less radioactive lipid (Figure 2.8A). Next, I determined that Hig2-deficient hepatocytes had increased oxidation by measuring acid-soluble metabolites in the media of Hig2-deficient hepatocytes after overnight [^{3}H] oleic acid loading (Figure 2.8B). As this method merely measures oxidation products, it would be valuable to confirm the results by directly measuring oxidation in Hig2-deficient hepatocytes. This could be done either by measuring the oxygen consumption rate (OCR) on a Seahorse flux analyzer during a mitochondrial stress test or by loading cells with [^{14}C] oleic acid and quantifying the radioactive CO_2 directly formed from respiration. I hypothesize that both of these assays would demonstrate that Hig2 deficiency directly increases oxidation.

LD protein deficiencies often increase lipolysis; hence, I measured lipolysis via two different assays. As hepatocytes contain glycerol kinase, glycerol release cannot be used as readout of lipolysis (316). Thus, I demonstrated that Hig2-deficient hepatocytes have increased TG turnover (Figure 2.8C) and increased lipolysis (Figure 2.8D).

The studies in this chapter support the hypothesis that Hig2 is a LD protein in hepatocytes that promotes both glucose intolerance and lipid deposition. Although the mechanism whereby Hig2 promotes lipid deposition is currently unclear, the lipid tracer experiments (Figure 2.8) suggest that Hig2 may inhibit lipolysis, β-oxidation or both. Lipolytic inhibition is a well-characterized mechanism whereby LD proteins promote lipid deposition. For example, Perilipin 1 potently inhibits adipocyte lipolysis (180) and Fsp27 interacts directly with ATGL to inhibit lipolysis (240). Additionally, although some LD proteins may directly interact with mitochondrial proteins, β-oxidation can often be a consequence of increased lipid fuel being shunted to mitochondria, as in Fsp27 and Cidea-deficient cells (203,220), although this is only speculation in the case of Hig2 deficiency. Furthermore, Hig2 has sequence similarity with G0S2, a known inhibitor of the lipase ATGL, in the region where it is known to bind with ATGL (Figure 2.9); thus, Hig2 could act similarly by physically inhibiting ATGL. This could be tested via a combination of biochemical and imaging experiments. Imaging of ATGL and Hig2 in hepatocytes could be done and colocalization

calculated. Additionally, co-immunoprecipitation experiments could be performed to determine if Hig2 and ATGL physically interact. Finally, ATGL imaging in Hig2-deficient cells could be completed to determine if ATGL is mislocalized by Hig2 deficiency. There are still many unanswered questions about the role of Hig2 as a LD protein in hepatocytes, but the studies presented herein have laid the groundwork for future experiments by determining that Hig2 is a LD protein in hepatocytes that promotes lipid deposition likely by inhibiting lipolysis.

A role for Hig2 as a LD protein in adipocytes

This section will discuss my interpretations, potential pitfalls, and future directions for the studies presented in Chapter III. In the studies detailed in chapter II, I found that Hig2 is indeed a LD protein in hepatocytes and that its expression promotes glucose intolerance and lipid deposition likely by inhibition of lipolysis. Through my expression profile analysis, I had determined that Hig2 was also expressed in WAT and BAT (Figure 2.10B). Although I am currently unable to detect Hig2 protein in adipose tissue via western blot, new antibodies should be developed for protein level verification in future studies. Additionally, Hig2 was highly expressed in the adipocyte fraction of omental and subcutaneous adipose tissue from bariatric surgery patients (Figure 3.1B-D) and increased with obesity in murine eWAT (Figure 3.1A), suggesting that its expression may promote obesity-associated lipid deposition. Furthermore, Hig2 expression significantly increased with adipogenic differentiation in the human

SGBS adipocyte cell line (Figure 3.1F). Interestingly, this was not the case for the murine 3T3-L1 adipocyte cell line (Figure 3.1E) or primary murine iWAT preadipocytes differentiated in culture (data not shown), suggesting a differential transcriptional regulation in mouse vs human. To fully confirm this, Hig2 expression should be measured in isolated human preadipocytes differentiated in culture. Additionally, Hig2 protein levels should be measured upon adipogenic differentiation in mouse and human adipocytes, as these may differ entirely from Hig2 mRNA expression. These aforementioned results raise the question of how human and murine Hig2 transcripts differ in their regulation. One key difference between the human Hig2 gene and the mouse Hig2 gene is that the mouse Hig2 gene is suggested to have two mRNA transcript variants; according to NCBI gene database, Hig2 transcript variant 1 is 288 nucleotides long and encodes a longer Hig2 isoform. Hig2 transcript variant 2 is 195 nucleotides long, contains an alternate 5' exon, and uses a downstream start codon, compared to variant 1; as such, it potentially codes a Hig2 protein with a shorter N-terminus. I have aligned these sequences with my Hig2 qPCR primers and have found that my primers detect both variants. In the future, non-overlapping primers should be designed and expression profiling should be done for each variant. Perhaps one variant is highly induced upon adipogenic differentiation, while the other is reduced. Although murine Hig2 transcript variation warrants further investigation, I did not

pursue it in this work because human Hig2 does not contain this transcript variation.

I strove to answer the same two questions in adipose tissue as I had in liver. One, is Hig2 a LD protein that promotes lipid deposition in adipocytes by inhibiting lipolysis and two, what is the role of adipocyte-specific Hig2 on whole body metabolism?

To begin to answer these questions, I imaged endogenous Hig2 in mature SGBS adipocytes and found that Hig2 localized to Bodipy-positive LDs in these cells (Figure 3.2A,B). One particular caveat of this experiment is that I imaged with the antibody we made in conjunction with Rockland Immunochemicals and what I considered endogenous staining could merely be non-specific staining. Considering it is difficult to knockdown genes in human adipocytes and Hig2 is particularly difficult to knock down (data not shown), I confirmed that this staining was specific using a blocking peptide (data not shown). Additionally, I observed that undifferentiated SGBS cells had little to no Hig2 staining (data not shown), which aligned with Hig2 mRNA expression (Figure 3.1F), suggesting that the staining is indeed specific. I was able to confirm that ectopically expressed HA-tagged Hig2 localizes to LDs in 3T3-L1 adipocytes (Figure 3.2C), but need better antibodies to determine the localization of endogenous Hig2 in murine cells. Interestingly, the LD localization pattern of Hig2 in culture adipocytes, particularly SGBS cells, is unique. Canonical LD proteins often form uniform rings around

LDs, much like GFP-Hig2 does in hepatocytes (Figure 2.1B), but in SGBS adipocytes, Hig2 does not localize to all LDs and coats certain LDs in a discontinuous pattern. This localization pattern warrants further investigation and suggests that Hig2 may be localized to certain contact sites on LDs, such as LD-mitochondrial contact sites, LD-ER contact sites, or LD-LD contact sites. Further imaging and biochemical fractionation experiments will need to be done to answer this question.

As I had determined that Hig2 was a LD protein in adipocytes, I proceeded to investigate whether its expression promoted lipid deposition by lipolytic inhibition and the role of adipocyte-specific Hig2 in whole body metabolism. To this end, I derived an adipocyte-specific Hig2-deficient mouse (Hig2AdKO) by using an adipocyte-specific adiponectin promoter-driven cre recombinase (Figure 3.3A) and confirmed that Hig2AdKO animals had adipocyte-specific deletion (Figure 3.3B-D), although this should be further confirmed with immunoblots using newly developed antibodies in the future. I challenged Hig2AdKO animals with HFD, evaluated metabolic parameters (insulin tolerance test, glucose tolerance test, serum and liver biochemical analyses, histology, tissue weights) and determined that Hig2AdKO animals displayed improved glucose tolerance (Figure 3.4B), concomitant with a redistribution of ectopic lipids. Hig2AdKO animals had significantly reduced eWAT weight (Figure 3.6A), increased liver weight (Figure 3.6D), and, although there was no significant pad weight change,

BAT that was largely cleared of lipids (Figure 3.6G). These data suggest that, as in liver, adipocyte-specific Hig2 expression promotes both lipid deposition and obesity-associated glucose intolerance. Interestingly, the data also suggest inter-organ communication, as the liver, an organ without Hig2 deletion, is affected. This will be discussed further later on in this chapter.

As Hig2 is deleted in both WAT and BAT, I wanted to try and determine which tissue was responsible for the phenotype in the Hig2AdKO animals. As the BAT of Hig2AdKO animals was strikingly cleared of lipids, I focused on specifically targeting brown adipocytes. There are multiple ways to modulate BAT activity, such as temperature, BAT denervation and genetic deletion. I started by using temperature. Room temperature (23°C) presents a cold stress for mice, thereby promoting beta adrenergic stimulation, activating BAT, and increasing both food consumption and metabolism (60). By moving the Hig2AdKO mice to thermoneutrality (30°C), I removed this thermal stress, greatly reducing BAT activity and minimizing its contribution to whole body metabolism. When I moved HFD-fed Hig2AdKO animals to 30°C for four weeks and metabolically characterized them (insulin tolerance test, glucose tolerance test, serum and liver biochemical analyses, histology, tissue weights), I determined that all differences present in Hig2AdKO animals at 23°C were abrogated by thermoneutral housing. At 30°C, the Hig2AdKO animals had no improvement in obesity-induced glucose intolerance and were actually more glucose intolerant than fl/fl controls (Figure

3.7B). Furthermore, Hig2AdKO animals had no alterations in ectopic lipid deposition at 30°C; there were no differences in eWAT weight (Figure 3.8A), liver weight (Figure 3.8D), or, most strikingly, BAT lipid deposition (Figure 3.8G). These data suggest that the metabolic improvements in Hig2AdKO animals require functionally active BAT. To further test this hypothesis, I proceeded to delete Hig2 specifically in brown adipocytes and compare the whole body metabolism to that of the Hig2AdKO mice. I derived a brown adipocyte-specific Hig2-deficient animal (Hig2BATKO) by using a brown adipocyte-specific Ucp1 promoter-driven cre recombinase (Figure 3.11A) and confirmed that the deletion was specific (Figure 3.11B,C,D). I challenged these animals with HFD and evaluated their metabolic parameters (insulin tolerance test, glucose tolerance test, serum and liver biochemistry, histology, and organ weights) and found that Hig2BATKO animals displayed improved glucose tolerance (Figure 3.12B). This result suggested that Hig2 deletion in brown adipocytes may be wholly responsible for the glucose tolerance improvements in Hig2AdKO animals (Figure 3.4B). Surprisingly, Hig2BATKO animals did not demonstrate the alteration in organ-specific lipid deposition, as they did not differ from fl/fl controls in eWAT weight (Figure 3.13A), liver weight (Figure 3.13D), or BAT lipid deposition (Figure 3.13G). These results suggest that either white adipocyte-specific Hig2 deletion is responsible for alterations in organ weights or that both white and brown adipocyte-specific Hig2 deletion are necessary to alter organ-

specific lipid deposition. Future experiments genetically targeting Hig2 specifically in white adipocytes are necessary to answer this question.

The mechanism whereby brown adipocyte-specific Hig2 deficiency improves glucose tolerance is currently unknown, but recent experiments suggest that, in addition to its thermogenic properties, activated BAT may function as an endocrine organ and can secrete beneficial molecules that improve overall metabolic health (308-312). For instance, transplanting BAT into WAT of diabetic mice promoted adipogenesis and restored euglycemia potentially through increases in circulating insulin-like growth factor 1 (IGF1) (313). Thus, it would be of value to measure circulating IGF1 levels in both adipocyte-specific and brown adipocyte-specific Hig2-deficient animals. Furthermore, BAT secretes a pool of the active thyroid hormone triiodothyronine (T_3) and although its contribution to systemic T_3 is currently unknown, T_3 has potent effects on metabolic rate, gluconeogenesis, and lipolysis (317). Fibroblast growth factor 21 (FGF21) has also recently been demonstrated to be synthesized in thermogenic BAT; it is a powerful promoter of glucose oxidation in a variety of tissues, such as liver and WAT (312). Thus, both T_3 and FGF21 should also be measured in adipocyte-specific and brown adipocyte-specific Hig2-deficient animals. To take an unbiased approach in addition to measuring the candidates listed above, proteomic analysis should be performed on serum from fl/fl and Hig2BATKO animals. As all of these products are thought to be secreted by

stimulated BAT, it will also be useful to measure them in thermoneutrally housed Hig2AdKO animals.

To elucidate the mechanism whereby Hig2 deficiency alters organ-specific lipid deposition in Hig2AdKO animals (Figure 3.6), I measured lipolysis and assessed gene and protein expression in adipose tissues of Hig2AdKO animals as compared with fl/fl controls. I hypothesized that Hig2 deficiency may increase eWAT lipolysis, thus reducing its weight. To test this hypothesis, I measured *ex vivo* glycerol release of basal and isoproterenol-stimulated eWAT explants (Figure 3.9A). I found no differences in basal or stimulated glycerol release (Figure 3.9A), or more systemic measures of lipolysis, such as serum NEFAs or serum glycerol (Table 3.1). Nonetheless, I assessed lipase and LD protein expression in eWAT from Hig2AdKO and fl/fl control mice. I was surprised to find that certain lipolysis-responsive genes such as ATGL and Fsp27 were increased in Hig2AdKO eWAT as compared with fl/fl controls (Figure 3.9B). Even more surprising was the highly significant increase in induction of phosphorylated HSL in the knockouts, independent of increases in other PKA substrates (Figure 3.9E,F). These results suggest that Hig2 deficiency may specifically increase HSL phosphorylation independent of other lipolysis measures. I hypothesized that if this selective increase in lipolytic signaling, particularly pHSL, may be associated with the improvements in Hig2AdKO animals, that the changes would be abrogated in a condition where the improvements were abrogated:

thermoneutrality. To test this hypothesis, I measured all of the same parameters at 30°C and found that gene expression increases were abrogated (Figure 3.10B) and that the induction of pHSL was also abrogated (Figure 3.10C,D). Taken together, these data suggest that although adipocyte-specific Hig2 deficiency increases phosphorylated HSL, it may not alter lipid deposition by increasing lipolysis.

These results pose two questions; one, how does Hig2 deficiency alter lipid deposition without altering canonical measures of lipolysis? Two, why is phosphorylated HSL induced at 23°C in Hig2-deficient animals independently of other PKA substrates? At this point, the mechanism whereby Hig2 alters lipid deposition in adipocytes is still unknown. Metabolic cage measurements of HFD-fed Hig2 animals suggest that these changes are not due to increases in energy expenditure, physical activity or changes in food intake in Hig2AdKO animals (Figure 3.5). To fully explore the gene changes in Hig2-deficient animals that could be responsible for altering lipid deposition, microarray analyses should be completed with fl/fl and Hig2AdKO BAT and WAT. Because Hig2AdKO animals display changes in multiple tissue weights, including liver, a tissue in which Hig2 is not deleted, I hypothesize that there might be inter-organ communication between these tissues. Adipose tissue secretes a variety of adipokines that are known to alter whole body insulin sensitivity and potentially lipid deposition (318). Adiponectin is one known beneficial adipokine that was unchanged between

genotypes (Table 3.1). Another beneficial adipokine that was not measured was the satiety factor Leptin. Conversely, detrimental adipokines, such as Adipsin, Resistin, and Lipocalin are known to promote insulin resistance and their secretion from Hig2-deficient adipose tissue could be reduced (319). It would be valuable to check the circulating levels of a variety of adipokines to determine if their altered levels are altering metabolism in the adipocyte-specific Hig2-deficient animals.

Additionally, it is currently unknown why Hig2 deficiency selectively increases pHSL independent of other PKA substrates. One explanation for this could be that, in addition to Perilipin 1, Hig2 provides a LD scaffold for HSL upon its activation. Perhaps HSL is highly activated, but partially mislocalized. I could test this hypothesis by isolating preadipocytes from Hig2AdKO animals, differentiating them in culture, and imaging for HSL to determine its localization. If Hig2 does act as a scaffold, I hypothesize that pHSL would be localized to the cytoplasm instead of the LD. Additional biochemical experiments, such as co-immunoprecipitation and mutagenesis would also need to be done to confirm that Hig2 physically interacts with pHSL and that a certain Hig2 sequence is required for binding. The results of the ex vivo glycerol assays suggest that, unlike Perilipin 1, Hig2 is not fully required for stimulated lipolysis, as isoproterenol-stimulated glycerol release was not blunted in Hig2-deficient cells.

Finally, the role of Hig2 as a hypoxia-inducible LD protein cannot be ruled out as a mechanism for the changes in the Hig2AdKO animal. Although controversial, it is thought that obese adipose tissue becomes more hypoxic due to enlarged adipocytes and increased tissue mass (140,320). I have shown that obesity increases Hig2 expression in murine eWAT (Figure 3.1A) and have not ruled out that this may be due to increased hypoxia. Furthermore, adipocyte-specific genetic deletion of upstream hypoxia-responsive factors Hif1α and Hif1β also suggests that they are required for obesity-associated glucose intolerance and lipid deposition, as these animals displayed improved glucose tolerance and reduced fat mass and eWAT adipocyte size (321). This may be through a reduction in signal transducer and activator of transcription 3 (STAT3) activation by suppressor of cytokine signaling 3 (SOCS3), as hypoxia increases SOCS3 and SOCS3 inhibits insulin signaling by binding to the insulin receptor and inhibiting autophosphorylation (321). Hig2 deficiency could function similarly and SOCS3 and STAT3 should be examined in Hig2-deficient adipose tissue, although other independent hypoxia-regulated pathways could also be involved. Although there are still many unanswered questions regarding the role of Hig2 as a LD protein in adipocytes, these studies have laid the groundwork for future experiments by establishing that Hig2 is a LD protein in human and mouse adipocytes and that adipocyte-specific Hig2 promotes lipid deposition.

The work in this thesis has established a role for Hig2 as a LD protein in liver and adipocytes. I have shown that Hig2 localizes to LDs in both tissues (Figure 2.1, 3.2) and that its deficiency reduces both obesity-associated glucose intolerance (Figure 2.6, 3.4, 3.12) and lipid deposition (Figure 2.4, 2.6, 3.6), likely through lipolytic inhibition in hepatocytes (Figure 2.8), but not through lipolytic inhibition in adipocytes (Figure 3.9, Table 3.1). As Hig2 is ubiquitously expressed (Figure 2.10), future experiments should be done to examine the role of Hig2 as a potential LD protein in other tissues. For instance, foam cells are critical for the development of atherosclerosis (322). Although I have not measured Hig2 expression in isolated foam cells, Hig2 could be critical for lipid deposition in macrophages. Hig2 could also play a role in myocellular or cardiac lipid deposition. As hypoxia is dysregulated in cancer and human breast, prostate and colon cancer tumors with upregulated lipogenesis are associated with poor prognosis (169), Hig2 could also function as a LD protein that promotes lipid deposition in cancer cells. It will be of interest to determine whether the mechanism whereby Hig2 promotes lipid deposition is conserved in each tissue. Lipolysis readouts from Hig2-deficient liver (increased) and Hig2-deficient adipose tissue (unchanged) suggest that this may not be the case, but experiments pinpointing the exact mechanism still need to be done. Additionally, the role of human Hig2 needs to be further investigated and it would be of great

therapeutic value to detect, characterize, and validate Hig2 mutations in human patients.

Bibliography

1. Abdel-Misih, S. R., and Bloomston, M. (2010) Liver anatomy. *Surg Clin North Am* **90**, 643-653
2. Gentric, G., Desdouets, C., and Celton-Morizur, S. (2012) Hepatocytes polyploidization and cell cycle control in liver physiopathology. *Int J Hepatol* **2012**, 282430
3. Jenne, C. N., and Kubes, P. (2013) Immune surveillance by the liver. *Nat Immunol* **14**, 996-1006
4. Ebe, Y., Hasegawa, G., Takatsuka, H., Umezu, H., Mitsuyama, M., Arakawa, M., Mukaida, N., and Naito, M. (1999) The role of Kupffer cells and regulation of neutrophil migration into the liver by macrophage inflammatory protein-2 in primary listeriosis in mice. *Pathol Int* **49**, 519-532
5. Lee, W. Y., Moriarty, T. J., Wong, C. H., Zhou, H., Strieter, R. M., van Rooijen, N., Chaconas, G., and Kubes, P. (2010) An intravascular immune response to Borrelia burgdorferi involves Kupffer cells and iNKT cells. *Nat Immunol* **11**, 295-302
6. Fausto, N., and Campbell, J. S. (2003) The role of hepatocytes and oval cells in liver regeneration and repopulation. *Mech Dev* **120**, 117-130
7. Grant, D. M. (1991) Detoxification pathways in the liver. *J Inherit Metab Dis* **14**, 421-430
8. Miller, L. L., Bly, C. G., Watson, M. L., and Bale, W. F. (1951) The dominant role of the liver in plasma protein synthesis; a direct study of the isolated perfused rat liver with the aid of lysine-epsilon-C14. *J Exp Med* **94**, 431-453
9. de Aguiar Vallim, T. Q., Tarling, E. J., and Edwards, P. A. (2013) Pleiotropic roles of bile acids in metabolism. *Cell Metab* **17**, 657-669
10. Berg, J. M., Tymoczko, J.L., Stryer, L. (2002) Glycogen Metabolism. in *Biochemistry*, W H Freeman, New York. pp
11. Nguyen, P., Leray, V., Diez, M., Serisier, S., Le Bloc'h, J., Siliart, B., and Dumon, H. (2008) Liver lipid metabolism. *J Anim Physiol Anim Nutr (Berl)* **92**, 272-283
12. Leturque, A., Brot-Laroche, E., and Le Gall, M. (2009) GLUT2 mutations, translocation, and receptor function in diet sugar managing. *Am J Physiol Endocrinol Metab* **296**, E985-992
13. Wang, Y., Viscarra, J., Kim, S. J., and Sul, H. S. (2015) Transcriptional regulation of hepatic lipogenesis. *Nat Rev Mol Cell Biol* **16**, 678-689
14. Sul, H. S., Latasa, M. J., Moon, Y., and Kim, K. H. (2000) Regulation of the fatty acid synthase promoter by insulin. *J Nutr* **130**, 315S-320S
15. Cooper, A. D. (1997) Hepatic uptake of chylomicron remnants. *J Lipid Res* **38**, 2173-2192
16. Hegele, R. A. (2009) Plasma lipoproteins: genetic influences and clinical implications. *Nat Rev Genet* **10**, 109-121
17. Pittman, R. C., Attie, A. D., Carew, T. E., and Steinberg, D. (1979) Tissue sites of degradation of low density lipoprotein: application of a method for determining the fate of plasma proteins. *Proc Natl Acad Sci U S A* **76**, 5345-5349
18. Innerarity, T. L., and Mahley, R. W. (1978) Enhanced binding by cultured human fibroblasts of apo-E-containing lipoproteins as compared with low density lipoproteins. *Biochemistry* **17**, 1440-1447

19. Ishibashi, S., Herz, J., Maeda, N., Goldstein, J. L., and Brown, M. S. (1994) The two-receptor model of lipoprotein clearance: tests of the hypothesis in "knockout" mice lacking the low density lipoprotein receptor, apolipoprotein E, or both proteins. *Proc Natl Acad Sci U S A* **91**, 4431-4435
20. Berg, J. M., Tymoczko, J.L., Stryer, L. (2002) Epinephrine and Glucagon Signal the Need for Glycogen Breakdown. in *Biochemistry*, W H Freeman, New York. pp
21. Pilkis, S. J., el-Maghrabi, M. R., and Claus, T. H. (1988) Hormonal regulation of hepatic gluconeogenesis and glycolysis. *Annual review of biochemistry* **57**, 755-783
22. Garrison, J. C., and Wagner, J. D. (1982) Glucagon and the Ca2+-linked hormones angiotensin II, norepinephrine, and vasopressin stimulate the phosphorylation of distinct substrates in intact hepatocytes. *J Biol Chem* **257**, 13135-13143
23. Loten, E. G., Assimacopoulos-Jeannet, F. D., Exton, J. H., and Park, C. R. (1978) Stimulation of a low Km phosphodiesterase from liver by insulin and glucagon. *J Biol Chem* **253**, 746-757
24. Gross, D. N., van den Heuvel, A. P., and Birnbaum, M. J. (2008) The role of FoxO in the regulation of metabolism. *Oncogene* **27**, 2320-2336
25. Yoon, J. C., Puigserver, P., Chen, G., Donovan, J., Wu, Z., Rhee, J., Adelmant, G., Stafford, J., Kahn, C. R., Granner, D. K., Newgard, C. B., and Spiegelman, B. M. (2001) Control of hepatic gluconeogenesis through the transcriptional coactivator PGC-1. *Nature* **413**, 131-138
26. Jitrapakdee, S. (2012) Transcription factors and coactivators controlling nutrient and hormonal regulation of hepatic gluconeogenesis. *Int J Biochem Cell Biol* **44**, 33-45
27. Koo, S. H., Flechner, L., Qi, L., Zhang, X., Screaton, R. A., Jeffries, S., Hedrick, S., Xu, W., Boussouar, F., Brindle, P., Takemori, H., and Montminy, M. (2005) The CREB coactivator TORC2 is a key regulator of fasting glucose metabolism. *Nature* **437**, 1109-1111
28. Perry, R. J., Camporez, J. P., Kursawe, R., Titchenell, P. M., Zhang, D., Perry, C. J., Jurczak, M. J., Abudukadier, A., Han, M. S., Zhang, X. M., Ruan, H. B., Yang, X., Caprio, S., Kaech, S. M., Sul, H. S., Birnbaum, M. J., Davis, R. J., Cline, G. W., Petersen, K. F., and Shulman, G. I. (2015) Hepatic acetyl CoA links adipose tissue inflammation to hepatic insulin resistance and type 2 diabetes. *Cell* **160**, 745-758
29. Ailhaud, G., Grimaldi, P., and Negrel, R. (1992) Cellular and molecular aspects of adipose tissue development. *Annu Rev Nutr* **12**, 207-233
30. Berry, D. C., Stenesen, D., Zeve, D., and Graff, J. M. (2013) The developmental origins of adipose tissue. *Development* **140**, 3939-3949
31. Rodbell, M. (1964) Metabolism of Isolated Fat Cells. I. Effects of Hormones on Glucose Metabolism and Lipolysis. *J Biol Chem* **239**, 375-380
32. Rodeheffer, M. S., Birsoy, K., and Friedman, J. M. (2008) Identification of white adipocyte progenitor cells in vivo. *Cell* **135**, 240-249
33. Tang, W., Zeve, D., Suh, J. M., Bosnakovski, D., Kyba, M., Hammer, R. E., Tallquist, M. D., and Graff, J. M. (2008) White fat progenitor cells reside in the adipose vasculature. *Science* **322**, 583-586

34. Yamamoto, N., Akamatsu, H., Hasegawa, S., Yamada, T., Nakata, S., Ohkuma, M., Miyachi, E., Marunouchi, T., and Matsunaga, K. (2007) Isolation of multipotent stem cells from mouse adipose tissue. *J Dermatol Sci* **48**, 43-52
35. Crossno, J. T., Jr., Majka, S. M., Grazia, T., Gill, R. G., and Klemm, D. J. (2006) Rosiglitazone promotes development of a novel adipocyte population from bone marrow-derived circulating progenitor cells. *J Clin Invest* **116**, 3220-3228
36. Gupta, R. K., Mepani, R. J., Kleiner, S., Lo, J. C., Khandekar, M. J., Cohen, P., Frontini, A., Bhowmick, D. C., Ye, L., Cinti, S., and Spiegelman, B. M. (2012) Zfp423 expression identifies committed preadipocytes and localizes to adipose endothelial and perivascular cells. *Cell Metab* **15**, 230-239
37. Medici, D., Shore, E. M., Lounev, V. Y., Kaplan, F. S., Kalluri, R., and Olsen, B. R. (2010) Conversion of vascular endothelial cells into multipotent stem-like cells. *Nat Med* **16**, 1400-1406
38. Tran, K. V., Gealekman, O., Frontini, A., Zingaretti, M. C., Morroni, M., Giordano, A., Smorlesi, A., Perugini, J., De Matteis, R., Sbarbati, A., Corvera, S., and Cinti, S. (2012) The vascular endothelium of the adipose tissue gives rise to both white and brown fat cells. *Cell Metab* **15**, 222-229
39. Cinti, S. (2001) The adipose organ: morphological perspectives of adipose tissues. *Proc Nutr Soc* **60**, 319-328
40. Bjorndal, B., Burri, L., Staalesen, V., Skorve, J., and Berge, R. K. (2011) Different adipose depots: their role in the development of metabolic syndrome and mitochondrial response to hypolipidemic agents. *J Obes* **2011**, 490650
41. Casteilla, L., Penicaud, L., Cousin, B., and Calise, D. (2008) Choosing an adipose tissue depot for sampling: factors in selection and depot specificity. *Methods Mol Biol* **456**, 23-38
42. Wang, Q. A., Tao, C., Gupta, R. K., and Scherer, P. E. (2013) Tracking adipogenesis during white adipose tissue development, expansion and regeneration. *Nat Med* **19**, 1338-1344
43. Jeffery, E., Church, C. D., Holtrup, B., Colman, L., and Rodeheffer, M. S. (2015) Rapid depot-specific activation of adipocyte precursor cells at the onset of obesity. *Nat Cell Biol* **17**, 376-385
44. Lee, M. J., Wu, Y., and Fried, S. K. (2013) Adipose tissue heterogeneity: implication of depot differences in adipose tissue for obesity complications. *Mol Aspects Med* **34**, 1-11
45. Tran, T. T., Yamamoto, Y., Gesta, S., and Kahn, C. R. (2008) Beneficial effects of subcutaneous fat transplantation on metabolism. *Cell Metab* **7**, 410-420
46. Krotkiewski, M., Bjorntorp, P., Sjostrom, L., and Smith, U. (1983) Impact of obesity on metabolism in men and women. Importance of regional adipose tissue distribution. *J Clin Invest* **72**, 1150-1162
47. Cannon, B., and Nedergaard, J. (2004) Brown adipose tissue: function and physiological significance. *Physiol Rev* **84**, 277-359
48. Harms, M., and Seale, P. (2013) Brown and beige fat: development, function and therapeutic potential. *Nat Med* **19**, 1252-1263

49. Hany, T. F., Gharehpapagh, E., Kamel, E. M., Buck, A., Himms-Hagen, J., and von Schulthess, G. K. (2002) Brown adipose tissue: a factor to consider in symmetrical tracer uptake in the neck and upper chest region. *Eur J Nucl Med Mol Imaging* **29**, 1393-1398
50. Nedergaard, J., Bengtsson, T., and Cannon, B. (2007) Unexpected evidence for active brown adipose tissue in adult humans. *Am J Physiol Endocrinol Metab* **293**, E444-452
51. Yeung, H. W., Grewal, R. K., Gonen, M., Schoder, H., and Larson, S. M. (2003) Patterns of (18)F-FDG uptake in adipose tissue and muscle: a potential source of false-positives for PET. *J Nucl Med* **44**, 1789-1796
52. Sanchez-Gurmaches, J., and Guertin, D. A. (2014) Adipocyte lineages: tracing back the origins of fat. *Biochim Biophys Acta* **1842**, 340-351
53. Ouellet, V., Routhier-Labadie, A., Bellemare, W., Lakhal-Chaieb, L., Turcotte, E., Carpentier, A. C., and Richard, D. (2011) Outdoor temperature, age, sex, body mass index, and diabetic status determine the prevalence, mass, and glucose-uptake activity of 18F-FDG-detected BAT in humans. *J Clin Endocrinol Metab* **96**, 192-199
54. Lee, P., Greenfield, J. R., Ho, K. K., and Fulham, M. J. (2010) A critical appraisal of the prevalence and metabolic significance of brown adipose tissue in adult humans. *Am J Physiol Endocrinol Metab* **299**, E601-606
55. Ishibashi, J., and Seale, P. (2010) Medicine. Beige can be slimming. *Science* **328**, 1113-1114
56. Petrovic, N., Walden, T. B., Shabalina, I. G., Timmons, J. A., Cannon, B., and Nedergaard, J. (2010) Chronic peroxisome proliferator-activated receptor gamma (PPARgamma) activation of epididymally derived white adipocyte cultures reveals a population of thermogenically competent, UCP1-containing adipocytes molecularly distinct from classic brown adipocytes. *J Biol Chem* **285**, 7153-7164
57. Peirce, V., Carobbio, S., and Vidal-Puig, A. (2014) The different shades of fat. *Nature* **510**, 76-83
58. Wu, J., Cohen, P., and Spiegelman, B. M. (2013) Adaptive thermogenesis in adipocytes: is beige the new brown? *Genes Dev* **27**, 234-250
59. Himms-Hagen, J., Melnyk, A., Zingaretti, M. C., Ceresi, E., Barbatelli, G., and Cinti, S. (2000) Multilocular fat cells in WAT of CL-316243-treated rats derive directly from white adipocytes. *Am J Physiol Cell Physiol* **279**, C670-681
60. Nedergaard, J., and Cannon, B. (2014) The browning of white adipose tissue: some burning issues. *Cell Metab* **20**, 396-407
61. Chondronikola, M., Volpi, E., Borsheim, E., Porter, C., Annamalai, P., Enerback, S., Lidell, M. E., Saraf, M. K., Labbe, S. M., Hurren, N. M., Yfanti, C., Chao, T., Andersen, C. R., Cesani, F., Hawkins, H., and Sidossis, L. S. (2014) Brown adipose tissue improves whole-body glucose homeostasis and insulin sensitivity in humans. *Diabetes* **63**, 4089-4099
62. Trayhurn, P., and Beattie, J. H. (2001) Physiological role of adipose tissue: white adipose tissue as an endocrine and secretory organ. *Proc Nutr Soc* **60**, 329-339
63. Yamauchi, T., and Kadowaki, T. (2008) Physiological and pathophysiological roles of adiponectin and adiponectin receptors in the integrated regulation of metabolic and cardiovascular diseases. *Int J Obes (Lond)* **32 Suppl 7**, S13-18

64. Kim, J. Y., van de Wall, E., Laplante, M., Azzara, A., Trujillo, M. E., Hofmann, S. M., Schraw, T., Durand, J. L., Li, H., Li, G., Jelicks, L. A., Mehler, M. F., Hui, D. Y., Deshaies, Y., Shulman, G. I., Schwartz, G. J., and Scherer, P. E. (2007) Obesity-associated improvements in metabolic profile through expansion of adipose tissue. *J Clin Invest* **117**, 2621-2637
65. Margetic, S., Gazzola, C., Pegg, G. G., and Hill, R. A. (2002) Leptin: a review of its peripheral actions and interactions. *Int J Obes Relat Metab Disord* **26**, 1407-1433
66. Myers, M. G., Cowley, M. A., and Munzberg, H. (2008) Mechanisms of leptin action and leptin resistance. *Annu Rev Physiol* **70**, 537-556
67. Kersten, S. (2001) Mechanisms of nutritional and hormonal regulation of lipogenesis. *EMBO Rep* **2**, 282-286
68. Evans, K., Burdge, G. C., Wootton, S. A., Clark, M. L., and Frayn, K. N. (2002) Regulation of dietary fatty acid entrapment in subcutaneous adipose tissue and skeletal muscle. *Diabetes* **51**, 2684-2690
69. Eissing, L., Scherer, T., Todter, K., Knippschild, U., Greve, J. W., Buurman, W. A., Pinnschmidt, H. O., Rensen, S. S., Wolf, A. M., Bartelt, A., Heeren, J., Buettner, C., and Scheja, L. (2013) De novo lipogenesis in human fat and liver is linked to ChREBP-beta and metabolic health. *Nat Commun* **4**, 1528
70. Lin, J., Yang, R., Tarr, P. T., Wu, P. H., Handschin, C., Li, S., Yang, W., Pei, L., Uldry, M., Tontonoz, P., Newgard, C. B., and Spiegelman, B. M. (2005) Hyperlipidemic effects of dietary saturated fats mediated through PGC-1beta coactivation of SREBP. *Cell* **120**, 261-273
71. Lin, J., Handschin, C., and Spiegelman, B. M. (2005) Metabolic control through the PGC-1 family of transcription coactivators. *Cell Metab* **1**, 361-370
72. Nagai, Y., Yonemitsu, S., Erion, D. M., Iwasaki, T., Stark, R., Weismann, D., Dong, J., Zhang, D., Jurczak, M. J., Loffler, M. G., Cresswell, J., Yu, X. X., Murray, S. F., Bhanot, S., Monia, B. P., Bogan, J. S., Samuel, V., and Shulman, G. I. (2009) The role of peroxisome proliferator-activated receptor gamma coactivator-1 beta in the pathogenesis of fructose-induced insulin resistance. *Cell Metab* **9**, 252-264
73. Solinas, G., Boren, J., and Dulloo, A. G. (2015) De novo lipogenesis in metabolic homeostasis: More friend than foe? *Mol Metab* **4**, 367-377
74. Minehira, K., Vega, N., Vidal, H., Acheson, K., and Tappy, L. (2004) Effect of carbohydrate overfeeding on whole body macronutrient metabolism and expression of lipogenic enzymes in adipose tissue of lean and overweight humans. *Int J Obes Relat Metab Disord* **28**, 1291-1298
75. Salans, L. B., Knittle, J. L., and Hirsch, J. (1968) The role of adipose cell size and adipose tissue insulin sensitivity in the carbohydrate intolerance of human obesity. *J Clin Invest* **47**, 153-165
76. Weyer, C., Foley, J. E., Bogardus, C., Tataranni, P. A., and Pratley, R. E. (2000) Enlarged subcutaneous abdominal adipocyte size, but not obesity itself, predicts type II diabetes independent of insulin resistance. *Diabetologia* **43**, 1498-1506
77. Roberts, R., Hodson, L., Dennis, A. L., Neville, M. J., Humphreys, S. M., Harnden, K. E., Micklem, K. J., and Frayn, K. N. (2009) Markers of de novo lipogenesis in adipose tissue:

associations with small adipocytes and insulin sensitivity in humans. *Diabetologia* **52**, 882-890

78. Huang, S., and Czech, M. P. (2007) The GLUT4 glucose transporter. *Cell Metab* **5**, 237-252
79. Strable, M. S., and Ntambi, J. M. (2010) Genetic control of de novo lipogenesis: role in diet-induced obesity. *Critical reviews in biochemistry and molecular biology* **45**, 199-214
80. Chakravarthy, M. V., Pan, Z., Zhu, Y., Tordjman, K., Schneider, J. G., Coleman, T., Turk, J., and Semenkovich, C. F. (2005) "New" hepatic fat activates PPARalpha to maintain glucose, lipid, and cholesterol homeostasis. *Cell Metab* **1**, 309-322
81. Chakravarthy, M. V., Lodhi, I. J., Yin, L., Malapaka, R. R., Xu, H. E., Turk, J., and Semenkovich, C. F. (2009) Identification of a physiologically relevant endogenous ligand for PPARalpha in liver. *Cell* **138**, 476-488
82. Tzameli, I., Fang, H., Ollero, M., Shi, H., Hamm, J. K., Kievit, P., Hollenberg, A. N., and Flier, J. S. (2004) Regulated production of a peroxisome proliferator-activated receptor-gamma ligand during an early phase of adipocyte differentiation in 3T3-L1 adipocytes. *J Biol Chem* **279**, 36093-36102
83. Kim, J. B., and Spiegelman, B. M. (1996) ADD1/SREBP1 promotes adipocyte differentiation and gene expression linked to fatty acid metabolism. *Genes Dev* **10**, 1096-1107
84. Lodhi, I. J., Wei, X., and Semenkovich, C. F. (2011) Lipoexpediency: de novo lipogenesis as a metabolic signal transmitter. *Trends Endocrinol Metab* **22**, 1-8
85. Kliewer, S. A., Sundseth, S. S., Jones, S. A., Brown, P. J., Wisely, G. B., Koble, C. S., Devchand, P., Wahli, W., Willson, T. M., Lenhard, J. M., and Lehmann, J. M. (1997) Fatty acids and eicosanoids regulate gene expression through direct interactions with peroxisome proliferator-activated receptors alpha and gamma. *Proc Natl Acad Sci U S A* **94**, 4318-4323
86. Krey, G., Braissant, O., L'Horset, F., Kalkhoven, E., Perroud, M., Parker, M. G., and Wahli, W. (1997) Fatty acids, eicosanoids, and hypolipidemic agents identified as ligands of peroxisome proliferator-activated receptors by coactivator-dependent receptor ligand assay. *Mol Endocrinol* **11**, 779-791
87. Yu, K., Bayona, W., Kallen, C. B., Harding, H. P., Ravera, C. P., McMahon, G., Brown, M., and Lazar, M. A. (1995) Differential activation of peroxisome proliferator-activated receptors by eicosanoids. *J Biol Chem* **270**, 23975-23983
88. Arner, P. (1999) Catecholamine-induced lipolysis in obesity. *Int J Obes Relat Metab Disord* **23 Suppl 1**, 10-13
89. Haemmerle, G., Zimmermann, R., Hayn, M., Theussl, C., Waeg, G., Wagner, E., Sattler, W., Magin, T. M., Wagner, E. F., and Zechner, R. (2002) Hormone-sensitive lipase deficiency in mice causes diglyceride accumulation in adipose tissue, muscle, and testis. *J Biol Chem* **277**, 4806-4815
90. Osuga, J., Ishibashi, S., Oka, T., Yagyu, H., Tozawa, R., Fujimoto, A., Shionoiri, F., Yahagi, N., Kraemer, F. B., Tsutsumi, O., and Yamada, N. (2000) Targeted disruption of hormone-sensitive lipase results in male sterility and adipocyte hypertrophy, but not in obesity. *Proc Natl Acad Sci U S A* **97**, 787-792

91. Wang, S. P., Laurin, N., Himms-Hagen, J., Rudnicki, M. A., Levy, E., Robert, M. F., Pan, L., Oligny, L., and Mitchell, G. A. (2001) The adipose tissue phenotype of hormone-sensitive lipase deficiency in mice. *Obes Res* **9**, 119-128
92. Jenkins, C. M., Mancuso, D. J., Yan, W., Sims, H. F., Gibson, B., and Gross, R. W. (2004) Identification, cloning, expression, and purification of three novel human calcium-independent phospholipase A2 family members possessing triacylglycerol lipase and acylglycerol transacylase activities. *J Biol Chem* **279**, 48968-48975
93. Villena, J. A., Roy, S., Sarkadi-Nagy, E., Kim, K. H., and Sul, H. S. (2004) Desnutrin, an adipocyte gene encoding a novel patatin domain-containing protein, is induced by fasting and glucocorticoids: ectopic expression of desnutrin increases triglyceride hydrolysis. *J Biol Chem* **279**, 47066-47075
94. Zimmermann, R., Strauss, J. G., Haemmerle, G., Schoiswohl, G., Birner-Gruenberger, R., Riederer, M., Lass, A., Neuberger, G., Eisenhaber, F., Hermetter, A., and Zechner, R. (2004) Fat mobilization in adipose tissue is promoted by adipose triglyceride lipase. *Science* **306**, 1383-1386
95. Akiyama, M., Sakai, K., Ogawa, M., McMillan, J. R., Sawamura, D., and Shimizu, H. (2007) Novel duplication mutation in the patatin domain of adipose triglyceride lipase (PNPLA2) in neutral lipid storage disease with severe myopathy. *Muscle Nerve* **36**, 856-859
96. Fischer, J., Lefevre, C., Morava, E., Mussini, J. M., Laforet, P., Negre-Salvayre, A., Lathrop, M., and Salvayre, R. (2007) The gene encoding adipose triglyceride lipase (PNPLA2) is mutated in neutral lipid storage disease with myopathy. *Nat Genet* **39**, 28-30
97. Kobayashi, K., Inoguchi, T., Maeda, Y., Nakashima, N., Kuwano, A., Eto, E., Ueno, N., Sasaki, S., Sawada, F., Fujii, M., Matoba, Y., Sumiyoshi, S., Kawate, H., and Takayanagi, R. (2008) The lack of the C-terminal domain of adipose triglyceride lipase causes neutral lipid storage disease through impaired interactions with lipid droplets. *J Clin Endocrinol Metab* **93**, 2877-2884
98. Schweiger, M., Schoiswohl, G., Lass, A., Radner, F. P., Haemmerle, G., Malli, R., Graier, W., Cornaciu, I., Oberer, M., Salvayre, R., Fischer, J., Zechner, R., and Zimmermann, R. (2008) The C-terminal region of human adipose triglyceride lipase affects enzyme activity and lipid droplet binding. *J Biol Chem* **283**, 17211-17220
99. Vaughan, M., Berger, J. E., and Steinberg, D. (1964) Hormone-Sensitive Lipase and Monoglyceride Lipase Activities in Adipose Tissue. *J Biol Chem* **239**, 401-409
100. Nye, C., Kim, J., Kalhan, S. C., and Hanson, R. W. (2008) Reassessing triglyceride synthesis in adipose tissue. *Trends Endocrinol Metab* **19**, 356-361
101. Seale, P., Kajimura, S., and Spiegelman, B. M. (2009) Transcriptional control of brown adipocyte development and physiological function--of mice and men. *Genes Dev* **23**, 788-797
102. Nedergaard, J., Golozoubova, V., Matthias, A., Asadi, A., Jacobsson, A., and Cannon, B. (2001) UCP1: the only protein able to mediate adaptive non-shivering thermogenesis and metabolic inefficiency. *Biochim Biophys Acta* **1504**, 82-106
103. Seale, P. (2015) Transcriptional Regulatory Circuits Controlling Brown Fat Development and Activation. *Diabetes* **64**, 2369-2375

104. Enerback, S., Jacobsson, A., Simpson, E. M., Guerra, C., Yamashita, H., Harper, M. E., and Kozak, L. P. (1997) Mice lacking mitochondrial uncoupling protein are cold-sensitive but not obese. *Nature* **387**, 90-94
105. Feldmann, H. M., Golozoubova, V., Cannon, B., and Nedergaard, J. (2009) UCP1 ablation induces obesity and abolishes diet-induced thermogenesis in mice exempt from thermal stress by living at thermoneutrality. *Cell Metab* **9**, 203-209
106. Lidell, M. E., Betz, M. J., Dahlqvist Leinhard, O., Heglind, M., Elander, L., Slawik, M., Mussack, T., Nilsson, D., Romu, T., Nuutila, P., Virtanen, K. A., Beuschlein, F., Persson, A., Borga, M., and Enerback, S. (2013) Evidence for two types of brown adipose tissue in humans. *Nat Med* **19**, 631-634
107. Ouellet, V., Labbe, S. M., Blondin, D. P., Phoenix, S., Guerin, B., Haman, F., Turcotte, E. E., Richard, D., and Carpentier, A. C. (2012) Brown adipose tissue oxidative metabolism contributes to energy expenditure during acute cold exposure in humans. *J Clin Invest* **122**, 545-552
108. Orava, J., Nuutila, P., Lidell, M. E., Oikonen, V., Noponen, T., Viljanen, T., Scheinin, M., Taittonen, M., Niemi, T., Enerback, S., and Virtanen, K. A. (2011) Different metabolic responses of human brown adipose tissue to activation by cold and insulin. *Cell Metab* **14**, 272-279
109. Blondin, D. P., Labbe, S. M., Tingelstad, H. C., Noll, C., Kunach, M., Phoenix, S., Guerin, B., Turcotte, E. E., Carpentier, A. C., Richard, D., and Haman, F. (2014) Increased brown adipose tissue oxidative capacity in cold-acclimated humans. *J Clin Endocrinol Metab* **99**, E438-446
110. Macleod, J. J. (1922) Insulin and the steps taken to secure an effective preparation. *Can Med Assoc J* **12**, 899-900
111. Chang, L., Chiang, S. H., and Saltiel, A. R. (2004) Insulin signaling and the regulation of glucose transport. *Mol Med* **10**, 65-71
112. Banting, F. G., Best, C. H., Collip, J. B., Campbell, W. R., and Fletcher, A. A. (1922) Pancreatic Extracts in the Treatment of Diabetes Mellitus. *Can Med Assoc J* **12**, 141-146
113. Sun, X. J., Rothenberg, P., Kahn, C. R., Backer, J. M., Araki, E., Wilden, P. A., Cahill, D. A., Goldstein, B. J., and White, M. F. (1991) Structure of the insulin receptor substrate IRS-1 defines a unique signal transduction protein. *Nature* **352**, 73-77
114. Sun, X. J., Wang, L. M., Zhang, Y., Yenush, L., Myers, M. G., Jr., Glasheen, E., Lane, W. S., Pierce, J. H., and White, M. F. (1995) Role of IRS-2 in insulin and cytokine signalling. *Nature* **377**, 173-177
115. Cheatham, B., Vlahos, C. J., Cheatham, L., Wang, L., Blenis, J., and Kahn, C. R. (1994) Phosphatidylinositol 3-kinase activation is required for insulin stimulation of pp70 S6 kinase, DNA synthesis, and glucose transporter translocation. *Mol Cell Biol* **14**, 4902-4911
116. Alessi, D. R., James, S. R., Downes, C. P., Holmes, A. B., Gaffney, P. R., Reese, C. B., and Cohen, P. (1997) Characterization of a 3-phosphoinositide-dependent protein kinase which phosphorylates and activates protein kinase Balpha. *Curr Biol* **7**, 261-269
117. Saltiel, A. R., and Kahn, C. R. (2001) Insulin signalling and the regulation of glucose and lipid metabolism. *Nature* **414**, 799-806

118. Taniguchi, C. M., Emanuelli, B., and Kahn, C. R. (2006) Critical nodes in signalling pathways: insights into insulin action. *Nat Rev Mol Cell Biol* **7**, 85-96
119. Pincus, I. J., and Rutman, J. Z. (1953) Glucagon, the hyperglycemic agent in pancreatic extracts; a possible factor in certain types of diabetes. *AMA Arch Intern Med* **92**, 666-677
120. Campbell, J. E., and Drucker, D. J. (2015) Islet alpha cells and glucagon--critical regulators of energy homeostasis. *Nat Rev Endocrinol* **11**, 329-338
121. Mayo, K. E., Miller, L. J., Bataille, D., Dalle, S., Goke, B., Thorens, B., and Drucker, D. J. (2003) International Union of Pharmacology. XXXV. The glucagon receptor family. *Pharmacol Rev* **55**, 167-194
122. Guilherme, A., Virbasius, J. V., Puri, V., and Czech, M. P. (2008) Adipocyte dysfunctions linking obesity to insulin resistance and type 2 diabetes. *Nat Rev Mol Cell Biol* **9**, 367-377
123. Postic, C., and Girard, J. (2008) Contribution of de novo fatty acid synthesis to hepatic steatosis and insulin resistance: lessons from genetically engineered mice. *J Clin Invest* **118**, 829-838
124. Howard, B. V. (1987) Lipoprotein metabolism in diabetes mellitus. *J Lipid Res* **28**, 613-628
125. McGarry, J. D., and Brown, N. F. (1997) The mitochondrial carnitine palmitoyltransferase system. From concept to molecular analysis. *Eur J Biochem* **244**, 1-14
126. Pessin, J. E., and Saltiel, A. R. (2000) Signaling pathways in insulin action: molecular targets of insulin resistance. *J Clin Invest* **106**, 165-169
127. Fery, F. (1994) Role of hepatic glucose production and glucose uptake in the pathogenesis of fasting hyperglycemia in type 2 diabetes: normalization of glucose kinetics by short-term fasting. *J Clin Endocrinol Metab* **78**, 536-542
128. Bechmann, L. P., Hannivoort, R. A., Gerken, G., Hotamisligil, G. S., Trauner, M., and Canbay, A. (2012) The interaction of hepatic lipid and glucose metabolism in liver diseases. *Journal of hepatology* **56**, 952-964
129. Reddy, J. K. (2001) Nonalcoholic steatosis and steatohepatitis. III. Peroxisomal beta-oxidation, PPAR alpha, and steatohepatitis. *Am J Physiol Gastrointest Liver Physiol* **281**, G1333-1339
130. Sun, Z., and Lazar, M. A. (2013) Dissociating fatty liver and diabetes. *Trends Endocrinol Metab* **24**, 4-12
131. Stefan, N., and Haring, H. U. (2011) The metabolically benign and malignant fatty liver. *Diabetes* **60**, 2011-2017
132. Cohen, J. C., Horton, J. D., and Hobbs, H. H. (2011) Human fatty liver disease: old questions and new insights. *Science* **332**, 1519-1523
133. Sun, K., Tordjman, J., Clement, K., and Scherer, P. E. (2013) Fibrosis and adipose tissue dysfunction. *Cell Metab* **18**, 470-477
134. Shoelson, S. E., Herrero, L., and Naaz, A. (2007) Obesity, inflammation, and insulin resistance. *Gastroenterology* **132**, 2169-2180
135. Savage, D. B., Petersen, K. F., and Shulman, G. I. (2007) Disordered lipid metabolism and the pathogenesis of insulin resistance. *Physiol Rev* **87**, 507-520

136. Rutkowski, J. M., Stern, J. H., and Scherer, P. E. (2015) The cell biology of fat expansion. *J Cell Biol* **208**, 501-512
137. Boden, G. (1997) Role of fatty acids in the pathogenesis of insulin resistance and NIDDM. *Diabetes* **46**, 3-10
138. Weisberg, S. P., McCann, D., Desai, M., Rosenbaum, M., Leibel, R. L., and Ferrante, A. W., Jr. (2003) Obesity is associated with macrophage accumulation in adipose tissue. *J Clin Invest* **112**, 1796-1808
139. Xu, H., Barnes, G. T., Yang, Q., Tan, G., Yang, D., Chou, C. J., Sole, J., Nichols, A., Ross, J. S., Tartaglia, L. A., and Chen, H. (2003) Chronic inflammation in fat plays a crucial role in the development of obesity-related insulin resistance. *J Clin Invest* **112**, 1821-1830
140. Trayhurn, P., Wang, B., and Wood, I. S. (2008) Hypoxia in adipose tissue: a basis for the dysregulation of tissue function in obesity? *Br J Nutr* **100**, 227-235
141. Huang-Doran, I., Sleigh, A., Rochford, J. J., O'Rahilly, S., and Savage, D. B. (2010) Lipodystrophy: metabolic insights from a rare disorder. *J Endocrinol* **207**, 245-255
142. Robbins, A. L., and Savage, D. B. (2015) The genetics of lipid storage and human lipodystrophies. *Trends Mol Med* **21**, 433-438
143. Bareja, A., Holt, J. A., Luo, G., Chang, C., Lin, J., Hinken, A. C., Freudenberg, J. M., Kraus, W. E., Evans, W. J., and Billin, A. N. (2014) Human and mouse skeletal muscle stem cells: convergent and divergent mechanisms of myogenesis. *PLoS One* **9**, e90398
144. Baron, A. D., Brechtel, G., Wallace, P., and Edelman, S. V. (1988) Rates and tissue sites of non-insulin- and insulin-mediated glucose uptake in humans. *Am J Physiol* **255**, E769-774
145. Thorens, B., and Mueckler, M. (2010) Glucose transporters in the 21st Century. *Am J Physiol Endocrinol Metab* **298**, E141-145
146. Frontera, W. R., and Ochala, J. (2015) Skeletal muscle: a brief review of structure and function. *Calcif Tissue Int* **96**, 183-195
147. Longnecker, D. (2014) Anatomy and Histology of the Pancreas. in *Pancreapedia: Exocrine Pancreas Knowledge Base*
148. Gromada, J., Franklin, I., and Wollheim, C. B. (2007) Alpha-cells of the endocrine pancreas: 35 years of research but the enigma remains. *Endocr Rev* **28**, 84-116
149. Strowski, M. Z., Parmar, R. M., Blake, A. D., and Schaeffer, J. M. (2000) Somatostatin inhibits insulin and glucagon secretion via two receptors subtypes: an in vitro study of pancreatic islets from somatostatin receptor 2 knockout mice. *Endocrinology* **141**, 111-117
150. Goodpaster, B. H., He, J., Watkins, S., and Kelley, D. E. (2001) Skeletal muscle lipid content and insulin resistance: evidence for a paradox in endurance-trained athletes. *J Clin Endocrinol Metab* **86**, 5755-5761
151. Amati, F., Dube, J. J., Alvarez-Carnero, E., Edreira, M. M., Chomentowski, P., Coen, P. M., Switzer, G. E., Bickel, P. E., Stefanovic-Racic, M., Toledo, F. G., and Goodpaster, B. H. (2011) Skeletal muscle triglycerides, diacylglycerols, and ceramides in insulin resistance: another paradox in endurance-trained athletes? *Diabetes* **60**, 2588-2597
152. Randle, P. J., Garland, P. B., Hales, C. N., and Newsholme, E. A. (1963) The glucose fatty-acid cycle. Its role in insulin sensitivity and the metabolic disturbances of diabetes mellitus. *Lancet* **1**, 785-789

153. Samuel, V. T., and Shulman, G. I. (2012) Mechanisms for insulin resistance: common threads and missing links. *Cell* **148**, 852-871
154. Weir, G. C., and Bonner-Weir, S. (2004) Five stages of evolving beta-cell dysfunction during progression to diabetes. *Diabetes* **53 Suppl 3**, S16-21
155. Mathis, D., Vence, L., and Benoist, C. (2001) beta-Cell death during progression to diabetes. *Nature* **414**, 792-798
156. Lee, J. S., Kim, S. H., Jun, D. W., Han, J. H., Jang, E. C., Park, J. Y., Son, B. K., Kim, S. H., Jo, Y. J., Park, Y. S., and Kim, Y. S. (2009) Clinical implications of fatty pancreas: correlations between fatty pancreas and metabolic syndrome. *World J Gastroenterol* **15**, 1869-1875
157. Greenberg, A. S., and Coleman, R. A. (2011) Expanding roles for lipid droplets. *Trends Endocrinol Metab* **22**, 195-196
158. Reue, K. (2011) A thematic review series: lipid droplet storage and metabolism: from yeast to man. *J Lipid Res* **52**, 1865-1868
159. Farese, R. V., Jr., and Walther, T. C. (2009) Lipid droplets finally get a little R-E-S-P-E-C-T. *Cell* **139**, 855-860
160. Thiam, A. R., Farese, R. V., Jr., and Walther, T. C. (2013) The biophysics and cell biology of lipid droplets. *Nat Rev Mol Cell Biol* **14**, 775-786
161. Pol, A., Gross, S. P., and Parton, R. G. (2014) Review: biogenesis of the multifunctional lipid droplet: lipids, proteins, and sites. *J Cell Biol* **204**, 635-646
162. Szymanski, K. M., Binns, D., Bartz, R., Grishin, N. V., Li, W. P., Agarwal, A. K., Garg, A., Anderson, R. G., and Goodman, J. M. (2007) The lipodystrophy protein seipin is found at endoplasmic reticulum lipid droplet junctions and is important for droplet morphology. *Proc Natl Acad Sci U S A* **104**, 20890-20895
163. Fei, W., Shui, G., Gaeta, B., Du, X., Kuerschner, L., Li, P., Brown, A. J., Wenk, M. R., Parton, R. G., and Yang, H. (2008) Fld1p, a functional homologue of human seipin, regulates the size of lipid droplets in yeast. *J Cell Biol* **180**, 473-482
164. Kadereit, B., Kumar, P., Wang, W. J., Miranda, D., Snapp, E. L., Severina, N., Torregroza, I., Evans, T., and Silver, D. L. (2008) Evolutionarily conserved gene family important for fat storage. *Proc Natl Acad Sci U S A* **105**, 94-99
165. Fujimoto, T., and Parton, R. G. (2011) Not just fat: the structure and function of the lipid droplet. *Cold Spring Harb Perspect Biol* **3**
166. Suzuki, M., Shinohara, Y., Ohsaki, Y., and Fujimoto, T. (2011) Lipid droplets: size matters. *J Electron Microsc (Tokyo)* **60 Suppl 1**, S101-116
167. Ducharme, N. A., and Bickel, P. E. (2008) Lipid droplets in lipogenesis and lipolysis. *Endocrinology* **149**, 942-949
168. Saka, H. A., and Valdivia, R. (2012) Emerging roles for lipid droplets in immunity and host-pathogen interactions. *Annu Rev Cell Dev Biol* **28**, 411-437
169. Bozza, P. T., and Viola, J. P. (2010) Lipid droplets in inflammation and cancer. *Prostaglandins Leukot Essent Fatty Acids* **82**, 243-250
170. Welte, M. A. (2007) Proteins under new management: lipid droplets deliver. *Trends Cell Biol* **17**, 363-369
171. Cermelli, S., Guo, Y., Gross, S. P., and Welte, M. A. (2006) The lipid-droplet proteome reveals that droplets are a protein-storage depot. *Curr Biol* **16**, 1783-1795

172. Camus, G., Vogt, D. A., Kondratowicz, A. S., and Ott, M. (2013) Lipid droplets and viral infections. *Methods Cell Biol* **116**, 167-190
173. Brasaemle, D. L. (2007) Thematic review series: adipocyte biology. The perilipin family of structural lipid droplet proteins: stabilization of lipid droplets and control of lipolysis. *J Lipid Res* **48**, 2547-2559
174. Kuhnlein, R. P. (2012) Thematic review series: Lipid droplet synthesis and metabolism: from yeast to man. Lipid droplet-based storage fat metabolism in Drosophila. *J Lipid Res* **53**, 1430-1436
175. Greenberg, A. S., Egan, J. J., Wek, S. A., Garty, N. B., Blanchette-Mackie, E. J., and Londos, C. (1991) Perilipin, a major hormonally regulated adipocyte-specific phosphoprotein associated with the periphery of lipid storage droplets. *J Biol Chem* **266**, 11341-11346
176. Greenberg, A. S., Egan, J. J., Wek, S. A., Moos, M. C., Jr., Londos, C., and Kimmel, A. R. (1993) Isolation of cDNAs for perilipins A and B: sequence and expression of lipid droplet-associated proteins of adipocytes. *Proc Natl Acad Sci U S A* **90**, 12035-12039
177. Tansey, J. T., Sztalryd, C., Gruia-Gray, J., Roush, D. L., Zee, J. V., Gavrilova, O., Reitman, M. L., Deng, C. X., Li, C., Kimmel, A. R., and Londos, C. (2001) Perilipin ablation results in a lean mouse with aberrant adipocyte lipolysis, enhanced leptin production, and resistance to diet-induced obesity. *Proc Natl Acad Sci U S A* **98**, 6494-6499
178. Servetnick, D. A., Brasaemle, D. L., Gruia-Gray, J., Kimmel, A. R., Wolff, J., and Londos, C. (1995) Perilipins are associated with cholesteryl ester droplets in steroidogenic adrenal cortical and Leydig cells. *J Biol Chem* **270**, 16970-16973
179. Lu, X., Gruia-Gray, J., Copeland, N. G., Gilbert, D. J., Jenkins, N. A., Londos, C., and Kimmel, A. R. (2001) The murine perilipin gene: the lipid droplet-associated perilipins derive from tissue-specific, mRNA splice variants and define a gene family of ancient origin. *Mamm Genome* **12**, 741-749
180. Brasaemle, D. L., Rubin, B., Harten, I. A., Gruia-Gray, J., Kimmel, A. R., and Londos, C. (2000) Perilipin A increases triacylglycerol storage by decreasing the rate of triacylglycerol hydrolysis. *J Biol Chem* **275**, 38486-38493
181. Tansey, J. T., Huml, A. M., Vogt, R., Davis, K. E., Jones, J. M., Fraser, K. A., Brasaemle, D. L., Kimmel, A. R., and Londos, C. (2003) Functional studies on native and mutated forms of perilipins. A role in protein kinase A-mediated lipolysis of triacylglycerols. *J Biol Chem* **278**, 8401-8406
182. Souza, S. C., Muliro, K. V., Liscum, L., Lien, P., Yamamoto, M. T., Schaffer, J. E., Dallal, G. E., Wang, X., Kraemer, F. B., Obin, M., and Greenberg, A. S. (2002) Modulation of hormone-sensitive lipase and protein kinase A-mediated lipolysis by perilipin A in an adenoviral reconstituted system. *J Biol Chem* **277**, 8267-8272
183. Brasaemle, D. L., Barber, T., Wolins, N. E., Serrero, G., Blanchette-Mackie, E. J., and Londos, C. (1997) Adipose differentiation-related protein is an ubiquitously expressed lipid storage droplet-associated protein. *J Lipid Res* **38**, 2249-2263
184. Xu, G., Sztalryd, C., Lu, X., Tansey, J. T., Gan, J., Dorward, H., Kimmel, A. R., and Londos, C. (2005) Post-translational regulation of adipose differentiation-related protein by the ubiquitin/proteasome pathway. *J Biol Chem* **280**, 42841-42847

185. Jiang, H. P., Harris, S. E., and Serrero, G. (1992) Molecular cloning of a differentiation-related mRNA in the adipogenic cell line 1246. *Cell Growth Differ* **3**, 21-30
186. Wolins, N. E., Quaynor, B. K., Skinner, J. R., Schoenfish, M. J., Tzekov, A., and Bickel, P. E. (2005) S3-12, Adipophilin, and TIP47 package lipid in adipocytes. *J Biol Chem* **280**, 19146-19155
187. Heid, H. W., Moll, R., Schwetlick, I., Rackwitz, H. R., and Keenan, T. W. (1998) Adipophilin is a specific marker of lipid accumulation in diverse cell types and diseases. *Cell Tissue Res* **294**, 309-321
188. Gross, D. N., Miyoshi, H., Hosaka, T., Zhang, H. H., Pino, E. C., Souza, S., Obin, M., Greenberg, A. S., and Pilch, P. F. (2006) Dynamics of lipid droplet-associated proteins during hormonally stimulated lipolysis in engineered adipocytes: stabilization and lipid droplet binding of adipocyte differentiation-related protein/adipophilin. *Mol Endocrinol* **20**, 459-466
189. Diaz, E., and Pfeffer, S. R. (1998) TIP47: a cargo selection device for mannose 6-phosphate receptor trafficking. *Cell* **93**, 433-443
190. Wolins, N. E., Rubin, B., and Brasaemle, D. L. (2001) TIP47 associates with lipid droplets. *J Biol Chem* **276**, 5101-5108
191. Miura, S., Gan, J. W., Brzostowski, J., Parisi, M. J., Schultz, C. J., Londos, C., Oliver, B., and Kimmel, A. R. (2002) Functional conservation for lipid storage droplet association among Perilipin, ADRP, and TIP47 (PAT)-related proteins in mammals, Drosophila, and Dictyostelium. *J Biol Chem* **277**, 32253-32257
192. Hickenbottom, S. J., Kimmel, A. R., Londos, C., and Hurley, J. H. (2004) Structure of a lipid droplet protein; the PAT family member TIP47. *Structure* **12**, 1199-1207
193. Scherer, P. E., Bickel, P. E., Kotler, M., and Lodish, H. F. (1998) Cloning of cell-specific secreted and surface proteins by subtractive antibody screening. *Nat Biotechnol* **16**, 581-586
194. Wolins, N. E., Skinner, J. R., Schoenfish, M. J., Tzekov, A., Bensch, K. G., and Bickel, P. E. (2003) Adipocyte protein S3-12 coats nascent lipid droplets. *J Biol Chem* **278**, 37713-37721
195. Wolins, N. E., Quaynor, B. K., Skinner, J. R., Tzekov, A., Croce, M. A., Gropler, M. C., Varma, V., Yao-Borengasser, A., Rasouli, N., Kern, P. A., Finck, B. N., and Bickel, P. E. (2006) OXPAT/PAT-1 is a PPAR-induced lipid droplet protein that promotes fatty acid utilization. *Diabetes* **55**, 3418-3428
196. Yamaguchi, T., Matsushita, S., Motojima, K., Hirose, F., and Osumi, T. (2006) MLDP, a novel PAT family protein localized to lipid droplets and enriched in the heart, is regulated by peroxisome proliferator-activated receptor alpha. *J Biol Chem* **281**, 14232-14240
197. Dalen, K. T., Dahl, T., Holter, E., Arntsen, B., Londos, C., Sztalryd, C., and Nebb, H. I. (2007) LSDP5 is a PAT protein specifically expressed in fatty acid oxidizing tissues. *Biochim Biophys Acta* **1771**, 210-227
198. Inohara, N., Koseki, T., Chen, S., Wu, X., and Nunez, G. (1998) CIDE, a novel family of cell death activators with homology to the 45 kDa subunit of the DNA fragmentation factor. *EMBO J* **17**, 2526-2533

199. Liang, L., Zhao, M., Xu, Z., Yokoyama, K. K., and Li, T. (2003) Molecular cloning and characterization of CIDE-3, a novel member of the cell-death-inducing DNA-fragmentation-factor (DFF45)-like effector family. *Biochem J* **370**, 195-203
200. Xu, L., Zhou, L., and Li, P. (2012) CIDE proteins and lipid metabolism. *Arteriosclerosis, thrombosis, and vascular biology* **32**, 1094-1098
201. Chen, Z., Guo, K., Toh, S. Y., Zhou, Z., and Li, P. (2000) Mitochondria localization and dimerization are required for CIDE-B to induce apoptosis. *J Biol Chem* **275**, 22619-22622
202. Gong, J., Sun, Z., and Li, P. (2009) CIDE proteins and metabolic disorders. *Curr Opin Lipidol* **20**, 121-126
203. Zhou, Z., Yon Toh, S., Chen, Z., Guo, K., Ng, C. P., Ponniah, S., Lin, S. C., Hong, W., and Li, P. (2003) Cidea-deficient mice have lean phenotype and are resistant to obesity. *Nat Genet* **35**, 49-56
204. Puri, V., Ranjit, S., Konda, S., Nicoloro, S. M., Straubhaar, J., Chawla, A., Chouinard, M., Lin, C., Burkart, A., Corvera, S., Perugini, R. A., and Czech, M. P. (2008) Cidea is associated with lipid droplets and insulin sensitivity in humans. *Proc Natl Acad Sci U S A* **105**, 7833-7838
205. Nordstrom, E. A., Ryden, M., Backlund, E. C., Dahlman, I., Kaaman, M., Blomqvist, L., Cannon, B., Nedergaard, J., and Arner, P. (2005) A human-specific role of cell death-inducing DFFA (DNA fragmentation factor-alpha)-like effector A (CIDEA) in adipocyte lipolysis and obesity. *Diabetes* **54**, 1726-1734
206. Zhou, L., Xu, L., Ye, J., Li, D., Wang, W., Li, X., Wu, L., Wang, H., Guan, F., and Li, P. (2012) Cidea promotes hepatic steatosis by sensing dietary fatty acids. *Hepatology* **56**, 95-107
207. Wang, W., Lv, N., Zhang, S., Shui, G., Qian, H., Zhang, J., Chen, Y., Ye, J., Xie, Y., Shen, Y., Wenk, M. R., and Li, P. (2012) Cidea is an essential transcriptional coactivator regulating mammary gland secretion of milk lipids. *Nat Med* **18**, 235-243
208. Li, J. Z., Ye, J., Xue, B., Qi, J., Zhang, J., Zhou, Z., Li, Q., Wen, Z., and Li, P. (2007) Cideb regulates diet-induced obesity, liver steatosis, and insulin sensitivity by controlling lipogenesis and fatty acid oxidation. *Diabetes* **56**, 2523-2532
209. Ye, J., Li, J. Z., Liu, Y., Li, X., Yang, T., Ma, X., Li, Q., Yao, Z., and Li, P. (2009) Cideb, an ER- and lipid droplet-associated protein, mediates VLDL lipidation and maturation by interacting with apolipoprotein B. *Cell Metab* **9**, 177-190
210. Li, J. Z., Lei, Y., Wang, Y., Zhang, Y., Ye, J., Xia, X., Pan, X., and Li, P. (2010) Control of cholesterol biosynthesis, uptake and storage in hepatocytes by Cideb. *Biochim Biophys Acta* **1801**, 577-586
211. Li, H., Song, Y., Li, F., Zhang, L., Gu, Y., Zhang, L., Jiang, L., Dong, W., Ye, J., and Li, Q. (2010) Identification of lipid droplet-associated proteins in the formation of macrophage-derived foam cells using microarrays. *Int J Mol Med* **26**, 231-239
212. Danesch, U., Hoeck, W., and Ringold, G. M. (1992) Cloning and transcriptional regulation of a novel adipocyte-specific gene, FSP27. CAAT-enhancer-binding protein (C/EBP) and C/EBP-like proteins interact with sequences required for differentiation-dependent expression. *J Biol Chem* **267**, 7185-7193

213. Puri, V., Virbasius, J. V., Guilherme, A., and Czech, M. P. (2008) RNAi screens reveal novel metabolic regulators: RIP140, MAP4k4 and the lipid droplet associated fat specific protein (FSP) 27. *Acta Physiologica* **192**, 103-115
214. Matsusue, K., Kusakabe, T., Noguchi, T., Takiguchi, S., Suzuki, T., Yamano, S., and Gonzalez, F. J. (2008) Hepatic steatosis in leptin-deficient mice is promoted by the PPARgamma target gene Fsp27. *Cell Metab* **7**, 302-311
215. Puri, V., Konda, S., Ranjit, S., Aouadi, M., Chawla, A., Chouinard, M., Chakladar, A., and Czech, M. P. (2007) Fat-specific protein 27, a novel lipid droplet protein that enhances triglyceride storage. *Journal of Biological Chemistry* **282**, 34213-34218
216. Gong, J., Sun, Z., Wu, L., Xu, W., Schieber, N., Xu, D., Shui, G., Yang, H., Parton, R. G., and Li, P. (2011) Fsp27 promotes lipid droplet growth by lipid exchange and transfer at lipid droplet contact sites. *J Cell Biol* **195**, 953-963
217. Jambunathan, S., Yin, J., Khan, W., Tamori, Y., and Puri, V. (2011) FSP27 Promotes Lipid Droplet Clustering and Then Fusion to Regulate Triglyceride Accumulation. *PLoS One* **6**, e28614
218. Sun, Z., Gong, J., Wu, H., Xu, W., Wu, L., Xu, D., Gao, J., Wu, J. W., Yang, H., Yang, M., and Li, P. (2013) Perilipin1 promotes unilocular lipid droplet formation through the activation of Fsp27 in adipocytes. *Nat Commun* **4**, 1594
219. Kuramoto, K., Okamura, T., Yamaguchi, T., Nakamura, T. Y., Wakabayashi, S., Morinaga, H., Nomura, M., Yanase, T., Otsu, K., Usuda, N., Matsumura, S., Inoue, K., Fushiki, T., Kojima, Y., Hashimoto, T., Sakai, F., Hirose, F., and Osumi, T. (2012) Perilipin 5, a Lipid Droplet-binding Protein, Protects Heart from Oxidative Burden by Sequestering Fatty Acid from Excessive Oxidation. *J Biol Chem* **287**, 23852-23863
220. Nishino, N., Tamori, Y., Tateya, S., Kawaguchi, T., Shibakusa, T., Mizunoya, W., Inoue, K., Kitazawa, R., Kitazawa, S., Matsuki, Y., Hiramatsu, R., Masubuchi, S., Omachi, A., Kimura, K., Saito, M., Amo, T., Ohta, S., Yamaguchi, T., Osumi, T., Cheng, J., Fujimoto, T., Nakao, H., Nakao, K., Aiba, A., Okamura, H., Fushiki, T., and Kasuga, M. (2008) FSP27 contributes to efficient energy storage in murine white adipocytes by promoting the formation of unilocular lipid droplets. *J Clin Invest* **118**, 2808-2821
221. Lass, A., Zimmermann, R., Haemmerle, G., Riederer, M., Schoiswohl, G., Schweiger, M., Kienesberger, P., Strauss, J. G., Gorkiewicz, G., and Zechner, R. (2006) Adipose triglyceride lipase-mediated lipolysis of cellular fat stores is activated by CGI-58 and defective in Chanarin-Dorfman Syndrome. *Cell Metab* **3**, 309-319
222. Yang, X., Lu, X., Lombes, M., Rha, G. B., Chi, Y. I., Guerin, T. M., Smart, E. J., and Liu, J. (2010) The G(0)/G(1) switch gene 2 regulates adipose lipolysis through association with adipose triglyceride lipase. *Cell Metab* **11**, 194-205
223. Ma, T., Lopez-Aguiar, A. G., Li, A., Lu, Y., Sekula, D., Nattie, E. E., Freemantle, S., and Dmitrovsky, E. (2014) Mice lacking G0S2 are lean and cold-tolerant. *Cancer Biol Ther* **15**, 643-650
224. Brown, J. M., Betters, J. L., Lord, C., Ma, Y., Han, X., Yang, K., Alger, H. M., Melchior, J., Sawyer, J., Shah, R., Wilson, M. D., Liu, X., Graham, M. J., Lee, R., Crooke, R., Shulman, G. I., Xue, B., Shi, H., and Yu, L. (2010) CGI-58 knockdown in mice causes hepatic steatosis but prevents diet-induced obesity and glucose intolerance. *J Lipid Res* **51**, 3306-3315

225. Radner, F. P., Streith, I. E., Schoiswohl, G., Schweiger, M., Kumari, M., Eichmann, T. O., Rechberger, G., Koefeler, H. C., Eder, S., Schauer, S., Theussl, H. C., Preiss-Landl, K., Lass, A., Zimmermann, R., Hoefler, G., Zechner, R., and Haemmerle, G. (2010) Growth retardation, impaired triacylglycerol catabolism, hepatic steatosis, and lethal skin barrier defect in mice lacking comparative gene identification-58 (CGI-58). *J Biol Chem* **285**, 7300-7311

226. Egan, J. J., Greenberg, A. S., Chang, M. K., and Londos, C. (1990) Control of endogenous phosphorylation of the major cAMP-dependent protein kinase substrate in adipocytes by insulin and beta-adrenergic stimulation. *J Biol Chem* **265**, 18769-18775

227. Zhang, H. H., Souza, S. C., Muliro, K. V., Kraemer, F. B., Obin, M. S., and Greenberg, A. S. (2003) Lipase-selective functional domains of perilipin A differentially regulate constitutive and protein kinase A-stimulated lipolysis. *J Biol Chem* **278**, 51535-51542

228. Granneman, J. G., Moore, H. P. H., Krishnamoorthy, R., and Rathod, M. (2009) Perilipin Controls Lipolysis by Regulating the Interactions of AB-hydrolase Containing 5 (Abhd5) and Adipose Triglyceride Lipase (Atgl). *Journal of Biological Chemistry* **284**, 34538-34544

229. Stralfors, P., and Belfrage, P. (1983) Phosphorylation of hormone-sensitive lipase by cyclic AMP-dependent protein kinase. *J Biol Chem* **258**, 15146-15152

230. Stralfors, P., Bjorgell, P., and Belfrage, P. (1984) Hormonal regulation of hormone-sensitive lipase in intact adipocytes: identification of phosphorylated sites and effects on the phosphorylation by lipolytic hormones and insulin. *Proc Natl Acad Sci U S A* **81**, 3317-3321

231. Anthonsen, M. W., Ronnstrand, L., Wernstedt, C., Degerman, E., and Holm, C. (1998) Identification of novel phosphorylation sites in hormone-sensitive lipase that are phosphorylated in response to isoproterenol and govern activation properties in vitro. *J Biol Chem* **273**, 215-221

232. Brasaemle, D. L., Levin, D. M., Adler-Wailes, D. C., and Londos, C. (2000) The lipolytic stimulation of 3T3-L1 adipocytes promotes the translocation of hormone-sensitive lipase to the surfaces of lipid storage droplets. *Biochim Biophys Acta* **1483**, 251-262

233. Clifford, G. M., Londos, C., Kraemer, F. B., Vernon, R. G., and Yeaman, S. J. (2000) Translocation of hormone-sensitive lipase and perilipin upon lipolytic stimulation of rat adipocytes. *J Biol Chem* **275**, 5011-5015

234. Egan, J. J., Greenberg, A. S., Chang, M. K., Wek, S. A., Moos, M. C., Jr., and Londos, C. (1992) Mechanism of hormone-stimulated lipolysis in adipocytes: translocation of hormone-sensitive lipase to the lipid storage droplet. *Proc Natl Acad Sci U S A* **89**, 8537-8541

235. Granneman, J. G., Moore, H. P., Granneman, R. L., Greenberg, A. S., Obin, M. S., and Zhu, Z. (2007) Analysis of lipolytic protein trafficking and interactions in adipocytes. *J Biol Chem* **282**, 5726-5735

236. Miyoshi, H., Souza, S. C., Zhang, H. H., Strissel, K. J., Christoffolete, M. A., Kovsan, J., Rudich, A., Kraemer, F. B., Bianco, A. C., Obin, M. S., and Greenberg, A. S. (2006) Perilipin promotes hormone-sensitive lipase-mediated adipocyte lipolysis via phosphorylation-dependent and -independent mechanisms. *J Biol Chem* **281**, 15837-15844

237. Su, C. L., Sztalryd, C., Contreras, J. A., Holm, C., Kimmel, A. R., and Londos, C. (2003) Mutational analysis of the hormone-sensitive lipase translocation reaction in adipocytes. *J Biol Chem* **278**, 43615-43619
238. Granneman, J. G., Moore, H. P., Mottillo, E. P., Zhu, Z., and Zhou, L. (2011) Interactions of perilipin-5 (Plin5) with adipose triglyceride lipase. *J Biol Chem* **286**, 5126-5135
239. Wang, H., Bell, M., Sreenivasan, U., Hu, H., Liu, J., Dalen, K., Londos, C., Yamaguchi, T., Rizzo, M. A., Coleman, R., Gong, D., Brasaemle, D., and Sztalryd, C. (2011) Unique regulation of adipose triglyceride lipase (ATGL) by perilipin 5, a lipid droplet-associated protein. *J Biol Chem* **286**, 15707-15715
240. Grahn, T. H., Kaur, R., Yin, J., Schweiger, M., Sharma, V. M., Lee, M. J., Ido, Y., Smas, C. M., Zechner, R., Lass, A., and Puri, V. (2014) Fat-specific protein 27 (FSP27) interacts with adipose triglyceride lipase (ATGL) to regulate lipolysis and insulin sensitivity in human adipocytes. *J Biol Chem* **289**, 12029-12039
241. Kaushik, S., and Cuervo, A. M. (2015) Degradation of lipid droplet-associated proteins by chaperone-mediated autophagy facilitates lipolysis. *Nat Cell Biol* **17**, 759-770
242. Bostrom, P., Andersson, L., Rutberg, M., Perman, J., Lidberg, U., Johansson, B. R., Fernandez-Rodriguez, J., Ericson, J., Nilsson, T., Boren, J., and Olofsson, S. O. (2007) SNARE proteins mediate fusion between cytosolic lipid droplets and are implicated in insulin sensitivity. *Nat Cell Biol* **9**, 1286-1293
243. Bostrom, P., Rutberg, M., Ericsson, J., Holmdahl, P., Andersson, L., Frohman, M. A., Boren, J., and Olofsson, S. O. (2005) Cytosolic lipid droplets increase in size by microtubule-dependent complex formation. *Arteriosclerosis, thrombosis, and vascular biology* **25**, 1945-1951
244. Chang, B. H., Li, L., Paul, A., Taniguchi, S., Nannegari, V., Heird, W. C., and Chan, L. (2006) Protection against fatty liver but normal adipogenesis in mice lacking adipose differentiation-related protein. *Mol Cell Biol* **26**, 1063-1076
245. McManaman, J. L., Bales, E. S., Orlicky, D. J., Jackman, M., MacLean, P. S., Cain, S., Crunk, A. E., Mansur, A., Graham, C. E., Bowman, T. A., and Greenberg, A. S. (2013) Perilipin-2-null mice are protected against diet-induced obesity, adipose inflammation, and fatty liver disease. *J Lipid Res* **54**, 1346-1359
246. Russell, T. D., Palmer, C. A., Orlicky, D. J., Bales, E. S., Chang, B. H., Chan, L., and McManaman, J. L. (2008) Mammary glands of adipophilin-null mice produce an amino-terminally truncated form of adipophilin that mediates milk lipid droplet formation and secretion. *J Lipid Res* **49**, 206-216
247. Kuramoto, K., Sakai, F., Yoshinori, N., Nakamura, T. Y., Wakabayashi, S., Kojidani, T., Haraguchi, T., Hirose, F., and Osumi, T. (2014) Deficiency of a lipid droplet protein, perilipin 5, suppresses myocardial lipid accumulation, thereby preventing type 1 diabetes-induced heart malfunction. *Mol Cell Biol* **34**, 2721-2731
248. Zhou, L., Park, S. Y., Xu, L., Xia, X., Ye, J., Su, L., Jeong, K. H., Hur, J. H., Oh, H., Tamori, Y., Zingaretti, C. M., Cinti, S., Argente, J., Yu, M., Wu, L., Ju, S., Guan, F., Yang, H., Choi, C. S., Savage, D. B., and Li, P. (2015) Insulin resistance and white adipose tissue inflammation are uncoupled in energetically challenged Fsp27-deficient mice. *Nat Commun* **6**, 5949

249. Tanaka, N., Takahashi, S., Matsubara, T., Jiang, C., Sakamoto, W., Chanturiya, T., Teng, R., Gavrilova, O., and Gonzalez, F. J. (2015) Adipocyte-specific disruption of fat-specific protein 27 causes hepatosteatosis and insulin resistance in high-fat diet-fed mice. *J Biol Chem* **290**, 3092-3105
250. Martinez-Botas, J., Anderson, J. B., Tessier, D., Lapillonne, A., Chang, B. H., Quast, M. J., Gorenstein, D., Chen, K. H., and Chan, L. (2000) Absence of perilipin results in leanness and reverses obesity in Lepr(db/db) mice. *Nat Genet* **26**, 474-479
251. Gandotra, S., Lim, K., Girousse, A., Saudek, V., O'Rahilly, S., and Savage, D. B. (2011) Human frame shift mutations affecting the carboxyl terminus of perilipin increase lipolysis by failing to sequester the adipose triglyceride lipase (ATGL) coactivator AB-hydrolase-containing 5 (ABHD5). *J Biol Chem* **286**, 34998-35006
252. Rubio-Cabezas, O., Puri, V., Murano, I., Saudek, V., Semple, R. K., Dash, S., Hyden, C. S., Bottomley, W., Vigouroux, C., Magre, J., Raymond-Barker, P., Murgatroyd, P. R., Chawla, A., Skepper, J. N., Chatterjee, V. K., Suliman, S., Patch, A. M., Agarwal, A. K., Garg, A., Barroso, I., Cinti, S., Czech, M. P., Argente, J., O'Rahilly, S., and Savage, D. B. (2009) Partial lipodystrophy and insulin resistant diabetes in a patient with a homozygous nonsense mutation in CIDEC. *EMBO Mol Med* **1**, 280-287
253. Schweiger, M., Lass, A., Zimmermann, R., Eichmann, T. O., and Zechner, R. (2009) Neutral lipid storage disease: genetic disorders caused by mutations in adipose triglyceride lipase/PNPLA2 or CGI-58/ABHD5. *Am J Physiol Endocrinol Metab* **297**, E289-296
254. Lefevre, C., Jobard, F., Caux, F., Bouadjar, B., Karaduman, A., Heilig, R., Lakhdar, H., Wollenberg, A., Verret, J. L., Weissenbach, J., Ozguc, M., Lathrop, M., Prud'homme, J. F., and Fischer, J. (2001) Mutations in CGI-58, the gene encoding a new protein of the esterase/lipase/thioesterase subfamily, in Chanarin-Dorfman syndrome. *Am J Hum Genet* **69**, 1002-1012
255. Yamaguchi, T., Omatsu, N., Matsushita, S., and Osumi, T. (2004) CGI-58 interacts with perilipin and is localized to lipid droplets. Possible involvement of CGI-58 mislocalization in Chanarin-Dorfman syndrome. *J Biol Chem* **279**, 30490-30497
256. Campagna, F., Nanni, L., Quagliarini, F., Pennisi, E., Michailidis, C., Pierelli, F., Bruno, C., Casali, C., DiMauro, S., and Arca, M. (2008) Novel mutations in the adipose triglyceride lipase gene causing neutral lipid storage disease with myopathy. *Biochem Biophys Res Commun* **377**, 843-846
257. Hirano, K., Ikeda, Y., Zaima, N., Sakata, Y., and Matsumiya, G. (2008) Triglyceride deposit cardiomyovasculopathy. *N Engl J Med* **359**, 2396-2398
258. Albert, J. S., Yerges-Armstrong, L. M., Horenstein, R. B., Pollin, T. I., Sreenivasan, U. T., Chai, S., Blaner, W. S., Snitker, S., O'Connell, J. R., Gong, D. W., Breyer, R. J., 3rd, Ryan, A. S., McLenithan, J. C., Shuldiner, A. R., Sztalryd, C., and Damcott, C. M. (2014) Null mutation in hormone-sensitive lipase gene and risk of type 2 diabetes. *N Engl J Med* **370**, 2307-2315
259. Magre, J., Delepine, M., Khallouf, E., Gedde-Dahl, T., Jr., Van Maldergem, L., Sobel, E., Papp, J., Meier, M., Megarbane, A., Bachy, A., Verloes, A., d'Abronzo, F. H., Seemanova, E., Assan, R., Baudic, N., Bourut, C., Czernichow, P., Huet, F., Grigorescu, F., de Kerdanet,

M., Lacombe, D., Labrune, P., Lanza, M., Loret, H., Matsuda, F., Navarro, J., Nivelon-Chevalier, A., Polak, M., Robert, J. J., Tric, P., Tubiana-Rufi, N., Vigouroux, C., Weissenbach, J., Savasta, S., Maassen, J. A., Trygstad, O., Bogalho, P., Freitas, P., Medina, J. L., Bonnicci, F., Joffe, B. I., Loyson, G., Panz, V. R., Raal, F. J., O'Rahilly, S., Stephenson, T., Kahn, C. R., Lathrop, M., Capeau, J., and Group, B. W. (2001) Identification of the gene altered in Berardinelli-Seip congenital lipodystrophy on chromosome 11q13. *Nat Genet* **28**, 365-370

260. Van Maldergem, L., Magre, J., Khallouf, T. E., Gedde-Dahl, T., Jr., Delepine, M., Trygstad, O., Seemanova, E., Stephenson, T., Albott, C. S., Bonnici, F., Panz, V. R., Medina, J. L., Bogalho, P., Huet, F., Savasta, S., Verloes, A., Robert, J. J., Loret, H., De Kerdanet, M., Tubiana-Rufi, N., Megarbane, A., Maassen, J., Polak, M., Lacombe, D., Kahn, C. R., Silveira, E. L., D'Abronzo, F. H., Grigorescu, F., Lathrop, M., Capeau, J., and O'Rahilly, S. (2002) Genotype-phenotype relationships in Berardinelli-Seip congenital lipodystrophy. *J Med Genet* **39**, 722-733
261. Ebihara, K., Kusakabe, T., Masuzaki, H., Kobayashi, N., Tanaka, T., Chusho, H., Miyanaga, F., Miyazawa, T., Hayashi, T., Hosoda, K., Ogawa, Y., and Nakao, K. (2004) Gene and phenotype analysis of congenital generalized lipodystrophy in Japanese: a novel homozygous nonsense mutation in seipin gene. *J Clin Endocrinol Metab* **89**, 2360-2364
262. Payne, V. A., Grimsey, N., Tuthill, A., Virtue, S., Gray, S. L., Dalla Nora, E., Semple, R. K., O'Rahilly, S., and Rochford, J. J. (2008) The human lipodystrophy gene BSCL2/seipin may be essential for normal adipocyte differentiation. *Diabetes* **57**, 2055-2060
263. Gimm, T., Wiese, M., Teschemacher, B., Deggerich, A., Schodel, J., Knaup, K. X., Hackenbeck, T., Hellerbrand, C., Amann, K., Wiesener, M. S., Honing, S., Eckardt, K. U., and Warnecke, C. (2010) Hypoxia-inducible protein 2 is a novel lipid droplet protein and a specific target gene of hypoxia-inducible factor-1. *Faseb Journal* **24**, 4443-4458
264. Denko, N., Schindler, C., Koong, A., Laderoute, K., Green, C., and Giaccia, A. (2000) Epigenetic regulation of gene expression in cervical cancer cells by the tumor microenvironment. *Clinical Cancer Research* **6**, 480-487
265. Togashi, A., Katagiri, T., Ashida, S., Fujioka, T., Maruyama, O., Wakumoto, Y., Sakamoto, Y., Fujime, M., Kawachi, Y., Shuin, T., and Nakamura, Y. (2005) Hypoxia-inducible protein 2 (HIG2), a novel diagnostic marker for renal cell carcinoma and potential target for molecular therapy. *Cancer research* **65**, 4817-4826
266. Kenny, P. A., Enver, T., and Ashworth, A. (2005) Receptor and secreted targets of Wnt-1/beta-catenin signalling in mouse mammary epithelial cells. *BMC Cancer* **5**, 3
267. Mattijssen, F., Georgiadi, A., Andasarie, T., Szalowska, E., Zota, A., Krones-Herzig, A., Heier, C., Ratman, D., De Bosscher, K., Qi, L., Zechner, R., Herzig, S., and Kersten, S. (2014) Hypoxia-inducible lipid droplet-associated (HILPDA) is a novel peroxisome proliferator-activated receptor (PPAR) target involved in hepatic triglyceride secretion. *J Biol Chem* **289**, 19279-19293
268. Viswakarma, N., Yu, S., Naik, S., Kashireddy, P., Matsumoto, K., Sarkar, J., Surapureddi, S., Jia, Y., Rao, M. S., and Reddy, J. K. (2007) Transcriptional regulation of Cidea, mitochondrial cell death-inducing DNA fragmentation factor alpha-like effector A, in

mouse liver by peroxisome proliferator-activated receptor alpha and gamma. *J Biol Chem* **282**, 18613-18624

269. Langhi, C., and Baldan, A. (2015) CIDEC/FSP27 is regulated by peroxisome proliferator-activated receptor alpha and plays a critical role in fasting- and diet-induced hepatosteatosis. *Hepatology* **61**, 1227-1238
270. Qi, L., Saberi, M., Zmuda, E., Wang, Y. G., Altarejos, J., Zhang, X. M., Dentin, R., Hedrick, S., Bandyopadhyay, G., Hai, T., Olefsky, J., and Montminy, M. (2009) Adipocyte CREB Promotes Insulin Resistance in Obesity. *Cell Metabolism* **9**, 277-286
271. Leavens, K. F., and Birnbaum, M. J. (2011) Insulin signaling to hepatic lipid metabolism in health and disease. *Critical reviews in biochemistry and molecular biology* **46**, 200-215
272. Charlton, M. (2004) Nonalcoholic fatty liver disease: a review of current understanding and future impact. *Clinical gastroenterology and hepatology : the official clinical practice journal of the American Gastroenterological Association* **2**, 1048-1058
273. Angulo, P. (2002) Nonalcoholic fatty liver disease. *N Engl J Med* **346**, 1221-1231
274. Birkenfeld, A. L., and Shulman, G. I. (2014) Nonalcoholic fatty liver disease, hepatic insulin resistance, and type 2 diabetes. *Hepatology* **59**, 713-723
275. Walther, T. C., and Farese, R. V., Jr. (2012) Lipid droplets and cellular lipid metabolism. *Annual review of biochemistry* **81**, 687-714
276. Greenberg, A. S., Coleman, R. A., Kraemer, F. B., McManaman, J. L., Obin, M. S., Puri, V., Yan, Q. W., Miyoshi, H., and Mashek, D. G. (2011) The role of lipid droplets in metabolic disease in rodents and humans. *J Clin Invest* **121**, 2102-2110
277. Patel, S., Yang, W., Kozusko, K., Saudek, V., and Savage, D. B. (2014) Perilipins 2 and 3 lack a carboxy-terminal domain present in perilipin 1 involved in sequestering ABHD5 and suppressing basal lipolysis. *Proc Natl Acad Sci U S A* **111**, 9163-9168
278. Yang, L., Ding, Y., Chen, Y., Zhang, S., Huo, C., Wang, Y., Yu, J., Zhang, P., Na, H., Zhang, H., Ma, Y., and Liu, P. (2012) The proteomics of lipid droplets: structure, dynamics, and functions of the organelle conserved from bacteria to humans. *J Lipid Res* **53**, 1245-1253
279. Nishimura, S., Tsuda, H., Nomura, H., Kataoka, F., Chiyoda, T., Tanaka, H., Tanaka, K., Susumu, N., and Aoki, D. (2011) Expression of hypoxia-inducible 2 (HIG2) protein in uterine cancer. *European journal of gynaecological oncology* **32**, 146-149
280. Folch, J., Lees, M., and Sloane Stanley, G. H. (1957) A simple method for the isolation and purification of total lipides from animal tissues. *J Biol Chem* **226**, 497-509
281. Gao, G., Zhou, X., Alvira, M. R., Tran, P., Marsh, J., Lynd, K., Xiao, W., and Wilson, J. M. (2003) High throughput creation of recombinant adenovirus vectors by direct cloning, green-white selection and I-Sce I-mediated rescue of circular adenovirus plasmids in 293 cells. *Gene Ther* **10**, 1926-1930
282. Gao, G. P., Yang, Y., and Wilson, J. M. (1996) Biology of adenovirus vectors with E1 and E4 deletions for liver-directed gene therapy. *J Virol* **70**, 8934-8943
283. Wang, H., Sreenivasan, U., Hu, H., Saladino, A., Polster, B. M., Lund, L. M., Gong, D. W., Stanley, W. C., and Sztalryd, C. (2011) Perilipin 5, a lipid droplet-associated protein, provides physical and metabolic linkage to mitochondria. *J Lipid Res* **52**, 2159-2168

284. Beylot, M., Neggazi, S., Hamlat, N., Langlois, D., and Forcheron, F. (2012) Perilipin 1 ablation in mice enhances lipid oxidation during exercise and does not impair exercise performance. *Metabolism: clinical and experimental* **61**, 415-423
285. Tove, S. B., Andrews, J. S., Jr., and Lucas, H. L. (1956) Turnover of palmitic, stearic, and unsaturated fatty acids in rat liver. *J Biol Chem* **218**, 275-281
286. Aibara, D., Matsusue, K., Matsuo, K., Takiguchi, S., Gonzalez, F. J., and Yamano, S. (2013) Expression of hepatic fat-specific protein 27 depends on the specific etiology of fatty liver. *Biological & pharmaceutical bulletin* **36**, 1766-1772
287. Quiroga, A. D., and Lehner, R. (2012) Liver triacylglycerol lipases. *Biochim Biophys Acta* **1821**, 762-769
288. Lass, A., Zimmermann, R., Oberer, M., and Zechner, R. (2011) Lipolysis - a highly regulated multi-enzyme complex mediates the catabolism of cellular fat stores. *Progress in lipid research* **50**, 14-27
289. Ong, K. T., Mashek, M. T., Bu, S. Y., Greenberg, A. S., and Mashek, D. G. (2011) Adipose triglyceride lipase is a major hepatic lipase that regulates triacylglycerol turnover and fatty acid signaling and partitioning. *Hepatology* **53**, 116-126
290. Reid, B. N., Ables, G. P., Otlivanchik, O. A., Schoiswohl, G., Zechner, R., Blaner, W. S., Goldberg, I. J., Schwabe, R. F., Chua, S. C., Jr., and Huang, L. S. (2008) Hepatic overexpression of hormone-sensitive lipase and adipose triglyceride lipase promotes fatty acid oxidation, stimulates direct release of free fatty acids, and ameliorates steatosis. *J Biol Chem* **283**, 13087-13099
291. Wu, J. W., Wang, S. P., Alvarez, F., Casavant, S., Gauthier, N., Abed, L., Soni, K. G., Yang, G., and Mitchell, G. A. (2011) Deficiency of liver adipose triglyceride lipase in mice causes progressive hepatic steatosis. *Hepatology* **54**, 122-132
292. UniProt, C. (2015) UniProt: a hub for protein information. *Nucleic Acids Res* **43**, D204-212
293. Sievers, F., Wilm, A., Dineen, D., Gibson, T. J., Karplus, K., Li, W., Lopez, R., McWilliam, H., Remmert, M., Soding, J., Thompson, J. D., and Higgins, D. G. (2011) Fast, scalable generation of high-quality protein multiple sequence alignments using Clustal Omega. *Mol Syst Biol* **7**, 539
294. Lee, Y. S., Li, P., Huh, J. Y., Hwang, I. J., Lu, M., Kim, J. I., Ham, M., Talukdar, S., Chen, A., Lu, W. J., Bandyopadhyay, G. K., Schwendener, R., Olefsky, J., and Kim, J. B. (2011) Inflammation Is Necessary for Long-Term but Not Short-Term High-Fat Diet-Induced Insulin Resistance. *Diabetes*
295. Sethi, J. K., and Vidal-Puig, A. J. (2007) Thematic review series: adipocyte biology. Adipose tissue function and plasticity orchestrate nutritional adaptation. *J Lipid Res* **48**, 1253-1262
296. Konige, M., Wang, H., and Sztalryd, C. (2014) Role of adipose specific lipid droplet proteins in maintaining whole body energy homeostasis. *Biochim Biophys Acta* **1842**, 393-401
297. Zechner, R., Zimmermann, R., Eichmann, T. O., Kohlwein, S. D., Haemmerle, G., Lass, A., and Madeo, F. (2012) FAT SIGNALS - Lipases and Lipolysis in Lipid Metabolism and Signaling. *Cell Metab* **15**, 279-291

298. Gandotra, S., Le Dour, C., Bottomley, W., Cervera, P., Giral, P., Reznik, Y., Charpentier, G., Auclair, M., Delepine, M., Barroso, I., Semple, R. K., Lathrop, M., Lascols, O., Capeau, J., O'Rahilly, S., Magre, J., Savage, D. B., and Vigouroux, C. (2011) Perilipin deficiency and autosomal dominant partial lipodystrophy. *N Engl J Med* **364**, 740-748
299. Himms-Hagen, J. (1984) Nonshivering thermogenesis. *Brain Res Bull* **12**, 151-160
300. Maloney, S. K., Fuller, A., Mitchell, D., Gordon, C., and Overton, J. M. (2014) Translating animal model research: does it matter that our rodents are cold? *Physiology (Bethesda)* **29**, 413-420
301. Hardy, O. T., Perugini, R. A., Nicoloro, S. M., Gallagher-Dorval, K., Puri, V., Straubhaar, J., and Czech, M. P. (2011) Body mass index-independent inflammation in omental adipose tissue associated with insulin resistance in morbid obesity. *Surgery for obesity and related diseases : official journal of the American Society for Bariatric Surgery* **7**, 60-67
302. Jiang, Z. Y., Zhou, Q. L., Coleman, K. A., Chouinard, M., Boese, Q., and Czech, M. P. (2003) Insulin signaling through Akt/protein kinase B analyzed by small interfering RNA-mediated gene silencing. *Proc Natl Acad Sci U S A* **100**, 7569-7574
303. Wabitsch, M., Brenner, R. E., Melzner, I., Braun, M., Moller, P., Heinze, E., Debatin, K. M., and Hauner, H. (2001) Characterization of a human preadipocyte cell strain with high capacity for adipose differentiation. *Int J Obes Relat Metab Disord* **25**, 8-15
304. DiStefano, M. T., Danai, L. V., Roth Flach, R. J., Chawla, A., Pedersen, D. J., Guilherme, A., and Czech, M. P. (2015) The Lipid Droplet Protein Hypoxia-inducible Gene 2 Promotes Hepatic Triglyceride Deposition by Inhibiting Lipolysis. *J Biol Chem* **290**, 15175-15184
305. Abreu-Vieira, G., Fischer, A. W., Mattsson, C., de Jong, J. M., Shabalina, I. G., Ryden, M., Laurencikiene, J., Arner, P., Cannon, B., Nedergaard, J., and Petrovic, N. (2015) Cidea improves the metabolic profile through expansion of adipose tissue. *Nat Commun* **6**, 7433
306. Ranjit, S., Boutet, E., Gandhi, P., Prot, M., Tamori, Y., Chawla, A., Greenberg, A. S., Puri, V., and Czech, M. P. (2011) Regulation of fat specific protein 27 by isoproterenol and TNF-alpha to control lipolysis in murine adipocytes. *J Lipid Res* **52**, 221-236
307. Nian, Z., Sun, Z., Yu, L., Toh, S. Y., Sang, J., and Li, P. (2010) Fat-specific protein 27 undergoes ubiquitin-dependent degradation regulated by triacylglycerol synthesis and lipid droplet formation. *J Biol Chem* **285**, 9604-9615
308. Villarroya, J., Cereijo, R., and Villarroya, F. (2013) An endocrine role for brown adipose tissue? *Am J Physiol Endocrinol Metab* **305**, E567-572
309. Whittle, A. J., Carobbio, S., Martins, L., Slawik, M., Hondares, E., Vazquez, M. J., Morgan, D., Csikasz, R. I., Gallego, R., Rodriguez-Cuenca, S., Dale, M., Virtue, S., Villarroya, F., Cannon, B., Rahmouni, K., Lopez, M., and Vidal-Puig, A. (2012) BMP8B increases brown adipose tissue thermogenesis through both central and peripheral actions. *Cell* **149**, 871-885
310. Virtue, S., Feldmann, H., Christian, M., Tan, C. Y., Masoodi, M., Dale, M., Lelliott, C., Burling, K., Campbell, M., Eguchi, N., Voshol, P., Sethi, J. K., Parker, M., Urade, Y., Griffin, J. L., Cannon, B., and Vidal-Puig, A. (2012) A new role for lipocalin prostaglandin d synthase in the regulation of brown adipose tissue substrate utilization. *Diabetes* **61**, 3139-3147

311. Rosell, M., Hondares, E., Iwamoto, S., Gonzalez, F. J., Wabitsch, M., Staels, B., Olmos, Y., Monsalve, M., Giralt, M., Iglesias, R., and Villarroya, F. (2012) Peroxisome proliferator-activated receptors-alpha and -gamma, and cAMP-mediated pathways, control retinol-binding protein-4 gene expression in brown adipose tissue. *Endocrinology* **153**, 1162-1173
312. Hondares, E., Iglesias, R., Giralt, A., Gonzalez, F. J., Giralt, M., Mampel, T., and Villarroya, F. (2011) Thermogenic activation induces FGF21 expression and release in brown adipose tissue. *J Biol Chem* **286**, 12983-12990
313. Gunawardana, S. C., and Piston, D. W. (2012) Reversal of type 1 diabetes in mice by brown adipose tissue transplant. *Diabetes* **61**, 674-682
314. Burri, L., Thoresen, G. H., and Berge, R. K. (2010) The Role of PPARalpha Activation in Liver and Muscle. *PPAR Res* **2010**
315. Alkhouri, N., Dixon, L. J., and Feldstein, A. E. (2009) Lipotoxicity in nonalcoholic fatty liver disease: not all lipids are created equal. *Expert Rev Gastroenterol Hepatol* **3**, 445-451
316. Robinson, J., and Newsholme, E. A. (1969) Some properties of hepatic glycerol kinase and their relation to the control of glycerol utilization. *Biochem J* **112**, 455-464
317. Silva, J. E., and Larsen, P. R. (1983) Adrenergic activation of triiodothyronine production in brown adipose tissue. *Nature* **305**, 712-713
318. Halberg, N., Wernstedt-Asterholm, I., and Scherer, P. E. (2008) The Adipocyte as an Endocrine Cell. *Endocrinology and Metabolism Clinics of North America* **37**, 753-+
319. Ouchi, N., Parker, J. L., Lugus, J. J., and Walsh, K. (2011) Adipokines in inflammation and metabolic disease. *Nat Rev Immunol* **11**, 85-97
320. Ye, J. (2009) Emerging role of adipose tissue hypoxia in obesity and insulin resistance. *Int J Obes (Lond)* **33**, 54-66
321. Jiang, C., Qu, A., Matsubara, T., Chanturiya, T., Jou, W., Gavrilova, O., Shah, Y. M., and Gonzalez, F. J. (2011) Disruption of hypoxia-inducible factor 1 in adipocytes improves insulin sensitivity and decreases adiposity in high-fat diet-fed mice. *Diabetes* **60**, 2484-2495
322. Yu, X. H., Fu, Y. C., Zhang, D. W., Yin, K., and Tang, C. K. (2013) Foam cells in atherosclerosis. *Clin Chim Acta* **424**, 245-252